Review

Visual prostheses for the blind

Robert K. Shepherd[1,2], Mohit N. Shivdasani[1,2], David A.X. Nayagam[1,2,3], Christopher E. Williams[1,2], and Peter J. Blamey[1,2]

[1] Bionics Institute, 384-388 Albert St East Melbourne, 3002, Victoria, Australia
[2] Medical Bionics Department, University of Melbourne, 384-388 Albert St East Melbourne, 3002, Victoria, Australia
[3] Department of Pathology, University of Melbourne, Parkville, 3010, Victoria, Australia

After more than 40 years of research, visual prostheses are moving from the laboratory into the clinic. These devices are designed to provide prosthetic vision to the blind by stimulating localized neural populations in one of the retinotopically organized structures of the visual pathway – typically the retina or visual cortex. The long gestation of this research reflects the many significant technical challenges encountered including surgical access, mechanical stability, hardware miniaturization, hermetic encapsulation, high-density electrode arrays, and signal processing. This review provides an introduction to the pathophysiology of blindness; an overview of existing visual prostheses, their advantages and drawbacks; the perceptual effects evoked by electrical stimulation; as well as the role played by plasticity and training in clinical outcomes.

Introduction

Neural prostheses restore or modulate neural activity in patients suffering from a variety of sensory or neurological disorders. Since the appearance of the first commercial devices in the 1970s, the field has grown to a $4.7 billion industry in 2012 with an annual growth rate of 20% [1]. Prominent innovations include neuromodulation devices to treat chronic refractory pain, cochlear implants that provide auditory cues for the profoundly deaf, and deep brain stimulators that reduce motor disorders in Parkinson's disease. Among the most exciting developments are visual prostheses, devices designed to provide artificial visual for the blind, resulting in increased independent living and quality of life. Here, we review the current status of both retinal and cortical based visual prostheses.

The retina is a highly specialized structure located at the back of the eye that converts light into nerve impulses. The outer retina contains ~150 million photoreceptors (see Glossary) that make excitatory and inhibitory connections with the first of a series of specialized cells that form the middle and inner layers of the retina. These cells in turn make synaptic connections to the ~1 million retinal ganglion cells (RGCs) that form the output of the retina, conducting action potentials via the optic nerve to the central visual pathway.

It is estimated that 285 million people are visually impaired worldwide; 39 million of whom are blind [2]. Although uncorrected refractive errors are the main cause of visual impairment, diseases associated with degeneration of the retinal photoreceptors result in severe visual loss with few or no therapeutic options for ongoing clinical management. Importantly, significant numbers of RGCs are spared following the loss of photoreceptors. Although there are major alterations to the neural circuitry of these surviving neurons [3], their presence provides the potential to restore vision using electrical stimulation delivered by an electrode array located close to the retina (Box 1). The clinical management of other forms of blindness, including

Glossary

Age-related macular degeneration (AMD): damage to the photoreceptors of the macula region of the retina leading to central blindness.
Choroid: located between the retina and the sclera, the choroid contains a rich network of blood vessels and connective tissue and is responsible for providing oxygen and nutrients to the outer layers of the retina.
Cones: a subtype of photoreceptor cell located in the outer retina responsible for color vision. They are optimized for performing in bright environments. Cones are densely packed in the central part of the visual field (the macula), but are relatively sparse in the peripheral retina. The human eye has approximately 6 million cone cells.
Fovea: a region of the macula responsible for sharp central vision.
Lateral geniculate nucleus (LGN): the main relay center in the brain of visual information coming from the retina. The axons of the LGN project directly to the visual cortex.
Macula: an oval-shaped region of the central retina that contains a high concentration of cone cells and is responsible for central vision.
Ophthalmoscope: or fundoscope is an optical instrument used to examine the inside surface (fundus) of the eye opposite the lens.
Optic nerve: The second cranial nerve consists of the processes of RGCs. It transmits visual information from the retina to the brain and is part of the central nervous system.
Phosphenes: artificial visual percepts not produced by light. Phosphenes can be evoked by electrical, mechanical, or magnetic stimulation of the retina or visual cortex.
Photoreceptor cells: A neuron specialized for transducing energy in the form of light to neural signals in the form of action potentials. In vertebrates, the two classic types of photoreceptor cells are rods and cones.
Retinal ganglion cells (RGCs): nerve cells whose axons connect the retina to the brain via the optic nerve. There are approximately 1 million RGCs in a normal human retina.
Retinitis pigmentosa (RP): an inherited, degenerative eye disease caused by an abnormality of photoreceptors leading to peripheral blindness.
Retinotopic: an orderly map of the retina reproduced in structures of the central visual system including the LGN and the visual cortex.
Rods: a subtype of photoreceptor cells that are sensitive to low light intensities. These cells are optimized for night vision and are concentrated in the peripheral retina. Rods are not sensitive to color. The human retina has approximately 100 million rod cells.
Visual cortex: Located at the back of the brain in the occipital cortex and receiving most of its input from the LGN, the primary visual cortex is a key site for vision processing.
Visual prostheses: devices designed to provide artificial vision for the blind.

Corresponding author: Shepherd, R.K. (rshepherd@bionicsinstitute.org).
Keywords: neural prosthesis; electrical stimulation; electrodes; blindness; bionic vision.

0167-7799/$ – see front matter
 http://dx.doi.org/10.1016/j.tibtech.2013.07.001

Box 1. Electrical stimulation of neural tissue

Generation of an action potential via an electrical stimulus

Neurons exhibit a resting membrane potential of typically –70 to –80 mV – the intracellular environment is maintained at a negative potential relative to the extracellular environment. As a negatively charged electrode (*cathode*) is positioned close to a neuron the potential difference across the neural membrane is artificially lowered – the neuron will become depolarized at that point. As the amount of charge delivered to the cathode increases, the depolarization of the neural membrane increases until it reaches a threshold potential. At this point, transmembrane voltage-sensitive Na^+ channels open and allow extracellular Na^+ into the intracellular environment, thus initiating an action potential. The propagation of the action potential along the axon is achieved via normal physiological processes independent of whether or not the activity is generated using natural or artificial means.

Principles of safe electrical stimulation of neural tissue

Stimulating electrodes must inject charge into the biological environment without damaging the surrounding tissue. Electrical stimulation is achieved via a series of electrochemical reactions that convert the charge carriers from electrons (in the electrode) to ions (in the electrolyte) and must be performed using specific electrode materials in combination with brief reversible stimulus waveforms to ensure that no toxic electrochemical products are introduced into the biological environment.

When a metal electrode is placed into an electrolyte, a layer of charge on the electrode surface will attract polarized water molecules, creating a capacitive layer at the electrode-tissue interface (Helmholtz double layer). At low charge densities ($<20\ \mu C/cm^2$) charge injection is dominated by this capacitance, no charge carrier crosses the electrode–tissue interface and no electrochemical reaction products are formed in the electrolyte [67,68]. In practice, activation of neural tissue requires charge densities higher than can be achieved via purely capacitive means. As charge density is increased, reversible electrochemical Faradaic reactions begin to dominate the charge injection process, including oxide formation/reduction and hydrogen-atom plating (Table I; [69]). Importantly, these reactions are localized to the electrode–tissue interface and can be readily reversed via the passage of an equal charge of opposite polarity – the charge-balanced biphasic pulse – ensuring that no new electrochemical species are released into the biological environment [67,68]. Safe electrical stimulation is restricted to charge injection via these processes and is dependent on the use of a charge-balanced stimulus waveform and the electrode material used. As an example, stainless steel electrodes are restricted to a maximum safe charge density of 40–50 $\mu C/cm^2$ geom. using these reversible processes compared with 210 $\mu C/cm^2$ geom. for platinum electrodes.

At higher stimulus intensities, charge injection is achieved via several irreversible electrochemical reactions, including electrode corrosion products, electrolysis of water, and oxidation of chloride ions (Table I). These electrochemical reaction products diffuse away from the electrode–tissue interface, resulting in tissue damage.

Platinum, iridium, and their alloys are the most extensively used metal electrodes for large surface area electrodes, whereas iridium oxide and titanium nitride are often used for microstimulation.

Table I. Reversible and irreversible electrochemical reactions associated with electrical stimulation using platinum electrodes

Oxide formation and reduction	$Pt + H_2O \leftrightarrow PtO + 2H^+ 2e^-$
H-atom plating	$Pt + H_2O + e^- \leftrightarrow Pt\text{-}H + OH^-$
Corrosion of the electrode	$Pt + 4Cl \rightarrow [PtCl_4]^{-2} + 2e^-$
Hydrogen generation	$2H_2O + 2e^- \rightarrow H_2\uparrow + 2OH^-$
Oxygen generation	$2H_2O \rightarrow O_2\uparrow + 4H^+ + 4e^-$
Oxidation of chloride ion	$2Cl^- \rightarrow Cl_2\uparrow + 2e^-$

glaucoma, diabetic retinopathy, and trauma is also associated with limited therapeutic options and can result in a nonfunctional retina or optic nerve. Although a retinal prosthesis is not suitable for these pathologies, electrical stimulation at other sites along the central visual pathway, particularly the visual cortex, has the potential to restore vision in these cases (Figure 1).

Attempts to stimulate the visual pathway electrically in order to evoke artificial visual percepts or 'phosphenes', are not new. In 1755 Charles LeRoy delivered current to a metal coil wrapped around the head of a blind man producing a flame-like phosphene that unfortunately also evoked terrible cries from the subject [4]. From the 1930s, exploratory procedures, performed by neurologists during neurosurgical procedures in awake patients, consistently demonstrated that phosphenes could be evoked by the application of localized electrical stimulation to specific regions of the cerebral cortex [5]. Brindley and colleagues pioneered the first clinical trial of a visual prosthesis in the late 1960s by implanting 80 electrodes over the visual cortex [6,7]. Although their subjects perceived reproducible phosphenes that looked like points, spots, or bars, the devices were limited by the technology available. Although a proposal for a retinal visual prosthesis was first described in the 1950s [8], the technical complexity of this approach delayed its development until the 1990s.

Over the past two decades there has been increased interest in the development of visual prostheses. Much of this impetus stems from the success of cochlear implants [9], advances in enabling technologies, and the lack of alternative therapeutic options for the treatment of these patients. There are at least 23 research groups developing visual prostheses [10]; the majority of which are retinal prostheses.

The normal and diseased retina

The human retina is a delicate and intricate network of photic-sensitive tissue lining the back of the eye. It transduces incident visible light, focused by the optics of the eye, into neural impulses, which form the perception of vision in the brain. The retina is comprised of an outer layer of photoreceptors, several specialist neural layers, and supporting architecture. Humans have two primary photoreceptors: rods and cones. The rods are optimized for low-light monochrome vision, whereas the cones are specialized for color vision in brighter environments. The photoreceptors are highly metabolically active and are supplied by the rich network of blood vessels in the adjacent layer of the eye, known as the choroid (Figure 2A). The light-sensing photoreceptor cells initiate a cascade of neural activity that propagates via a convergent retinal network to the RGCs whose axons form the optic nerve (Figure 2A).

Viewing the retina through the pupil via an ophthalmoscope (a fundus image), the most notable feature is the surface vasculature, which originates from the pale circular region known as the optic disc, and provides nourishment to the inner retinal layers (Figure 2B). The optic disc is the point where the axons of the RGCs form the optic nerve and exit the eye. Near the centre of the retina is an oval pigmented region known as the macula, which does

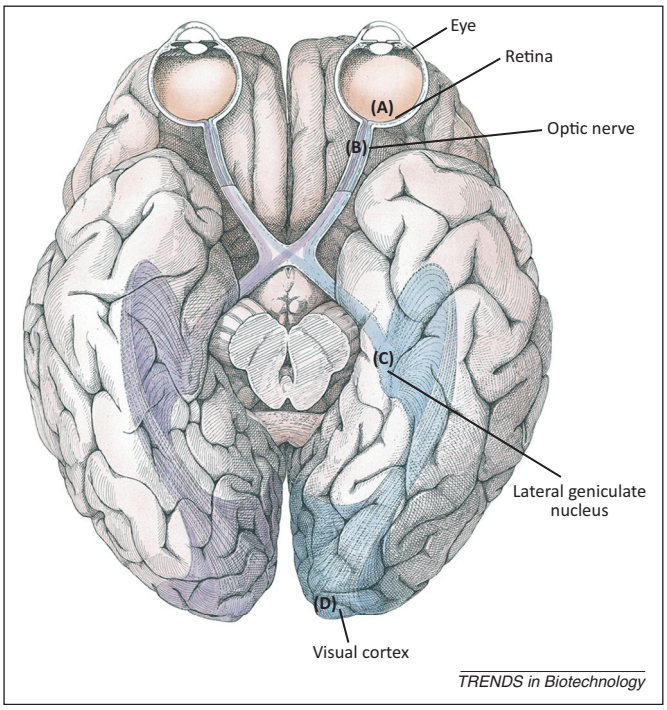

Figure 1. Overview of the visual pathway from the retina to the primary visual cortex. Visual prostheses can potentially target several sites along this pathway including: **(A)** planar electrode arrays placed at the epiretinal, subretinal, or suprachoroidal locations adjacent to the retina; **(B)** cuff electrodes around or penetrating electrodes into the optic nerve; **(C)** penetrating electrodes into the lateral geniculate nucleus; and **(D)** surface or penetrating electrodes over the visual cortex. These structures have a well-organized topographic map of the retina, that is, the spatial organization of the retina is maintained throughout the visual pathway. This is referred to as retinotopic organization. Adapted from [70].

not contain large blood vessels. This region is specialized for central, high-acuity vision, which is greatest at the fovea – a small depression in the centre of the macula containing almost exclusively cone photoreceptors (Figure 2B) [11].

Retinitis pigmentosa and age-related macular degeneration

Retinitis pigmentosa (RP) and age-related macular degeneration (AMD) are two degenerative diseases of the retina that result in blindness, secondary to photoreceptor loss (Figure 2D). RP is the collective term for a group of relatively rare hereditary deficits that lead to blindness in midlife, as a result of a gradual degeneration of photoreceptors. In typical rod–cone dystrophy, the lesion is initially restricted to the peripheral retina, resulting in tunnel vision (Figure 2F), but over time the central macular region can also be affected. Importantly, there is currently no cure for RP. AMD is a leading cause of vision loss in older adults; in western countries it accounts for ~50% of all severe visual impairment and blindness [12]. It gradually destroys the high-resolution macula region of the retina while typically leaving peripheral vision intact (Figure 2G). There are two forms of AMD. Dry AMD makes up the majority of cases (85–90%). With no effective treatment options, the disease process ultimately leads to a severe loss of central visual field. Wet AMD makes up 10–15% of cases and is characterized by abnormal proliferation of blood vessels in the choroid. As the disease progresses, this vascularization results in blood and fluid accumulation, damaging the photoreceptors of the macular region and resulting in severe loss of central vision (Figure 2H). Wet AMD progresses rapidly, and without intervention can cause severe damage within a few months. At present it is possible to use anti-vascular endothelial growth factor (anti-VEGF) drugs or retinal laser treatment to reduce the formation of new blood vessels; however, it is not possible to reverse the progression of the pathology.

Remodeling of the retina following loss of photoreceptors

Although significant populations of RGCs survive following photoreceptor degeneration, the loss of afferent input produces major changes in both the structure and function of the remaining neural retina [3]. The extent of retinal remodeling can vary substantially, but is ubiquitous following loss of photoreceptors. A cascade of early neurochemical changes precede structural and functional revisions including the migration and rewiring of retinal circuitry, gliosis, ectopic neurite outgrowth, and RGC degeneration [3,13]. These alterations influence the sensitivity of RGCs to electrical stimulation as well as the neural processing through the retinal network [3]. Importantly, electrical stimulation of the long-term blind retina evokes stable, retinotopically organized visual precepts [14].

Other potential forms of blindness that could be treated with visual prostheses

Other causes of incurable blindness include glaucoma, diabetic retinopathy, traumatic eye injury, peripheral visual pathway, or retinofugal lesions (such as optic nerve tumors), and central disorders [15]. Retinal prostheses are not suitable for these conditions because the injury foci are central to the RGCs, however, electrode arrays that directly stimulate more central structures within the visual pathway (Figure 1) provide viable alternatives.

Design principles of visual prostheses

Visual prostheses can be broadly categorized into groups based on their underlying technology or the anatomical location in which the electrode array is implanted. From a technological perspective there are two basic designs. (i) Optical sensors such as an array of photodiodes that are implanted close to the retina. The normal optical properties of the eye focus light onto the photodiodes, which convert this energy into electrical pulses designed to depolarize proximal RGCs [16,17]. (ii) A classic sensory prosthesis that includes an external video camera, vision processor, and power supply, a transcutaneous telemetry link, an implantable stimulator connected to a leadwire, and electrode array located at the level of the retina or central visual pathway [18–20] (Figure 3; Box 2).

There are several design advantages to using a photodiode array; primarily the absence of wires, which simplifies the surgery. Additionally, because a photodiode array utilizes existing ocular optics and eye position to localize the visual field, there is no need to take into account the subject's gaze. The major limiting factor associated with the use of photodiodes is their inability to provide sufficient

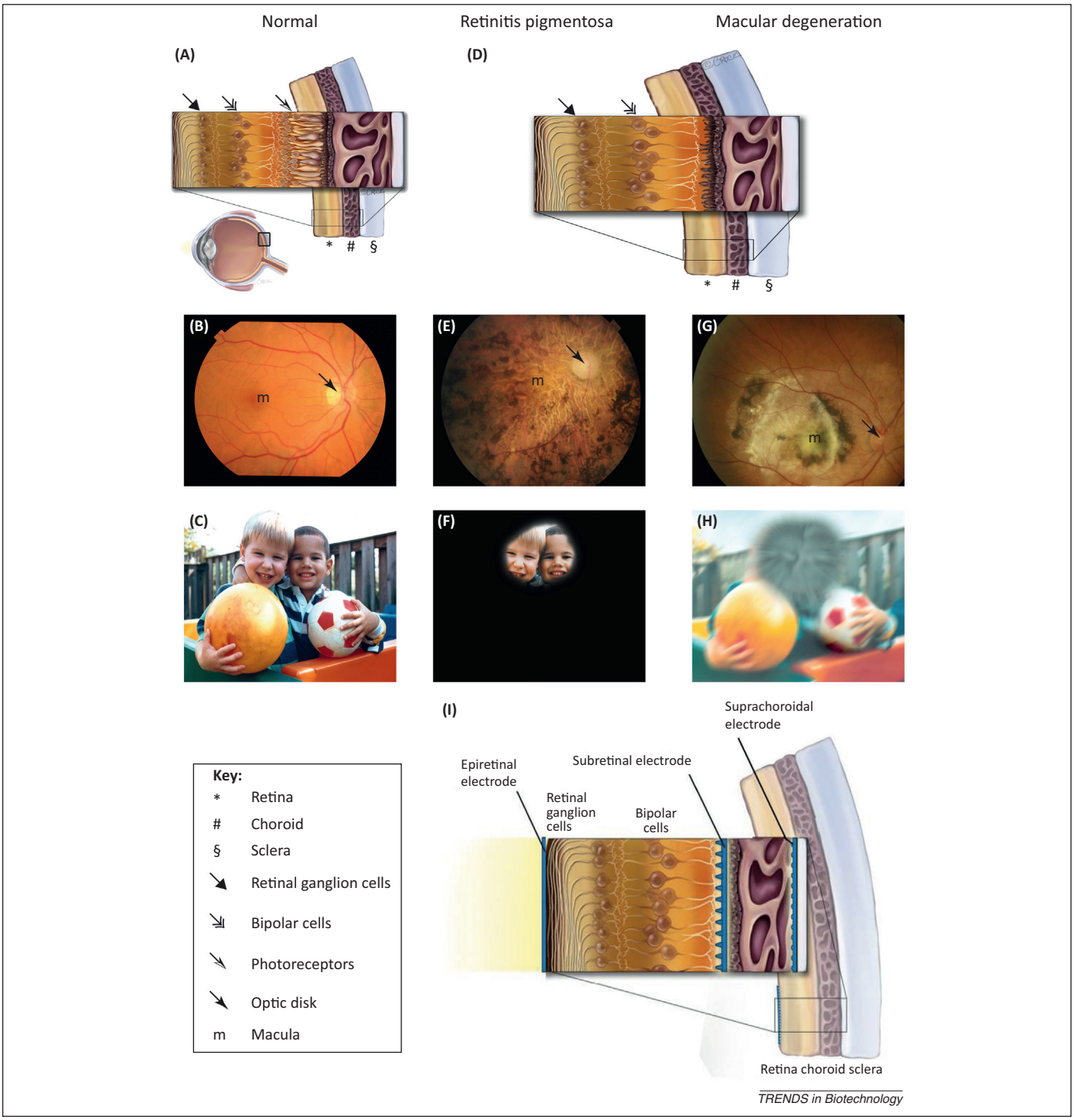

Figure 2. The anatomy of the eye in normal vision and following loss of photoreceptors. **(A)** Schematic of a normal retina, choroid, and sclera. The retina consists of several processing layers extending from the rods and cones of the outer retina through bipolar cells of the middle retina to the retinal ganglion cells (RGCs) that make up the inner retina. Axons of the RGCs project via the optic disc to form the optic nerve. Inset: horizontal section through the eye with the boxed region illustrating the location of the magnified schematics in panels A and D. **(B)** Color fundus image of a normal retina illustrating the optic disk (arrow) and macula region (m). **(C)** Simulated normal visual field. **(D)** Schematic of a retina with widespread photoreceptor degeneration. **(E)** Fundus image of a retina with retinitis pigmentosa (RP). **(F)** Simulated tunnel vision of a patient with RP. **(G)** Fundus image of a retina with age-related macular degeneration (AMD). **(H)** Simulated visual field of a patient with AMD, showing loss of central vision. **(I)** Potential sites to place an electrode array close to the retina including epiretinal, subretinal, and suprachoroidal positions. Panels A, D and I: courtesy of Bionic Vision Australia (Image by C. Roce). Panels B, E and G: courtesy of the Centre for Eye Research Australia. Panels C, F and H: courtesy of the National Institutes of Health National Eye Institute.

energy necessary for retinal stimulation [21]. To overcome this limitation one photodiode based device includes an external power source and a leadwire assembly [16,22], and a second design intends to use pulsed infrared light to provide both power and visual information directly to a photodiode array implanted in the retina [17].

The most common form of a visual prosthesis incorporates an electrode array located on or close to the retina. There are several anatomical sites where these electrodes

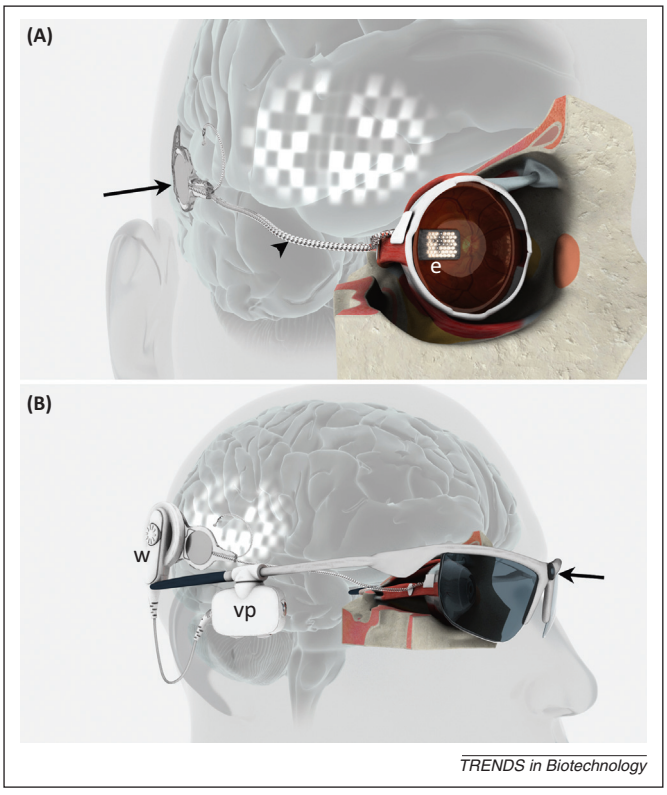

Figure 3. **(A)** Schematic diagram of a generic retinal prosthesis illustrating a receiver–stimulator unit implanted in the mastoid bone behind the ear (arrow), a leadwire assembly (arrowhead) connecting the output of the stimulator to an array of electrodes (e) implanted in the retina. The electrode array can be tacked in front of the retina (epiretinal); inserted between the choroid and the retina (subretinal); or inserted between the sclera and the choroid (suprachoroidal). A similar architecture would be suitable for a visual prosthesis based on stimulation of the visual cortex. **(B)** Overall schema of a retinal prosthesis that includes a video camera incorporated onto glasses (arrow), an external vision processor (vp) that provides both data and power across the skin via a wireless link (w) to the implanted receiver-stimulator, leadwire and electrode array illustrated in (A). The camera continuously feeds video signals to the vision processor that contains the patient's phosphene map, visual processing algorithms, and stimulation strategies. Each frame of the input video generates a sequence of commands at the vision processor that defines the electrodes and stimulus parameters required to generate a prosthetic image of the scene. (Images by Jack Parry; courtesy of the Bionics Institute).

can be placed, including the inner surface of the retina (epiretinal), between the retina and choroid (subretinal), or between the choroid and the sclera (suprachoroidal) (Figure 2I). Potential complications associated with a retinal prosthesis include mechanical stability of the implant in a location subject to extensive movement in the form of micro- and macrosaccades. An intended recipient of a visual prosthesis with vision impairment is expected to have a similar number of saccades as a normally sighted person; between 100 000 and 150 000 eye movements per day [23]. Mechanical stability can be a particular issue for epiretinal devices where the implant must be fixed to the inner retina. Heat generation using high-density electrode arrays and neural stimulating circuitry located within the eye is also a potential safety issue for retinal prostheses. International standards require that no outer surface of an active implant be 2 °C above body temperature (ISO 14708-1). Power dissipation levels <19 mW/mm^2 at the retinal surface are considered to operate within this safe range [24].

Epiretinal

Placing an electrode array on the inner surface of the retina ensures the electrodes stimulate the output of the retina – the axons of the RGCs. Such proximity to RGCs results in low thresholds for neural activation, minimizing the physical size required of individual electrodes, and theoretically maximizing the resolution and acuity of prosthetic vision over electrodes positioned in other retinal locations. Surgically, the electrode array is fixed to the inner retinal surface using one or two retinal tacks. The devices make use of platinum, iridium oxide, or conductive diamond electrodes coupled to stimulation electronics within a hermetic capsule that is contained entirely within the vitreous chamber. The implant housings are fixed in place of the lens or attached extraocularly to the sclera. The capsule is coupled to a receiving coil that is inductively linked to an external coil fitted to a pair of glasses that also houses the camera. There are several research groups and companies developing epiretinal devices. [18,25–27]. Second Sight Medical Products recently received regulatory approval in both Europe and the USA to treat late-stage RP with

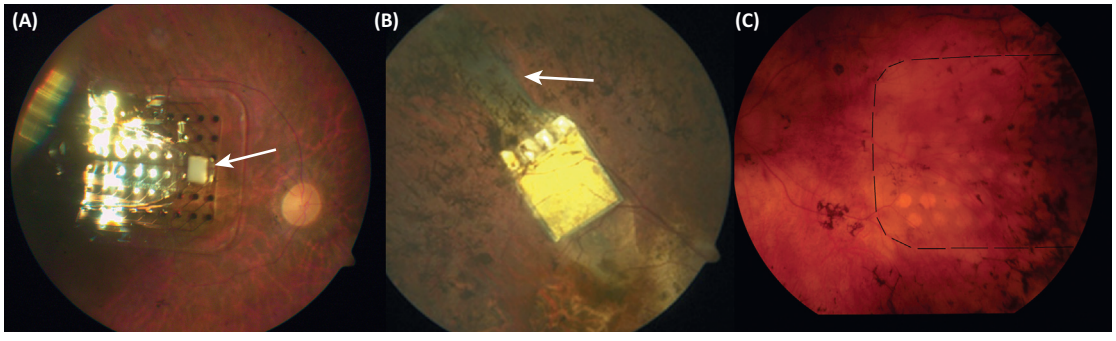

Figure 4. Fundus images of three retinal prostheses in clinical use in late stage RP patients. **(A)** Epiretinal Argus II electrode array containing 60 platinum electrodes fixed to the inner retina via a retinal tack (arrow) (Image courtesy of Second Sight Medical Products Inc.). **(B)** Subretinal Alpha IMS retinal implant containing 1500 photodiode electrodes on a 3 × 3 mm matrix. A leadwire (arrow) delivers additional power to the electrodes to ensure that the stimulus levels are sufficient to excite retinal tissue. (Image courtesy of the Center for Ophthalmology, University of Tübingen, Germany). **(C)** Bionic Vision Australia's prototype suprachoroidal electrode array developed by the Bionics Institute containing 24 platinum electrodes. The edge of the array is illustrated by the broken line (Image courtesy of the Centre for Eye Research Australia).

Box 2. Building a neural prosthesis

Apart from the photodiode technology being developed by some visual prosthesis groups, the majority of modern commercial neural prostheses consist of several essential components including an electrode array for stimulation and/or recording from neural tissue; a leadwire assembly connecting the electrode array to implanted stimulation and/or recording circuitry; a power source; and a transcutaneous wireless link to an external controller that provides data defining the stimulation parameters to be delivered to the electrode array (e.g., a visual processor, see Figure 3 in main text).

A stimulating/recording electrode array must be developed for each application because its design features will be dependent on factors including the underlying anatomy and pathophysiology of the target site and surgical access. An electrode array designed for long-term use in humans must ensure: minimal insertion trauma; biocompatibility; that the electrical stimulus is localized to discrete groups of target neurons; mechanical and electrical stability; that it is designed to minimize the risks of infection (including smooth surfaces, elimination of cavities, and careful selection of bio materials); that the stimulus regime is not damaging in the long-term; and that it is designed for safe removal and replacement [68].

The implanted electronics that make up the active components of a visual prosthesis must be protected from the corrosive biological environment by hermetically sealing them from body fluids. The long-term reliability of any prosthesis is associated with the efficacy of its hermetic seal. The gold standard sealing technique is to encase the electronics within a titanium capsule that is sealed using a laser welder [71,72]. This hermetic sealing technique can be problematic for retinal prostheses where size restrictions are an important design constraint. The use of polymers for hermetic encapsulation is an attractive alternative because many have excellent biocompatibility, ease of fabrication, flexibility, electromagnetic transmission, and cost compared with titanium. However, there remain technical challenges in obtaining long-term effective hermetic bonding using polymers [71] and this remains an important area of research.

In order for the hermetically sealed electronics to deliver electrical pulses to the electrode array and/or receive biological signals from the neural interface, the implant must also incorporate a feed-through assembly that allows the sealed electronics to make electrical connection to the electrodes without compromising the seal [72]. There are significant design pressures on manufactures to develop devices with a large electrode count. This places considerable pressure on the development of reliable high density feed-through assemblies and is an important limiting factor in developing high-density electrode arrays.

Active implants such as visual prostheses require a power source to operate. There are two alternative power sources that are in common use. Many devices receive their power via a battery located within the hermetically sealed capsule (e.g., a deep brain stimulator). This approach presents surgical restrictions on the implant site as a result of its size. For devices such as retinal prostheses, power is typically provided via an external source whenever the implant is in use. An inductive link comprised of coils on each side of the skin coupled via a radiofrequency carrier signal (see Figure 3B in main text).

their 60 electrode Argus II device (Figure 4A). Two technical challenges associated with the epiretinal approach are related to the significant constraints on device size with this surgical approach, and the fixation and long-term mechanical stability of the electrode array on the retinal surface using penetrating retinal tacks. Additional safety issues include the potential for mechanical damage to the retina and an increased risk of inflammation with devices that run leadwires from the vitreous through the sclera.

Subretinal

Significant neural processing occurs within the outer and middle layers of the retina peripheral to the RGCs; epiretinal prostheses cannot take advantage of this processing. Subretinal electrode arrays are designed to be positioned at the level of the outer retina where, in a healthy eye, photoreceptors would be located [16,17,22,28,29] (Figure 2I). Although this is a logical choice for an implant whose function is to replace lost photoreceptors, it comes with its own challenges. The surgical approach is technically difficult and the electrode array and associated electronics must be extremely thin (<400 μm) to minimize retinal damage or detachment. In addition, there is the potential for a subretinal electrode array to impede blood supply from the choroid to the surviving retina. Finally, although at least some of the impetus for the development of a subretinal neural prosthesis is to take advantage of the normal processing that occurs in the outer and middle retina [22], this becomes a moot point after the remodeling that occurs following photoreceptor loss [3]. Several groups are developing this approach, with the Alpha-IMS manufactured by Retina Implant AG recently gaining European regulatory approval for the treatment of late stage RP [16,22] (Figure 4B). There are technical challenges with manufacturing a long-term hermetic encapsulation with the thin profile of these implants. Some have chosen photodiodes as the sensing elements [16,17]; whereas another group has developed an array of 256 electrodes driven by an implantable stimulator containing 256 current drivers [30]. Many of the safety concerns associated with epiretinal implants are also an issue for epiretinal devices.

Suprachoroidal

Although electrodes located in a tissue pocket between the choroid and sclera (the so-called suprachoroidal position) are some distance from their target neurons in the inner retina, this approach has been adopted by several groups. This placement offers a safe and simple surgical approach and a mechanically stable location [31]. Clinical complications are minimized with the suprachoroidal approach, because multiple layers of the eye do not have to be breached in order to position the electrode array [19,32–36]. A major limitation of this approach is an increase in stimulus thresholds as a result of the greater distance between the electrode array and the retina when compared with epi- and subretinal devices. Experimental studies have demonstrated that the retina can be effectively stimulated at safe levels using this electrode position [32,37]. Moreover the choroid – which separates the electrode array from the retina in this approach – undergoes significant shrinkage in RP [38]. Recently, two groups have conducted successful clinical trials using this approach; both demonstrated that long-term severely blind patients can perceive discriminable percepts in response to electrical stimulation within safe limits of charge injection [19,39] (Figure 4C).

Visual prostheses based on stimulation of the central visual pathway

Stimulation of the visual pathway at sites central to the retina has the potential to provide prosthetic vision for a

wider range of pathologies, including those that result in damage to the optic nerve. Although clinical trials of cortical-based devices were undertaken early in the development of visual prostheses [7,40], there is currently no central visual prosthesis undergoing a clinical trial.

Optic nerve

Using a spiral cuff electrode, the optic nerve has been targeted as an implant site for a clinical trial in two blind patients, which resulted in the generation of usable phosphenes [41] and the ability to record electrically evoked potentials [42]. More recently, there has been interest in targeting the optic nerve using an array of penetrating electrodes [43]. Highly focal excitation would be necessary in order to provide reliable retinotopic cues. Given this technological challenge, it is unclear how this approach would surpass the advantages of retinal based implants.

Lateral geniculate nucleus

One group has proposed placing stimulating electrodes in the LGN of the thalamus [44]. The LGN is a well characterized retinotopic structure within the central visual pathway. This study showed that it was possible to elicit neural responses in the visual cortex from thalamic microstimulation, providing proof of concept for this stimulation site. Although there have been no clinical trials to date, the surgical approach would be similar to that used in deep brain stimulation to treat movement disorders associated with Parkinson's disease [45].

Visual cortex

Early clinical studies provided strong evidence that visual sensations could be readily evoked through stimulation of the cortical surface [7,40] or via penetrating microelectrodes [46]. This research has recently been advanced by taking advantage of improved electrode technologies [20,47–49]. Most groups propose placing individual modules or tiles, each containing multiple stimulating electrodes, along with associated stimulating circuitry within a hermetically sealed chamber. Multiple tiles can be inserted into the visual cortex to provide many individually addressable electrodes.

The primary visual cortex is thought to be an ideal location for a visual prosthesis for several reasons; it is well organized retinotopically, it has adequate space for multiple implanted components, and is known to have a large area devoted to central vision. However, it is unclear whether a prosthesis that bypasses all visual processing occurring within the retina and LGN will contain sufficient information for higher-order brain centers to recognize accurately percepts generated from electrical stimulation. As an example, there is a rich descending corticothalamic modulation feedback loop that occurs in normal vision processing (the LGN receives the majority of its input from the visual cortex [44]); a cortical based prosthesis would bypass this processing stage. In addition, although the plastic brain plays an important role in improved clinical outcomes with sensory prostheses [50], it remains unclear whether direct stimulation of the visual cortex will recruit the same level of plastic reorganization as stimulation arising from the retina. In this context, it should be noted that stimulation delivered to the RGCs via a retinal prosthesis is already several neural processing stages beyond the photoreceptors, and this may also result in a level of perceptual complexity.

Perceptual effects of visual prostheses

Phosphenes are visual sensations produced by stimuli other than light, including mechanical, magnetic, or electrical stimulation of the retina or brain [4]. The phosphenes evoked by electrical stimuli have typically been described in the literature as flashes of light, often amorphous but sometimes with a clear well-defined shape. Studies have also reported complex phosphenes which can be darker than the patient's naturally perceived background, sometimes with both bright and dark areas in the same phosphene [27]. The brightness, shape, size, duration and location of a phosphene can be manipulated by varying the location and configuration of electrodes being stimulated and the electrical waveforms used [51–53].

Importantly, when stimulating multiple electrodes on an array, phosphenes can interact with one another to change the perceived image [54,55]. Despite the complexities of phosphenes evoked through electrical stimulation, they form the basic building blocks of prosthetic vision. For example, psychophysical studies have demonstrated that by stimulating appropriate electrodes on an array, it is possible to create the perception of retinotopically organized patterns and simple shapes such as lines of different orientations and geometric objects (e.g., triangle or square), regardless of whether the device is placed in the epiretinal [18], subretinal [53], or suprachoroidal [39,19] space.

A camera and an image processing algorithm are required to provide a visual representation of the subjects' surroundings. Subjects implanted with the Argus II epiretinal system and using an external camera to source their visual field can perform object localization, motion discrimination, and discrimination of oriented gratings with a best visual acuity to date of 20/1260 [18,56]. If a 16X zoom camera mode is enabled, then acuity measures increase to 20/200, but the field of view is correspondingly reduced from 20° down to a few degrees, making scanning of an image more time consuming [57]. The Alpha-IMS subretinal device with 25 times more electrodes than the Argus II has demonstrated best visual acuity of 20/546 [22], allowing patients implanted with this device to be able to detect and localize light and motion, identify, localize and discriminate high contrast objects, and read large font letters [22]. Phosphenes generated by stimulation of the visual cortex are sometimes described as more complex than those induced by retinal implants, although well-defined, localized and resolvable phosphenes are possible [7], and there are reports of blind subjects reading by incorporation of a camera with the device [58].

Head/eye movement issues

An important technical issue associated with camera-based visual prostheses is related to the change in the position of a phosphene within the subject's visual field with eye movement, but not with passive movement of the head while maintaining a fixed eye gaze [7]. As already noted, photovoltaic devices are not burdened with this

issue because the technology enables a natural refreshed image to be sampled by the device each time the eye makes a microsaccade [16,22]. This is a major advantage of photodiode-based devices because it eliminates the need to incorporate sophisticated eye tracking techniques to correct the image sampled by a camera for eye movement. However, the use of a camera enables the application of vision processing algorithms to pre-process the image, before applying stimulation to the electrodes, a feature that will become more powerful as implant groups gain clinical experience.

Role of plasticity and training

The fundamental findings by Hubel and Wiesel and their colleagues the 1960s and 1970s highlighted the importance of visual experience during development on the normal establishment of retinotopic maps and ocular dominance column plasticity in the visual cortex. Importantly, in pathologies where the onset of blindness occurs after periods of normal development, as is the case in RP and AMD, the primary visual cortex does not exhibit extensive retinotopic remapping following prolonged periods of sensory deprivation [59,60]. Consistent with these observations, clinical data demonstrate that useful retinotopically organized visual cues can be evoked via a visual prosthesis decades after the onset of adult onset blindness [39].

Visual experience obtained through the use of a device is expected to result in improved performance as a result of plasticity within the central visual pathway. Strong support for the positive role of learning and plasticity comes from 30 years of experience of cochlear implant use in profoundly deaf adults. Studies examining factors that affect clinical performance consistently demonstrate that the duration of cochlear implant experience has a significant positive effect on speech understanding [61,62]. These clinical results are supported by animal studies that show electrophysiological evidence of cortical reorganization in deafened animals reared using cochlear implants [63], although the extent of plastic change in response to activation of a visual prosthesis in a long-term blind subject must be tempered given the relatively simple retino-geniculate-visual cortex pathway when compared to the complexity of the multiple pathways that occur between the eighth nerve and the auditory cortex.

Careful device fitting and ongoing training are important for the clinical success of these devices. In order to maximize the benefits of plasticity, training using everyday tasks, not just object recognition, is required [64]. Device fitting can be a time-consuming procedure that will require ongoing monitoring. The threshold and dynamic range necessary to evoke a useable phosphene must be determined for each electrode on the array. This task becomes problematic with high-density electrode arrays. Finally, the successful clinical application of visual prostheses must be a productive collaboration between the patients, their support family, researchers, clinicians, and low vision rehabilitation specialists.

Future directions and concluding remarks

In the 1970s, cochlear implants were branded as 'an aid to lip reading'. Over the subsequent 30 years they significantly exceeded these expectations and expanded the patient base from profoundly deaf adults to now include both severely deaf adults and children. We can expect similar outcomes for visual prostheses over the following decades as both the technology and clinical experience in managing patients using these devices become more sophisticated.

In the shorter term, there remain considerable technical challenges that must be addressed before visual prostheses receive widespread clinical acceptance. The existing research and commercial device development cover a very broad range of options for each of the outstanding questions listed in Box 3.

The possible electrode locations include the epiretinal, subretinal, suprachoroidal, and visual cortex, each with its own strengths and weaknesses. Safety, stability, and effectiveness are likely to be different in each of these electrode locations and there are insufficient long-term data in humans to determine the likely range of performance for each location. In the future, we may see combinations of electrodes in different sites, such as a small high-resolution array with many electrodes in an epiretinal position close to the fovea in combination with an array of larger electrodes in the suprachoroidal location to provide peripheral vision across a much wider field of view.

There is presently a trend towards larger numbers of electrodes, but there is no clear evidence that more electrodes correspond to better performance on visual tasks. Performance will also depend on the proportion of electrodes that produce visual percepts, the spatial separation and size of electrodes, and the size of the perceptual space that corresponds to the whole array. For example, legal blindness is defined in the USA as an acuity of 20/200 and an angular field of view greater than 20°. A person who can correctly identify letters on the lowest line of the Snellen chart (i.e., a person with 20/20 vision) is able to discern individual lines that are separated by a visual angle of one arc minute. It would require 1200 electrodes over a 20° angle to achieve a resolution of one arc minute. This corresponds to 1.44 million electrodes within a 7-mm

Box 3. Outstanding questions

The following are key questions that remain to be answered in order to advance the field of visual prostheses.

- What is the most suitable location for the electrode array?
- What is the optimal number of electrodes for a visual prosthesis?
- What is the optimum field of view for a visual prosthesis?
- What is the most suitable method of powering a visual prosthesis?
- How will simultaneous stimulation of electrodes affect the visual percepts?
- Is the use of eye tracking technology necessary for visual prosthesis users?
- How should visual acuity be measured for a visual prosthesis?
- How should clinical performance be measured with a visual prosthesis?
- How best do we engage the plastic brain using visual prostheses?
- Can we selectively stimulate retinal neurons in order to take maximum advantage of the natural vision processing?
- Will electrical stimulation of the retina halt or slow down the retinal remodeling that occurs following photoreceptor loss?
- Is it possible to combine electrical stimulation of the retina with therapeutic drugs administration (e.g., neurotrophins) to slow/stop the retinal remodeling?
- Is it possible to provide color vision via a visual prosthesis?

square area of the retina. If an acuity of 20/200 is acceptable, then 15 000 electrodes within a 7-mm^2 area would suffice. These electrodes may be too small to produce reliable phosphenes within the safe limits of electrical charge injection, and the phosphenes may overlap too much to provide the required acuity. The optimal number and spacing of electrodes in the visual cortex is likely to be different as the cortical retinotopic map of the macula is expanded relative to the macula itself. As more is learned about the psychophysics of artificial vision, a clearer notion of the optimum number of electrodes will emerge from the data.

The size constraints, energy dissipation capacity, and mobility of the eye are likely to lead to retinal prostheses with a power and wireless data module mounted on the skull, connected via a small number of very flexible wires to a stimulator situated in or on the eyeball. Stimulation of a large number of electrodes at reasonably high pulse rates is also likely to require stimulation of several electrodes in parallel rather than one electrode at a time. Understanding how to control the percepts produced by simultaneous stimulation and ensuring that the total stimulation is at a safe level are nontrivial problems for the future.

Stimulation of electrodes at fixed positions on the retina produces phosphenes that appear to move through space as the eye moves relative to the head. In devices with an external camera, eye tracking technology will be used to account for eye movements, also resulting in a more natural scanning of objects using the eyes, instead of using head movements to direct the camera. The devices that use light-sensitive devices on the retina avoid the need for eye tracking, and it is not yet clear whether eye tracking will be required for cortical stimulation devices. Sophisticated image processing techniques such as feature extraction, edge detection, depth mapping, face and letter recognition, may also be useful for performing particular tasks. Access to different zoom factors in the external vision processor may also be useful for tasks such as reading. This would be analogous to wearing reading glasses, for example.

Another very challenging issue may be the fitting and training of patients using devices with a large number of electrodes. The fitting and optimization methods that are currently used with small numbers of electrodes, such as measurement of thresholds and dynamic ranges for individual electrodes, will most likely need to be replaced with procedures for adjusting more global parameters for groups of electrodes, or for interpolating values between a sparse set of electrodes that are measured individually. The ultimate goal of visual prostheses is to provide improvement in the quality of life of blind patients by improving their performance on real-world tasks. The acuity measures that have been proposed for evaluation of prostheses will need to be augmented by measures of performance that are sufficiently difficult to allow significant improvement, and sufficiently useful to indicate an improved quality of life. The collection of these data in a way that allows comparative performance measures of various devices will require alignment of regulators, researchers, and commercial interests.

Finally, stimulation of fibers of passage is a potential issue for retinal implants, particularly for the epiretinal approach, and can also be an issue with the LGN and cortical approaches [65]. A clinical study using epiretinal stimulation where the electrode array is lying adjacent to the RGC axons, showed that patients reported arc-like or banana-like phosphenes, and these shapes were consistent with the modeled trajectory of the RGC axons travelling towards the optic nerve in each patient [66].

Despite these challenges, visual prostheses are destined to enable major advances in the clinical management of blind patients. Ultimately these devices will provide a level of prosthetic vision that will allow users to read large font print and recognize faces.

Acknowledgments

We thank our colleagues in Bionic Vision Australia (BVA) for their contributions to the BVA research effort. Fundus images were generously provided by Drs Lauren Ayton, Peter Dimitrov, and Penny Allen from CERA (suprachoroidal electrode array), Brian Mech from Second Sight Medical Products Inc. (the Argus II device), and Dr Katarina Stingl and Prof Eberhart Zrenner from the Center for Ophthalmology, University of Tuebingen, Germany (Alpha IMS subretinal implant). Dr Lauren Ayton, Dr Paige Shaklee, and two anonymous reviewers gave helpful comments on an earlier version of this manuscript. The Bionics Institute acknowledges the support it receives from the Victorian Government through its Operational Infrastructure Support Program. This research was supported by the Australian Research Council (ARC) through its Special Research Initiative (SRI) in Bionic Vision Science and Technology grant to Bionic Vision Australia. The Bionics Institute would also like to acknowledge support from the Potter Foundation and the Bertalli Family Trust.

References

1 Cavuoto, J. *et al.* (2011) *The Market for Neurotechnology: 2012–2016*. pp. 1–345, Neurotech Reports
2 World Health Organization (2012) *Visual Impairment and Blindness*. World Health Organization
3 Jones, B.W. *et al.* (2012) Retinal remodeling. *Jpn. J. Ophthalmol.* 56, 289–306
4 Marg, E. (1991) Magnetostimulation of vision: direct noninvasive stimulation of the retina and the visual brain. *Optom. Vis. Sci.* 68, 427–440
5 Penfield, W. and Perot, P. (1963) The brain's record of auditory and visual experience. *Brain* 86, 595–696
6 Brindley, G.S. (1970) Sensations produced by electrical stimulation of the occipital poles of the cerebral hemispheres, and their use in constructing visual prostheses. *Ann. R. Coll. Surg. Engl.* 47, 106–108
7 Brindley, G.S. and Lewin, W.S. (1968) The sensations produced by electrical stimulation of the visual cortex. *J. Physiol.* 196, 479–493
8 Tassicker, G.E. (1956) Preliminary report on a retinal stimulator. *Br. J. Physiol. Opt.* 13, 102–105
9 Clark, G.M. (2003) *Cochlear Implants: Fundamentals and Applications*. Springer-Verlag
10 Cohen, E.D. (2007) Safety and effectiveness considerations for clinical studies of visual prosthetic devices. *J. Neural Eng.* 4, S124–S129
11 Batterbury, M. and Bowling, B. (2005) *Ophthalmology: An Illustrated Color Text*. Elservier Churchill Livingstone
12 Finger, R.P. *et al.* (2011) Incidence of blindness and severe visual impairment in Germany: projections for 2030. *Invest. Ophthalmol. Vis. Sci.* 52, 4381–4389
13 Chua, J. *et al.* (2009) Functional remodeling of glutamate receptors by inner retinal neurons occurs from an early stage of retinal degeneration. *J. Comp. Neurol.* 514, 473–491
14 Weiland, J.D. *et al.* (2011) Retinal prostheses: current clinical results and future needs. *Ophthalmology* 118, 2227–2237
15 Pascolini, D. and Mariotti, S.P. (2012) Global estimates of visual impairment: 2010. *Br. J. Ophthalmol.* 96, 614–618

16 Zrenner, E. *et al.* (2011) Subretinal electronic chips allow blind patients to read letters and combine them to words. *Proc. R. Soc. B* 278, 1489–1497
17 Mathieson, K. *et al.* (2012) Photovoltaic retinal prosthesis with high pixel density. *Nat. Photonics* 6, 391–397
18 Humayun, M.S. *et al.* (2012) Interim results from the international trial of Second Sight's visual prosthesis. *Ophthalmology* 119, 779–788
19 Fujikado, T. *et al.* (2011) Testing of semichronically implanted retinal prosthesis by suprachoroidal-transretinal stimulation in patients with retinitis pigmentosa. *Invest. Ophthalmol. Vis. Sci.* 52, 4726–4733
20 Normann, R.A. *et al.* (2009) Toward the development of a cortically based visual neuroprosthesis. *J. Neural Eng.* 6, 035001
21 Fernandes, R.A. *et al.* (2012) Artificial vision through neuronal stimulation. *Neurosci. Lett.* 519, 122–128
22 Stingl, K. *et al.* (2013) Artificial vision with wirelessly powered subretinal electronic implant alpha-IMS. *Proc. Biol. Sci.* 280, 20130077
23 Yarbus, A.L. (1967) *Eye Movements and Vision*. Plenum Press
24 Opie, N.L. *et al.* (2012) Retinal prosthesis safety: alterations in microglia morphology due to thermal damage and retinal implant contact. *Invest. Ophthalmol. Vis. Sci.* 53, 7802–7812
25 Hadjinicolaou, A.E. *et al.* (2012) Electrical stimulation of retinal ganglion cells with diamond and the development of an all diamond retinal prosthesis. *Biomaterials* 33, 5812–5820
26 Klauke, S. *et al.* (2011) Stimulation with a wireless intraocular epiretinal implant elicits visual percepts in blind human. *Invest. Ophthalmol. Vis. Sci.* 52, 449–455
27 Keseru, M. *et al.* (2012) Acute electrical stimulation of the human retina with an epiretinal electrode array. *Acta Ophthalmol.* 90, e1–e8
28 Rizzo, J.F., III (2011) Update on retinal prosthetic research: the Boston Retinal Implant Project. *J. Neuroophthalmol.* 31, 160–168
29 Stingl, K. *et al.* (2013) Safety and efficacy of subretinal visual implants in humans: methodological aspects. *Clin. Exp. Optom.* 96, 4–13
30 Rizzo, J.F., III *et al.* (2011) Development of the Boston retinal prosthesis. *Conf. Proc. IEEE Eng. Med. Biol. Soc.* 2011, 3135–3138
31 Villalobos, J. *et al.* (2013) A wide-field suprachoroidal retinal prosthesis is stable and well tolerated following chronic implantation. *Invest. Ophthalmol. Vis. Sci.* 54, 3751–3762
32 Shivdasani, M.N. *et al.* (2010) Evaluation of stimulus parameters and electrode geometry for an effective suprachoroidal retinal prosthesis. *J. Neural Eng.* 7, 036008
33 Morimoto, T. *et al.* (2011) Chronic implantation of newly developed suprachoroidal-transretinal stimulation prosthesis in dogs. *Invest. Ophthalmol. Vis. Sci.* 52, 6785–6792
34 Villalobos, J. *et al.* (2012) Development of a surgical approach for a wide-view suprachoroidal retinal prosthesis: evaluation of implantation trauma. *Graefes Arch. Clin. Exp. Ophthalmol.* 250, 399–407
35 Zhou, J.A. *et al.* (2008) A suprachoroidal electrical retinal stimulator design for long-term animal experiments and in vivo assessment of its feasibility and biocompatibility in rabbits. *J. Biomed. Biotechnol.* 2008, 547428
36 Suaning, G.J. *et al.* (2010) Discrete cortical responses from multi-site supra-choroidal electrical stimulation in the feline retina. *Conf. Proc. IEEE Eng. Med. Biol. Soc.* 2010, 5879–5882
37 Cicione, R. *et al.* (2012) Visual cortex responses to suprachoroidal electrical stimulation of the retina: effects of electrode return configuration. *J. Neural Eng.* 9, 036009
38 Ayton, L.N. *et al.* (2012) Choroidal thickness profiles in retinitis pigmentosa. *Clin. Exp. Ophthalmol.* 41, 396–403
39 Blamey, P.H. *et al.* (2013) Psychophysics of a suprachoroidal retinal prosthesis. In *ARVO 2013 Annual Meeting*. pp. 1044
40 Dobelle, W.H. *et al.* (1974) Artifical vision for the blind: electrical stimulation of visual cortex offers hope for a functional prosthesis. *Science* 183, 440–444
41 Veraart, C. *et al.* (2004) Vision rehabilitation with the optic nerve visual prosthesis. *Conf. Proc. IEEE Eng. Med. Biol. Soc.* 6, 4163–4164
42 Brelen, M.E. *et al.* (2010) Measurement of evoked potentials after electrical stimulation of the human optic nerve. *Invest. Ophthalmol. Vis. Sci.* 51, 5351–5355
43 Sun, J. *et al.* (2011) Spatiotemporal properties of multipeaked electrically evoked potentials elicited by penetrative optic nerve stimulation in rabbits. *Invest. Ophthalmol. Vis. Sci.* 52, 146–154
44 Panetsos, F. *et al.* (2011) Consistent phosphenes generated by electrical microstimulation of the visual thalamus. An experimental approach for thalamic visual neuroprostheses. *Front. Neurosci.* 5, 1–12
45 Lozano, A.M. and Lipsman, N. (2013) Probing and regulating dysfunctional circuits using deep brain stimulation. *Neuron* 77, 406–424
46 Schmidt, E.M. *et al.* (1996) Feasibility of a visual prosthesis for the blind based on intracortical microstimulation of the visual cortex. *Brain* 119, 507–522
47 Schiller, P.H. *et al.* (2011) New methods devised specify the size and color of the spots monkeys see when striate cortex (area V1) is electrically stimulated. *Proc. Natl. Acad. Sci. U.S.A.* 108, 17809–17814
48 Troyk, P. *et al.* (2003) A model for intracortical visual prosthesis research. *Artif. Organs* 27, 1005–1015
49 Brunton, E. *et al.* (2012) A comparison of microelectrodes for a visual cortical prosthesis using finite element analysis. *Front. Neuroeng.* 5, 23
50 Fallon, J.B. *et al.* (2008) Cochlear implants and brain plasticity. *Hear. Res.* 238, 110–117
51 Perez Fornos, A. *et al.* (2012) Temporal properties of visual perception on electrical stimulation of the retina. *Invest. Ophthalmol. Vis. Sci.* 53, 2720–2731
52 Nanduri, D. *et al.* (2012) Frequency and amplitude modulation have different effects on the percepts elicited by retinal stimulation. *Invest. Ophthalmol. Vis. Sci.* 53, 205–214
53 Wilke, R. *et al.* (2011) Spatial resolution and perception of patterns mediated by a subretinal 16-electrode array in patients blinded by hereditary retinal dystrophies. *Invest. Ophthalmol. Vis. Sci.* 52, 5995–6003
54 Horsager, A. *et al.* (2010) Spatiotemporal interactions in retinal prosthesis subjects. *Invest. Ophthalmol. Vis. Sci.* 51, 1223–1233
55 Horsager, A. *et al.* (2011) Temporal interactions during paired-electrode stimulation in two retinal prosthesis subjects. *Invest. Ophthalmol. Vis. Sci.* 52, 549–557
56 Dorn, J.D. *et al.* (2013) The detection of motion by blind subjects with the Epiretinal 60-Electrode (Argus II) retinal prosthesis. *JAMA Ophthalmol.* 131, 183–189
57 Shael, J.A. *et al.* (2013) Acuboost: enhancing the maximum acuity of the Argus II Retinal Prosthesis System. In *ARVO 2013 Annual Meeting*. pp. 1389
58 Dobelle, W.H. *et al.* (1976) "Braille" reading by a blind volunteer by visual cortex stimulation. *Nature* 259, 111–112
59 Xie, J. *et al.* (2012) Preservation of retinotopic map in retinal degeneration. *Exp. Eye Res.* 98, 88–96
60 Baseler, H.A. *et al.* (2011) Large-scale remapping of visual cortex is absent in adult humans with macular degeneration. *Nat. Neurosci.* 14, 649–655
61 Blamey, P. *et al.* (2013) Factors affecting auditory performance of postlinguistically deaf adults using cochlear implants: an update with 2251 patients. *Audiol. Neurootol.* 18, 36–47
62 Lazard, D.S. *et al.* (2012) Pre-, per- and postoperative factors affecting performance of postlinguistically deaf adults using cochlear implants: a new conceptual model over time. *PLoS ONE* 7, e48739
63 Fallon, J.B. *et al.* (2009) Cochlear implant use following neonatal deafness influences the cochleotopic organization of the primary auditory cortex in cats. *J. Comp. Neurol.* 512, 101–114
64 Dagnelie, G. (2012) Retinal implants: emergence of a multidisciplinary field. *Curr. Opin. Neurol.* 25, 67–75
65 Histed, M.H. *et al.* (2009) Direct activation of sparse, distributed populations of cortical neurons by electrical microstimulation. *Neuron* 63, 508–522
66 Nanduri, D. *et al.* (2011) Percept properties of single electrode stimulation in retinal prosthesis subjects. *ARVO Meet. Abstr.* 52, 442
67 Cogan, S.F. (2008) Neural stimulation and recording electrodes. *Annu. Rev. Biomed. Eng.* 10, 275–309
68 Shepherd, R.K. *et al.* (in press) Medical bionics. In *Comprehensive Biomedical Physics* (Zhou, S-A. and Zhou, L., eds), Elsevier
69 Huang, C.Q. *et al.* (2001) Stimulus induced pH changes in cochlear implants: an in vitro and in vivo study. *Ann. Biomed. Eng.* 29, 791–802
70 Hubel, D.H. (1988) *Eye, Brain and Vision*. Scientific Amercian Library
71 Amanat, N. *et al.* (2010) Welding methods for joining thermoplastic polymers for the hermetic enclosure of medical devices. *Med. Eng. Phys.* 32, 690–699
72 Guenther, T. *et al.* (2012) Bionic vision: system architectures: a review. *Expert Rev. Med. Devices* 9, 33–48

Progress in Retinal and Eye Research 50 (2016) 89–107

Contents lists available at ScienceDirect

Progress in Retinal and Eye Research

journal homepage: www.elsevier.com/locate/prer

The Argus® II Retinal Prosthesis System

Yvonne Hsu-Lin Luo [a, b, 1], Lyndon da Cruz [a, b, *, 1]

[a] NIHR Biomedical Research Centre, Moorfields Eye Hospital NHS Foundation Trust, 162 City Road, London EC1V 2PD, UK
[b] Institute of Ophthalmology, University College London, 11–43 Bath Street, London EC1V 9EL, UK

ARTICLE INFO

Article history:
Received 2 May 2015
Received in revised form
25 August 2015
Accepted 17 September 2015
Available online 25 September 2015

Keywords:
Retinal prosthesis
Visual prosthesis
Artificial retina
Retinitis pigmentosa
Retinal dystrophy

ABSTRACT

The Argus® II Retinal Prosthesis System (Second Sight Medical Products) is the first prosthetic vision device to obtain regulatory approval in both Europe and the USA. As such it has entered the commercial market as a treatment for patients with profound vision loss from end-stage outer retinal disease, predominantly retinitis pigmentosa. To date, over 100 devices have been implanted worldwide, representing the largest group of patients currently treated with visual prostheses.

The system works by direct stimulation of the relatively preserved inner retina via epiretinal microelectrodes, thereby replacing the function of the degenerated photoreceptors. Visual information from a glasses-mounted video camera is converted to a pixelated image by an external processor, before being transmitted to the microelectrode array at the macula. Elicited retinal responses are then relayed via the normal optic nerve to the cortex for interpretation.

We reviewed the animal and human studies that led to the development of the Argus® II device. A sufficiently robust safety profile was demonstrated in the phase I/II clinical trial of 30 patients. Improvement of function in terms of orientation and mobility, target localisation, shape and object recognition, and reading of letters and short unrehearsed words have also been shown. There remains a wide variability in the functional outcomes amongst the patients and the factors contributing to these performance differences are still unclear. Future developments in terms of both software and hardware aimed at improving visual function have been proposed. Further experience in clinical outcomes is being acquired due to increasing implantation.

Contents

* Corresponding author. NIHR Biomedical Research Centre, Moorfields Eye Hospital NHS Foundation Trust, 162 City Road, London EC1V 2PD, UK.
E-mail address: lyndon.dacruz@moorfields.nhs.uk (Y.H.-L. Luo).

[1] Percentage of work contributed by each author in the production of the manuscript is as follows: Yvonne Hsu-Lin Luo: 50% (wrote the initial draft); Lyndon da Cruz: 50% (revised the manuscript).

http://dx.doi.org/10.1016/j.preteyeres.2015.09.003
1350-9462/

1. Introduction

The Argus® II Retinal Prosthesis System (Second Sight Medical Products Inc., Sylmar, California, USA) is a commercially available device that aims to restore a basic level of vision to patients with profound vision loss from outer retinal dystrophies. The device elicits visual perceptions by means of electrical stimulation of the residual diseased retina. It was the first device to go into widespread clinical use with regulatory permission in multiple countries.

The discovery by Foerster (1929) that it is possible to elicit transient and reproducible visual percepts (known as phosphenes) upon direct electrical stimulation of the visual pathway took place almost a century ago. Since then extensive research efforts have been focused on understanding and controlling such phosphene responses. The ability to reliably elicit and modify phosphenes in a controllable way by manipulating the stimulating parameters, such that they reflect the surrounding visual scenes, has been the common goal of all electrical stimulation-based visual prostheses.

The Argus® II has become the most widely used and most successful retinal prosthesis currently available in terms of regulatory approval. Since obtaining the CE mark in 2011 and FDA approval as a humanitarian device in 2013, commercial implantation has begun in many countries worldwide. Use of the device has been predominantly for patients with profound vision loss from retinitis pigmentosa and to a lesser extent, choroideremia as well as for a planned cohort with extensive geographic atrophy from age-related macular degeneration (AMD) (ClinicalTrials.gov Identifier: NCT02227498). To date, over 100 devices have been implanted and the number is likely to increase. With its integration into clinical practice, it seems timely to review the pioneering work leading up to the regulatory approval of this product, as well as the subsequent clinical outcomes with the use of this device. In particular, we will evaluate the practical implications of using this device for the patients in real-life settings based on published literature.

The issues of electrical stimulation safety, choice of stimulating wave forms, biocompatibility and hermeticity in the development of the device will not be discussed in this review as these topics have already been covered comprehensively elsewhere (Humayun, 2001; Margalit et al., 2002). Stronks and Dagnelie (2014) gave a didactic account of how different stimulating parameters such as amplitude and frequency affects the phosphene brightness and size, while Ahuja et al. (2013) discussed the factors affecting electrode thresholds in detail. These topics will therefore also not be discussed in any detail.

1.1. Retina: the site of choice for electrical stimulation

In 1952, Hodgkin and Huxley first described the electrical nature of signal propagation in all nervous systems by the means of action potentials (Hodgkin and Huxley, 1952). During electrical stimulation of any neural tissue with an external electrode, the injection of electrical charges creates a localised depolarisation and subsequent initiation of action potentials. As such, electrical stimulation at any point along the visual pathway could elicit visual phosphenes. Commencing with cortical stimulation by Brindley et al., in 1968 (Brindley and Lewin, 1968a) and later by others (Dobelle, 2000; Normann et al., 2009), electrical stimulation has also been described at the levels of lateral geniculate nucleus (Panetsos et al., 2009, 2011), the optic nerve (Sakaguchi et al., 2009, 2012; Wang et al., 2011) and the retina.

Of all of the anatomical sites listed above, retinal stimulation (e.g. the epiretinal implant Argus® II and the subretinal implant alpha-IMS) has been the most successful. There are many reasons for this and they can be best summarised as: a) greater accessibility at lower surgical risk than the intracranial visual pathways; b) straightforward monitoring of the device by direct visualisation; and c) potentially predictable and reproducible retinotopy by applying stimulation at a pre-processing site.

With the advent of modern vitreoretinal surgical techniques, access to the retina and the subsequent implantation of stimulating electrodes are comparatively easier than other sites of implantation. This is exemplified by the widespread implantation of the Argus® II System in many countries by many different surgeons over a relatively short period, at a level of surgical morbidity acceptable to regulators (Humayun et al., 2012; Rizzo et al., 2014). Despite the relative accessibility and safety discussed here, implantation still requires advanced vitreoretinal surgical skills. Complications and problems were also easily identified during the phase I/II clinical trials due to the ability to directly visualise the device (Humayun et al., 2012).

The other advantage of a retinal prosthesis is the theoretically predictable retinotopy by stimulating the visual system at a site before significant processing of the signal has occurred. Brindley and Lewin (1968b) have demonstrated that although stimulation of cortical electrodes gave rise to phosphenes in locations in agreement with the classic Holmes' retinotopic map of the visual cortex (Holmes, 1945), many of the phosphenes were complex and non-discrete in nature. This was predominantly thought to be due to the fact that the retina, as well as the rest of the pre-cortical visual pathway, carried out significant processing of the signal.

This was borne out in the discovery of organisational processing in the retina, as demonstrated by the dichotomous centre/surround responses of the retinal ganglion cell (RGC) receptive fields to light stimuli. Furthermore, as there are around 120 million photoreceptors while only 1.5 million ganglion cells, many photoreceptors converge onto a single bipolar cell *especially at the periphery*, with further convergence taking place from the bipolar cells to RGCs (Kolb, 2003). Conversely within the macular region of the retina, the photoreceptor:bipolar cell:RGC ratio approaches 1:1:1, with minimal convergence. It is thus envisaged that focal electrical stimulating patterns with a multi-electrode array in the macular region would more likely manifest retinotopic correlations along the visual pathway. There is, however, a particular limitation to this rationale, due to the arcuate displacement of axons and the piling up of ganglion cell bodies when approaching the fovea.

The retina as a viable site for electrical stimulation to generate phosphene perception was first demonstrated by contact lens electrode stimulation in Retinitis Pigmentosa (RP) patients (Potts and Inoue, 1969, 1970; Potts et al., 1968). Given the advantages of retinal stimulation, there are two main physical approaches to access the retina: the epiretinal approach – whereby the multi-electrode array is placed on the retinal surface in direct contact with the nerve fibre layer; and the subretinal approach – whereby the array is placed underneath the retina and is in closest contact with the bipolar cells. Both approaches have achieved reliable phosphene activation and have shown comparable functional improvements in human clinical trials. The Argus® II Retinal Prosthesis System adopts the epiretinal approach, as do the Epi-Ret3 (Menzel-Severing et al., 2012) and the Intelligent IRIS Implant (Velikay-Parel et al., 2009, 2013), which were developed by two German consortium groups. The subretinal approach is adopted by the alpha-IMS device (Stingl et al., 2013).

1.2. Candidates for treatment

All current retinal prostheses (including the Argus® II Retinal Prosthesis) work by electrically eliciting patterned focal responses in the residual inner retina. Ideal candidates for treatment would therefore have conditions where the outer retina (i.e. photoreceptors and/or retinal pigment epithelium) has been destroyed by any mechanism, while the inner retina (e.g. bipolar cells, RGCs, horizontal cells and amacrine cells) remains relatively intact. The largest single condition that manifests this combination of outer retinal loss with relative inner retina preservation is RP (Milam et al., 1998).

RP denotes a group of hereditary outer retinal dystrophies, affecting around 1 in 4000 live births and more than a million people worldwide (Hartong et al., 2006). Affected individuals suffer from progressive visual loss which can be profound (0.5% with no light perception and 25% with ≤20/200 vision in both eyes) (Grover et al., 1999). Post mortem histological studies of eyes of patients with moderate to severe RP have shown that even though all cellular layers of the retina underwent degeneration and cell loss with disease progression, the bipolar cell layer and the RGC layer remained relatively unaffected, with 78% and 30% preservation respectively, even in cases of severe RP (Santos, 1997; Stone, 1992). Treatment options for RP, other than for the associated cataract, epiretinal membrane and macular oedema, are limited (Guadagni et al., 2015). As such, they represent an ideal group of patients who may benefit from retinal prosthesis treatment.

Owing to the exploratory nature of the study, the recruitment criteria for entry into the Argus® II phase I/II clinical trial was RP patients with logMAR 2.9 (bare light perception) vision or worse (Humayun et al., 2012). If visual loss in the eyes was asymmetrical, the worse seeing eye was chosen as the study eye to minimise potential harm to the patient.

1.3. Components of the Argus® II Retinal Prosthesis

Although called *retinal* prostheses and popularly known as the '*bionic eye*', devices such as the Argus® II at best predominantly attempt to replace photoreceptor function. As such, they depend on some native residual function of the inner retina and optic nerve. The success of a retinal prosthesis, therefore, depends on how well it is able to replace the functions of the degenerated or absent photoreceptors, namely: a) the efficient capture of the visual image; b) the transduction of the captured image into meaningful neural electric signals; and c) the subsequent activation of the residual inner retina (bipolar cells and RGCs), from where visual information can be relayed by the optic nerve to the visual cortex.

To achieve these goals, the Argus® II Retinal Prosthesis System employs 3 external components and 3 internal components. The 3 external components are: (see Fig. 1)

1. A glasses mounted video-camera – for real-time image capture.
2. A portable computer (the Visual Processing Unit, VPU) – for processing of the captured scenes and translation into electrical stimulating parameters conveying spatial–temporal information.
3. An external coil (built into the side arm of the glasses) – for wireless transmission of the processed data from the VPU and electrical power to the internal components using radio-frequency (RF) telemetry.

The 3 internal components entail: (see Fig. 2)

Fig. 1. Photograph of a patient fitted with the Argus® II Retinal Prosthesis System. The external components consisted of a glasses mounted video-camera, a portable computer (the Video Processing Unit, VPU), and an external coil. The VPU enables real-time processing of the captured scenes and translation into electrical stimulating parameters conveying spatial–temporal information. The external coil allows for wireless transmission of the processed data from the VPU and electrical power to the internal components using radiofrequency (RF) telemetry.

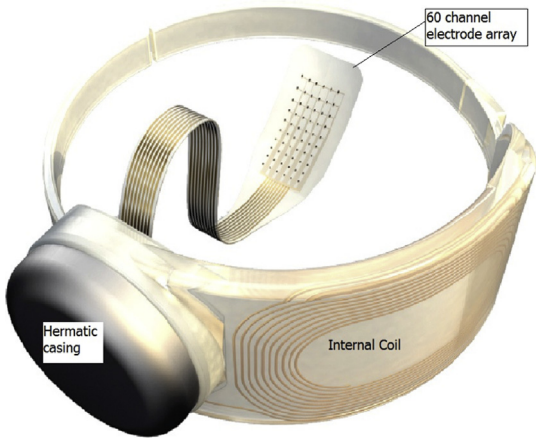

Fig. 2. Illustration of the internal components of the Argus® II Retinal Prosthesis System. The internal components consist of an internal coil, an inbuilt Application-Specific-Internal-Circuit (ASIC) housed in the hermetic casing, and a 60 channel stimulating electrode array. The internal coil acts as a wireless receiver of RF telemetry, converting radio waves back to electromagnetic waves to recover both data and electrical power. The ASIC generates the appropriate electrical pulses according to the data received, which are then relayed to the electrode array where direct stimulation of the retinal surface takes place.
(Reproduced with permission from Second Sight Medical Products Inc.)

1. An internal coil – as a wireless receiver of RF telemetry, converting radio waves back to electrical signals to recover both data and electrical power.
2. An inbuilt Application-Specific-Integrated-Circuit (ASIC) – for generating appropriate electrical pulses in accordance with the stimulating parameter data recovered from the internal coil, which are then relayed to the multi-electrode array.
3. A 60-channel microelectrode (6 × 10) epiretinal array – consisting of 60 platinum electrodes (diameter = 200 μm) spaced 575 μm (centre-to-centre) apart, embedded in a thin film of polyimide. Each microelectrode is connected to the ASIC in a parallel circuit via a metallised polymer connecting cable, such that each electrode can be activated independently according to the stimulating parameters. The array comes into direct contact with the retinal surface, allowing injection of electrical charges locally to stimulate the underlying retinal tissues (see Fig. 3).

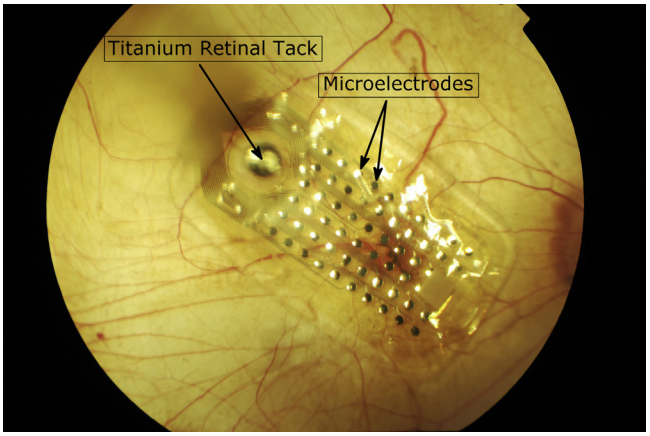

Fig. 3. Colour fundus photograph of the microelectrode array with 60 platinum electrodes, implanted in a patient with choroideremia. The array rests on the retinal surface in direct contact with the retina, to allow efficient stimulation of the underlying retinal tissues. The array is held in place with a spring adjusted titanium tack that passes through retina, choroid and the sclera.

1.4. Surgical implantation

Surgical implantation of the Argus® II Retinal Prosthesis involves the standard vitreoretinal surgery techniques of pars plana vitrectomy (Machemer et al., 1971, 1972) and scleral buckling procedures (Friedman, 1958; Schepens, 1957). If the patient is phakic, lensectomy is usually performed from the outset, as subsequent cataract formation would render clinical monitoring difficult.

A standard 3-port pars plana vitrectomy is first performed, with removal of the posterior hyaloid face to prevent future development of an epiretinal membrane. Any pre-existing epiretinal membrane is removed at the time of surgery in order to optimise electrical contact between the microelectrodes and the retinal surface. A 360° conjunctival peritomy is performed to allow isolation of all 4 recti muscles in preparation for placing the encircling band carrying the extraocular portion of the device.

The internal coil and ASIC are sealed in protective hermetic cases, which have a concave under surface, conforming to the curvature of the globe.

These are placed flush on bare sclera surface and sutured onto the sclera, usually in the supero-temporal quadrant of the globe, at a pre-determined distance from the limbus (approximately 5 mm) depending on the axial length of the globe (see Fig. 4). A 5 mm pars plana sclerotomy in the supero-temporal quadrant allows introduction of the microelectrode array into the vitreous cavity (see Fig. 5) – this is the only intraocular portion of the device. With appropriate scleral placement of the extraocular part of the device, the microelectrode array would rest naturally on the retinal surface at the posterior pole with minimal tension. Gentle manipulation of the array position is possible to optimise placement in the macular region. Once the array position is satisfactory, a spring-tensioned, titanium retinal tack is inserted at the heel of the array, to ensure close apposition of the array and the retinal surface (see Fig. 6). The sclerotomy is then sutured close around the traversing cable connecting the array to the ASIC to avoid scleral leakage and hypotony.

The internal coil and ASIC cases on the sclera are further stabilised by an encircling band, which passes under each of the 4 recti muscles around the globe before being gently tightened and held with a Watzke's sleeve. Finally, an allograft (e.g. Tutoplast®) or autologous fascia-lata patch is sutured over the hermetic cases before the conjunctival closure over the device. Surgical time generally falls between 1.5 and 4 h (Rizzo et al., 2014).

1.5. History

Research into the possibility of retinal prosthetic vision began in the early 1990s with Mark Humayun, Robert Greenberg and Eugene

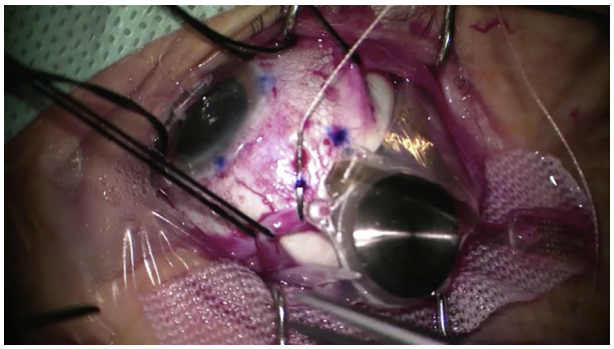

Fig. 4. Intra-operative photograph of the ASIC in hermetic casing being sutured onto sclera 5 mm from the limbus.
(Still image captured from surgical video, courtesy of Stanislao Rizzo with permission.)

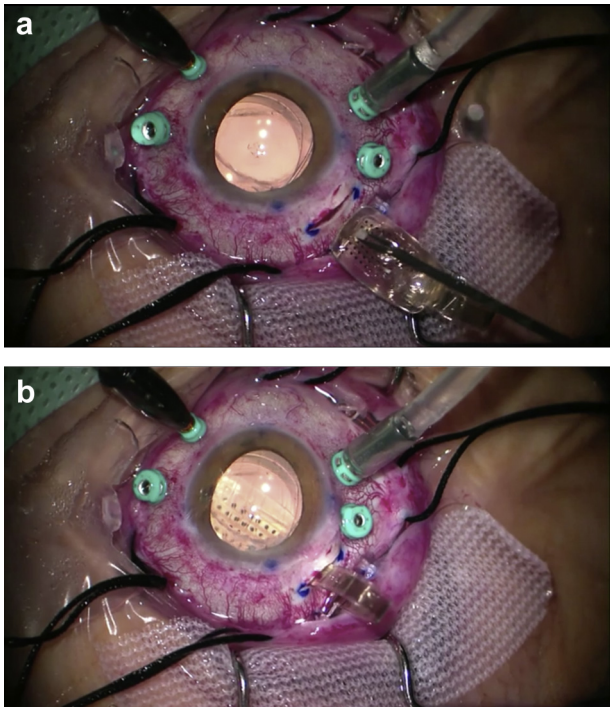

Fig. 5. a & b: Intra-operative photographs showing the insertion of the microelectrode into the vitreous cavity via a 5 mm pars plana sclerotomy.
(Still images captured from surgical video, courtesy of Stanislao Rizzo with permission.)

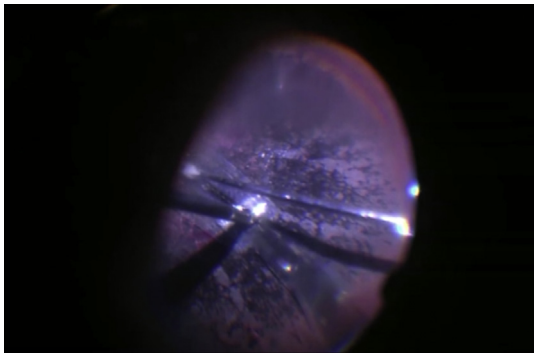

Fig. 6. Intra-operative photographs showing the Titanium tack being compressed into the heel of the microelectrode array, thereby fixing the array to the retinal surface.
(Still image captured from surgical video, courtesy of Stanislao Rizzo with permission.)

de Juan at Johns Hopkins University. They first demonstrated that focal electrical stimulation with a platinum electrode could elicit localised retinal responses in isolated animal retinas (Humayun et al., 1994) (discussed in detail in section 2.1.1). The group subsequently moved to the University of Southern California (USC), and started a collaboration with the Second Sight company that would eventually lead to the development of the Argus I and Argus® II retinal prostheses.

1.6. Argus I system

The prototype retinal prosthesis, the Argus I, began its phase I clinical trial involving 6 patients in 2002 (Humayun et al., 2003, 2005; Yanai et al., 2003). The main differences between the first generation device and the Argus® II device are:

1. The stimulating array of Argus I consisted of 16 microelectrodes (4×4 configuration), of either 260 μm or 520 μm in diameter, or both sizes alternating in a checkerboard pattern, with a centre-to-centre inter-electrode separation of 800 μm (see Fig. 7 inset) (Horsager et al., 2009).
2. In the Argus I system, the hermetic casing containing the internal coil and ASIC was placed subcutaneously in the temporal bone recess, with the connecting cable leaving the periorbital space via a lateral canthotomy and tunnelled along the temporal bone subcutaneously to reach the temporal recess (see Fig. 7). This approach was similar to that of the cochlear implant and the alpha-IMS subretinal implant (Zrenner et al., 2011), and required dissection of the temporal region with the assistance of maxillofacial/otolaryngology expertise and extended surgical time. As such, this approach has been revised in the subsequent Argus® II design to simplify the implantation.
3. In the Argus I system the external coil is situated over the temporal bone, held magnetically to the subcutaneous internal coil.

Initial results from this clinical trial with a follow-up period of up to 33 months supported safety and long term functioning of the device. A wide range of electrode thresholds were observed both within and across the subjects, but many electrodes were able to elicit visual percepts within the safety charge density limit (Brummer and Turner, 1977; Brummer et al., 1983).

Variability in the performances across the subjects was also noted, but was generally encouraging with the subjects being able to enumerate and localise high contrast objects with greater accuracy than by chance. Two subjects were also able to orientate shape (in the form of letter 'L') and identify 3 common objects (i.e.

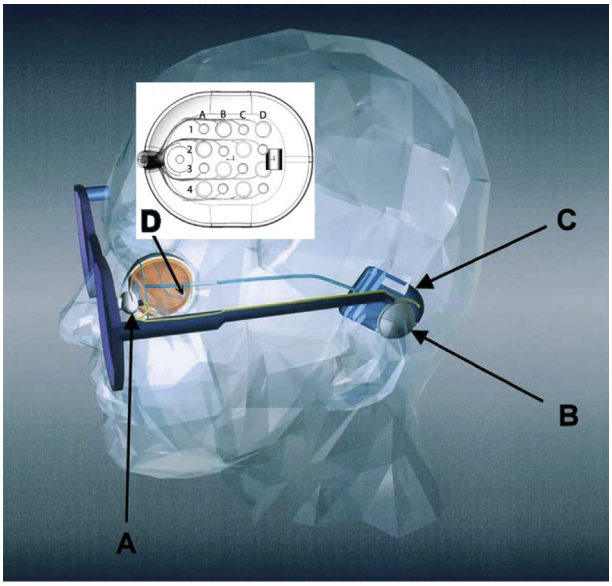

Fig. 7. Illustration of Argus I retinal implant in situ. (A) video-camera mounted in glasses frame; (B) the external coil for wireless RF telemetry transmission held magnetically to the underlying subcutaneous internal coil; (C) the hermetic casing containing the internal coil and ASIC embedded subcutaneously in the temporal bone recess, with the connecting cable leaving the periorbital space via a lateral cantotomy and tunnelled along the temporal bone subcutaneously to reach the temporal recess; (D) multielectrode array implanted intraocularly on the epiretinal surface. The inset shows the multielectrode array consisting of 16 electrodes (4×4 configuration). The electrodes are alternating 260 μm and 520 μm in diameter in a checkerboard pattern. The centre-to-centre inter-electrode separation is 800 μm.
(Modified and reproduced with permission from Horsager et al. (2009) and Humayun et al. (2003).)

plate, cup and knife) with greater accuracy than by chance. Furthermore, using high contrast square wave gratings, one subject was able to differentiate the orientation of the gratings in 4 directions (vertical, horizontal, diagonal to right, diagonal to left) significantly better than by chance. The best level of resolution achievable was equivalent to logMAR 2.21 vision, in keeping with the theoretical resolution possible with the 4 × 4 array (Caspi et al., 2009). The ability to carry out these tasks supported the notion that the subjects are capable of interpreting patterned electrical stimulation. Based on these results, the next generation retinal prosthesis – the Argus® II – with 60 microelectrodes, was developed.

2. Background

2.1. Proof of concept

The development of the Argus® II Retinal Prosthesis, as with all retinal prostheses, was based on the following assumptions:

1. The inner retina (RGCs with/without bipolar cells) of end-stage RP patients remains functionally intact for transmission of information along the visual pathway to the visual cortex.
2. The residual inner retina can be activated focally with localised electrical stimulation to elicit discrete phosphenes without causing damage or toxicity to the retina.
3. Retinotopy is relatively preserved in the residual inner retina and along the visual pathway, such that simultaneous multifocal stimulations would form geometric patterns of phosphenes in accordance with retinotopic locations.
4. The elicited geometric patterns of phosphenes can be relayed in a spatio-temporally correct manner along the visual pathway and interpreted by the primary visual cortex as recognisable visual patterns.
5. Limited pixels can still provide useful visual function.

The evidence for the first premise has already been discussed in section 1.1. The rest of this section will therefore focus on animal and human studies that support the remaining concepts.

2.1.1. Focal retinal stimulation

2.1.1.1. Animal studies. To establish whether focal electrical stimulation of the inner retina could be achieved using microelectrodes and stimulating parameters within the established safety density charge limits (Humayun et al., 1994; Rose and Robblee, 1990) carried out a series of experiments: on the retinas of bullfrogs in an eye cup preparation; on a normal retina from an intact rabbit eye under terminal anaesthesia; and on rabbit eyes with the outer retinal function abolished by intravenous sodium iodate infusion. Using a pair of epiretinal platinum electrodes of 200 μm in diameter separated by 200 μm (the same diameter as that of the final Argus® II device) the authors demonstrated that the thresholds for activating these 3 retinal preparations were: 2.98 μC/cm^2, 8.92 μC/cm^2 and 11.0 μC/cm^2 for bullfrog, normal rabbit retina and rabbit retina with abolished outer retinal function respectively. Even though stimulation of the retinal tissue with outer retinal dysfunction required higher stimulating charge density, all of them were within the predetermined safety limit for long term retina stimulation with platinum electrodes (limit = 50–150 μC/cm^2) (Rose and Robblee, 1990). Similar responses have also been achieved by electrically stimulating transgenic P23H-1 rats' retinas, which had lost responses to light stimuli secondary to photoreceptor degeneration (Sekirnjak et al., 2009).

Humayun et al. (1994) also demonstrated that the retinal responses elicited were localised to the area of electrical stimulation, as the recording electrode only detected activity when it was placed in between the stimulating electrode and the optic disc, but not when it was distal to the stimulating electrode–optic disc path (e.g. when it was placed nasal to the optic disc while the stimulating electrode was placed in the temporal retina). This indicated that the RGC responses elicited by electrical stimulation are only recordable from axons close to the point of stimulation, but not from axons of cells residing far away from the electrical stimuli. However, this study did not examine axons from distal cells that passed through the area of stimulation. Overall it at least showed probable gross retinotopic localisation of retinal responses, allowing for the possibility of simultaneous multi-focal stimulation to form geometric patterns, which could then potentially give rise to pixelated vision.

The issue of the inadvertent activation of bypassing axons from RGCs distal to the point of stimulation remains one of concern for creating discrete phosphenes. This is a potential problem due to the layering of axons in the macula region and the arcuate displacement of nerve fibres away from the fovea to minimise the visual obstruction of light falling on the central high-density photoreceptors. Stimulation of the RGC axon fibres, instead of the cell body (soma), would theoretically convey the perception of peripheral retinal activation, rather than a retinotopically correct pattern of photoreceptor activation. This may be more problematic with epiretinal electrodes, which are anatomically closer to the nerve fibre layer (hence the axon fibres), than the RGC soma. Furthermore, with a diameter of 200 μm, each electrode encompasses the equivalent area of hundreds of photoreceptors (see Fig. 8), further reducing the achievable resolution.

With the assumption that selective activation of localised RGCs will lead to production of discrete phosphenes, further work has been carried out to determine the nature of retinal activation with epiretinal electrodes, and to explore methods of focal retinal stimulation (e.g. by varying stimulating parameters and/or reducing the stimulating electrode size). Using isolated rabbit

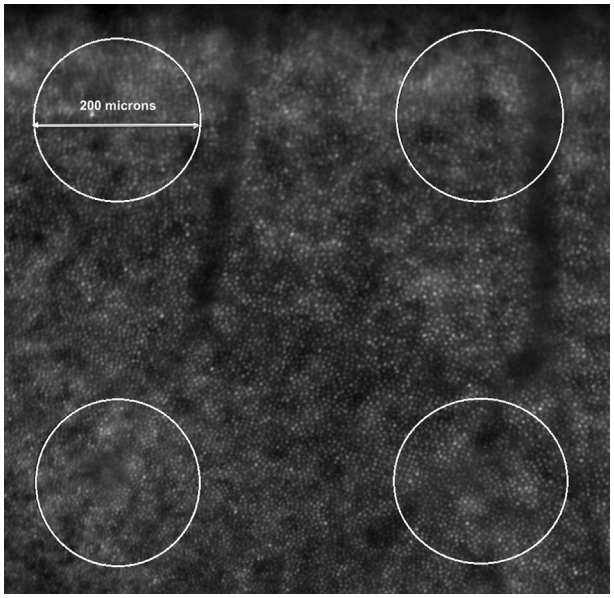

Fig. 8. Adaptive optics (Imagine Eyes – rtx1™) retinal image of a healthy subject, taken at 3° temporal to fixation. Individual cone photoreceptors can be seen as discrete dots. Within this macular region, the ratio of photoreceptors:bipolar cells:retinal ganglion cells approaches 1:1:1, allowing maximal visual resolution. In comparison, the 4 white circles are representative of the retinal surface areas covered by the Argus® II retinal prosthesis microelectrodes, with a diameter of 200 μm each, drawn to scale. Activation of one microelectrode would therefore result in equivalent simultaneous activation of hundreds of photoreceptors. The resolution achievable is thus limited. (Reproduced with permission from Luo and daCruz (2014).)

retinas and ultra fine electrodes (2 μm), Jensen et al. (2003a) set out to investigate the differences in the thresholds of stimulating RGC axons versus cell bodies. They discovered that the electrical threshold of activation was lowest with mono-polar cathode stimulation applied directly over the RGC soma (assuming the soma is located within its light receptive field), and that the threshold increased as the stimulation moved further away from the soma. With cathode stimulation, the RGC soma threshold was about half of that of the axon. However, this difference was not observed when anode stimulation was applied, which showed similar thresholds for both RGC soma and axon activation. In addition, application of cadmium chloride, a synaptic blocker, did not abolish the retinal responses, suggesting that the responses may originate in the RGC, rather than from bipolar cells.

In a separate study by the same group using mono-polar cathode stimulation, the authors found that with smaller electrode sizes (5 μm in diameter), and shorter stimulating durations (0.1 ms pulses), the threshold for directly activating RGC was much lower (37 times lower) than that required to activate the RGC indirectly via synaptic transmission. Even with a 125 μm electrode and 2 ms stimulating pulse, the average threshold for direct RGC activation was still half of that of trans-synaptic RGC activation (Jensen et al., 2003b). While the results from Jensen et al.'s group pointed towards a potential way of selective RGC soma activation, the conical configuration of the needle-shaped stimulating electrode and the mono-polar cathode stimulation were very different from the intended multi-electrode array design (which has a disciform planar configuration), and the safer charge-balanced biphasic stimulation (which reduces the Faradaic reaction at the electrode–tissue interface, hence minimising tissue damage) (Lilly et al., 1955). However, despite the fact that both Jensen et al. and Greenberg et al.'s (1999) computer modelling demonstrated lower thresholds for RGC soma compared with the axons, other evidence suggests that the RGC axons appear to be the preferred site of activation (Nanduri, 2011). As such, whether it is the RGC soma or axon that is preferentially stimulated by the Argus® II device *in vivo*, remains ambiguous.

To expand the study on other animal retinas and test out settings and configurations which were similar to the intended retinal prosthesis design, Sekirnjak et al. (2008) carried out experiments on the retinas of rats, guinea pigs and later, macaque monkeys (which bear close resemblance to human retinas). They used multi-electrode arrays with micro-electrodes of 6 μm–25 μm in diameter and charge-balanced biphasic stimulations to investigate retinal responses (Sekirnjak, 2006; Sekirnjak et al., 2008). The threshold charge densities from their experiments were typically 100 $\mu C/cm^2$, which were within the established safety limit. Addition of various synaptic blockers did not abolish the retinal responses, again indicating that the responses were of RGC origin. In a subset of macaque monkey RGCs, the parasol cells (both ON and OFF) were further stimulated with 9–15 μm electrodes (comparable to the size of individual RGC somas) (Sekirnjak et al., 2008). It was shown that these parasol cells responded to a single electrical pulse with a single evoked response at sub-millisecond latency (~0.2 ms), and that the response was confined within the activated cell, without spreading to its neighbours (i.e. spatially specific). Further work on other ganglion cell types of macaque monkeys' retinas were carried out by Jepson et al. (2013), including ON and OFF midget cells and small bi-stratified ganglion cells as well as the ON and OFF parasol cells. All these ganglion cells could also be independently activated with sub-millisecond latency within established safety limits. Given that the parasol cells form a significant part of the magnocellular pathway, while midget cells form the parvocellular pathway, the authors postulated that epiretinal electrical stimulation has the potential to elicit signals of high temporal and spatial resolution in primate retinas using high-density multi-electrode arrays. Selective activation of ON and OFF RGCs has also been demonstrated in isolated rabbit retinas by Twyford et al. (2014), using a conical epiretinal electrode with a base diameter of 15 μm (comparable to the surface area of a 40 μm disc electrode), and high frequency electrical stimulations (HFS) of 2 kHz. They have shown that within the low magnitude range (20–60 μA) of HFS, modulation of the amplitude elicited opposing spiking responses in ON and OFF RGCs, lending to the prospect of developing a retinal prosthesis capable of cell-type specific, selective activation in the future (Guo et al., 2014).

More recently, an Australian research group at the University of New South Wales has proposed the use of a complex epiretinal stimulating unit, whereby a central stimulating electrode is surrounded by 6 hexagonally-arranged return electrodes, which collectively return the delivered current (Abramian et al., 2010, 2011; Lovell et al., 2005). Electrical charge spread from single electrode stimulation has previously been demonstrated both by computer modelling and later experimentally in rabbit as well as salamander retinas (Behrend et al., 2011). This could be responsible for the clinical observation that some Argus I subjects reported phosphene sizes that were more than twice the physical size of the single stimulating electrode (Horsager et al., 2009). The presence of electric currents in the return electrodes supported the notion of charge spread from the stimulating electrode. The hypothesis behind this arrangement of stimulating and return electrodes was that it might isolate a particular stimulating electrode from neighbouring active stimulating electrodes. This isolation of the stimulating electrode would theoretically minimise the effect of 'cross-talking' from charge leakages (Addi et al., 2008), improving the 'focus' of retinal stimulation. In this stimulating unit, each electrode was 50 μm in diameter and could act both as a stimulating or returning electrode. In a multi-electrode array (with centre-to-centre electrode distance of 200 μm), this configuration allowed great flexibility in the stimulating pattern. Other methods of improving focal retinal stimulation have also been described, including minimising the distance between the stimulating element and the target cells (Palanker et al., 2004), and the design of a bipolar stimulating/return pixel to minimise charge spread (Mathieson et al., 2012).

2.1.1.2. Human studies. Following experiments in vertebrate retinas, Humayun et al. (1999) carried out acute experiments in 5 blind volunteers (3 with RP; one with an unknown retinal degeneration since birth; and one with extensive AMD) to investigate the effect of focal epiretinal stimulation. Using handheld probes of bipolar platinum electrodes of 200 μm in diameter, the authors performed intra-operative stimulations with the patients awake under local anaesthesia. With a focal stimulation, all 5 patients reported perception of a transient phosphene, ranging from "pin" to "pea" in size. The location of each of the perceived phosphenes in space corresponded broadly to that predicted retinotopically by the position of retinal stimulation within the 4 quadrants of the macula, except in the patient who was blind since birth. This may have been due to the lack of development of retinotopic organisation at the visual cortex level from sensory deprivation. Simultaneous stimulation of 2 sites separated <1 mm apart produced the perception of 2 separate phosphenes in one patient, while stimulation with an elongated piece of platinum wire gave rise to an elongated percept ("a pencil held at arm's length"). These findings strongly supported the notion that focal electrical stimulations could elicit discrete phosphenes in a retinotopic manner in a diseased human retina with outer retinal degeneration.

To explore whether multiple discrete phosphenes could be elicited simultaneously to form recognisable geometric patterns, further experiments were carried out by the same group of

researchers using platinum multi-electrode arrays of 3 × 3 and 5 × 5 configurations on 2 different blind RP patients (Humayun et al., 1999). Each electrode was 400 μm in diameter with an inter-electrode separation of 200 μm, and was embedded in a silicone matrix. The first patient with the 5 × 5 array perceived a horizontal line when a row of electrodes was activated, and a vertical line when a column of electrodes was activated. The phosphenes appeared to merge together such that a continuous line (rather than discrete linear dots) was seen. When the electrodes in 2 columns and 1 row in the form of a "U" shape were stimulated, the patient reported an "H" shaped percept. In the second patient with the 3 × 3 array, when the 8 electrodes forming the perimeter of the array were activated, a "box" with an empty centre was described. Both patients reported visual percepts which appeared to correspond to the pattern of multi-electrode stimulation, indicating that visual percepts could be modified by the stimulation pattern to give rise to form vision.

To further elucidate the effect of outer retinal loss on electrically elicited visual percepts, Weiland et al. (1999) carried out an experiment on 2 patients with normal retinas, prior to their eye exenteration for orbital cancer. Krypton and argon laser retinal ablations (each about 1 disc diameter in size) were applied to the infero-temporal macula and supero-temporal macula respectively. Krypton red destroyed photoreceptors, while argon green destroyed both the outer and inner retinal layers, leaving only RGC nuclei and axons. Charge balanced, biphasic stimulations with a platinum wire electrode (125 μm in diameter) were applied to areas of normal retina as well as the krypton and argon laser-ablated areas. Supra-threshold stimuli applied to a normal retinal area elicited a large, dark percept, while stimulation of the krypton-ablated area elicited a discrete, small white dot and stimulation of the argon-ablated area elicited a linear, thread-like percept that was somewhat fainter. Both patients reported similar visual percepts when the same retinal areas were stimulated and these visual percepts were repeatable.

Rizzo et al. (2003a, 2003b) from the Boston Retinal Implant Group also explored the feasibility of multi-focal epiretinal stimulation using iridium oxide electrodes, to give visual percepts of recognisable geometric shapes. Using arrays of variable electrode sizes (50 μm, 100 μm and 400 μm in diameter), epiretinal stimulations were performed in 5 blind RP patients and 1 patient with a normal healthy retina who was awaiting an exenteration procedure for orbital cancer. Rizzo et al. (2003a) observed that in general, the stimulation thresholds were much lower in the normal retina compared to diseased RP retinas. For the 50 μm electrodes, the threshold to produce phosphenes exceeded that of the established charge density limit (quoted from established literature to be 1 mC/cm^2 with cathodic stimulation) (Beebe and Rose, 1988). Even with the 100 μm and 400 μm electrodes, only the normal retina thresholds were below the established charge density limit. Severely damaged retinas from RP appeared to have 4–19 times higher thresholds than normal retinas, which raised the concern for long-term electrical stimulation in severe RP patients. However in a later study, the iridium oxide safety charge limit was found to be higher than previously estimated, measuring up to 4 mC/cm^2 with a 0.2 ms stimulating pulse (Weiland et al., 2002), suggesting that safe chronic stimulation was possible.

In a follow-on study, contrary to Humayun et al. and Weiland et al.'s findings, Rizzo et al. (2003b) showed that out of the 5 blind RP patients, only 3 patients experienced perception of a single discrete phosphene with single electrode stimulation. Single electrode stimulations were carried out by either 100 μm or 400 μm electrodes. Of the 185 visual percepts elicited in the 3 patients, only 6%, 35% and 85% of these phosphenes were perceived as small single dots. Other phosphenes were more complex in nature, such as a "line", or a "cluster of 2 or 3 images". Even in the patient with a normal retina, only 57% of single electrode stimulations yielded single discrete phosphenes. When simple geometric patterns of electrodes were stimulated (e.g. a line or letter "L" or "T"), out of 84 stimulations, the proportion of phosphenes matching the expected retinotopic representation was 55%, 21% and 29% respectively in the 3 RP patients, and 43% in the normal retina patient.

When the same stimulating parameters were applied to the same electrodes at different times to test the reproducibility of phosphenes, the results were variable between the patients. One RP patient reported similar phosphenes in 2 out of 2 trials, while the other 2 patients reported similar phosphenes in 19/23 trials and 9/12 trials respectively. The patient with normal retina reported reproducibility in 9/11 trials. Notably in one RP patient, when 2 electrodes spaced 1860 μm apart were stimulated simultaneously, one phosphene was reported 5 out of 6 times while two phosphenes were observed once. Subsequent sequential stimulation of one followed by 2 electrodes for comparison yielded a single brighter percept twice, a brighter and larger percept once, a larger percept once, and the sensation of "motion" once.

J. Rizzo et al. confirmed that single discrete phosphenes could be achieved with single electrode stimulations in some patients, but noted that there was considerable variability amongst the patients (later borne out in the chronic implantation and stimulation studies). The patterns of the phosphenes elicited were often not predictable from the patterns of electrode array stimulation.

2.1.2. Cortical responses from electrically stimulating diseased retina

A further requirement of a functional retinal prosthesis is the successful relay of the elicited electrical signals from the retina to the visual cortex. Several research groups have looked into the cortical responses to epiretinal electrical stimulation, using electrophysiology measurements in both animals and humans. These are discussed further here.

2.1.2.1. Animal studies. Cortical activities from epiretinal stimulation were first demonstrated in rabbit retinas, using subcutaneously implanted/extradural electrodes over the visual cortex (Nadig, 1999; Walter and Heimann, 2000). The cortical electrically-evoked potentials (EEPs) were comparable to that of visually-evoked potentials (VEPs) in both wave forms and in responses to changes in stimulus strength and frequency, suggesting that EEPs also originated from focal retinal activation.

Further demonstration of eliciting EEPs by focal electrical stimulation has been made in normal and *rd1* mice, and normal and RCD1 dogs (Chen et al., 2006; Güven et al., 2005). These two animal studies showed that EEP elicitation was also achievable in animal models of outer retinal degeneration. There was a distinct early response (latency < 10 ms) and late response (latency > 50 ms). Synaptic blockade using cadmium chloride ($CaCl_2$) abolished the late responses, but not the early responses, indicating that the early responses were from direct activation of RGC. Epiretinal electrical stimulation thus elicited cortical responses both via direct activation of RGC and via trans-synaptic signal transmission.

With the aim of visualising neuronal activity changes in the visual cortex, Walter et al. (2005) performed direct optical imaging of the cortical surface following epiretinal stimulation in rabbits. With neuronal activation visualised as darkening of the cortical area, topographical changes in the area of activation could be seen to follow sequential pairs of epiretinal electrodes being activated. The cortical activation was temporally matched and appeared to follow the visuotopic organisation of the cortex. This confirmed that retinotopic stimulation gives rise to focal, visuotopically preserved patterns of cortical activation.

2.1.2.2. Human studies. Apart from working on *rd1* mice and RCD1 dogs, Chen et al. also performed measurements of EEP in one human with RP, using gold disc scalp electrodes over the occipital cortex. The epiretinal stimulation was carried out by an implantable epiretinal electrode array. Eight epiretinal electrodes were activated simultaneously, using supra-threshold currents. EEPs were recordable from the human RP patient on 2 separate occasions 3 weeks apart. On both occasions, EEPs were recorded with a latency of >50 ms. This was unexpected as previous works from Humayun et al. (1996) and computer modelling from Greenberg et al. (1999) suggested RGC as the main site of electrical activation. The authors have commented that this may be due to the lack of sensitivity of scalp electrodes in detecting the early signal response.

More recently, EEPs have been recorded in both Argus I and Argus® II patients (Dagnelie and Stronks, 2014; Humayun et al., 2003; Stronks et al., 2013). Stronks et al. (2013) reported EEP recordings from 4 Argus® II retinal implant patients. Despite using all available electrodes for stimulation for each patient to maximise the cortical response, the signal–noise ratios were still low, thus requiring prolonged recording time and more substantial signal processing than standard VEPs. Nevertheless, the authors were able to identify characteristic features in the waveform. In particular the second peak, P2, was identified as the most reproducible outcome measure as it correlated well with the patients' subjective report of the phosphene elicited by the supra-threshold stimulus. However, although the patients reported a decline in their perceived phosphene brightness over time with continuous stimulation, this was not reflected in the P2 recordings.

Despite numerous animal and human studies providing objective evidence of cortical activation in response to epiretinal stimulation, little is understood about how these cortical activities reflect image processing and/or interpretation along the visual pathway and at the cortical level. Neither is the correlation between EEPs and visual function well understood.

2.2. Simulation of potential visual outcomes with retinal prosthesis

While physically replacing millions of photoreceptors with microelectrodes is not technically feasible, the actual number of microelectrodes required to restore functioning vision may be far lower. With the cortical implant, Brindley and Lewin (1968b) first demonstrated the feasibility of partially restoring vision by the means of pixelated scenes – visual patterns made up of punctate spots of light (phosphenes). With this in mind, researchers set out to estimate the number of pixels (hence the number of functioning microelectrodes for focal retinal stimulation) theoretically required to provide useful function, using a combination of psychophysical experiments and computer simulations. For the purpose of practical application in Argus® II subjects, simulations were performed to establish the number of pixels required for 3 levels of visual tasks: navigational vision, facial and object recognition, and reading vision.

2.2.1. Navigational vision

Cha et al. (1992b) used a monochromic monitor mounted on a pair of goggles for projecting scenes. The monitor was further covered by a perforated mask to create pixelated images. Seven normally sighted volunteers were asked to wear the goggles and navigate through a maze. The obstacles and configuration of the maze were altered randomly per trial to prevent route learning by the participants. They found that the field of view and the number of pixels were the two strongest determinants of navigational ability, and collectively accounted for 83.7% of the variance in walking speed. Training and practice improved the performance of maze navigation (i.e. walking speed and number of contact with obstacles), and each subject required about 40 trials for the performance to be stabilised. The authors estimated that a minimum of 25×25 (625 in total) pixels projected centrally to the fovea, with a field of view of 30°, was required for normal walking speed to navigate through the maze. Sommerhalder et al. (2006) also reported a very similar estimation of pixel requirements for navigation, recommending a visual field of $23° \times 33°$ and a minimum of 500 pixels, while earlier work by Sterling (1971) indicated that a much lower number of 200 pixels might be adequate for recognition of small obstacles.

To allow comparisons of several more feasible designs of electrode arrays in navigation and mobility performances, Dagnelie et al. (2007) looked at the differences in navigational performance with 3 different densities of simulated pixelated vision: 4×4, 6×10 and 16×16 pixels. The authors used a combination of real mobility navigation – whereby the normal sighted participants wore a prosthetic vision simulator to walk through a maze; and a virtual reality navigation – whereby the participants navigated through a virtual maze with a game controller, again only watching a simulated pixelated vision display. The authors found that with adequate practice, an experienced user could navigate with the same efficiency using 6×10 pixelated vision, as with 16×16 vision. To further emulate the effect of phosphene "drop-outs" as encountered in the real-life use of the Argus® II Retinal Prosthesis System (due to poor electrode–retinal contact and/or unresponsiveness of the underlying retinal tissue to electrical stimulation within the safety charge density limit), the same group of researchers evaluated the effect of introducing random removal of pixels, and addition of background noise (i.e. random sparks, to mimic the spontaneous background photopsia experienced by many end-stage RP patients) in a virtual maze navigation (Wang et al., 2008). The simulated prosthetic vision display was also "gaze-locked", such that the presented scene did not vary with eye movement, to emulate the fact that the same area of retina was always stimulated by the electrode array, irrespective of eye movement. The authors concluded that a phosphene drop-out rate of 30% significantly extended the time required to perform the virtual maze navigation (by 40%), while addition of background noise and variation in luminance contrast did not significantly affect navigation.

2.2.2. Object & facial recognition

Object and facial recognition form an important aspect of visual function as well as playing a significant role in social interaction. Apart from the number of pixels as discussed previously, a second important factor in the rendition of prosthetic vision is the ability to perceive differences in image grey levels (i.e. luminance contrast). By varying the stimulating parameters (e.g. amplitude and frequency), the luminance contrast of different pixels can be adjusted, giving the perception of different grey levels. The greater the range of grey levels perceivable, the better the scene recognition (Terasawa et al., 2002).

Humayun (2001) set out to determine the pixel number and grey levels required for facial recognition. Using a head-mounted, customised Low Vision Enhancement System (LVES) display, simulated pixelated facial images were projected over the entire macular region of 8 normally sighted volunteers. The dot size, spacing, drop-out rates, grid size (visual field) and number of grey levels were varied in the simulation, to emulate the 3 different array designs: 4×4 (covering a $7.3° \times 7.3°$ visual angle), 6×10 (covering a $11.3° \times 19.3°$ visual angle) and 16×16 array. While unsurprisingly the best performance was seen in the 25×25 array with 6 grey levels (over 75% accuracy), reasonable facial recognition could be achieved with the 16×16 array with a minimum visual field of 10°, drop-out rate of less than 30% and 4 grey levels.

Recognition of common daily objects (e.g. cup, spoon, plate and pen) was only achievable with the 16 × 16 array, while the 6 × 10 array allowed description of the object shape, but not accurate identification (Hayes et al., 2003; Humayun, 2001).

Thompson (2003) tested a range of 16 different simulation conditions with varying combinations of the following parameters: dot size, drop-out rate, gap width (i.e. inter-dot distance), grid (array) size, grey levels and image contrast. The performance with each condition was compared with that of a standard condition to assess the effect of varying these parameters. The standard condition settings were: 16 × 16 array, 31.5 arc-min dot size, 4.5 arc-min gap size, 30% dot drop-out rate, and 6 grey levels. While each of the parameters was shown to affect the recognition speed, image contrast in particular, had a great impact on performance. For high contrast images (i.e. darkest grey level = 0% luminance; brightest grey level = 100% luminance), good facial recognition was achievable except when the simulated image was reduced to 70% random dot drop-out rate and 2 grey levels. For low contrast images (i.e. darkest grey level = 44% luminance; brightest grey level = 56% luminance), reasonable facial recognition was also possible with up to 70% dot drop-out rate, but a minimum of 4 grey levels and at least 17% of target image size was required. With more difficult images, the performance of the participants was shown to improve with practice.

2.2.3. Reading vision

As early as 1964, Brindley et al. estimated that 50 channels would permit recognition of one “printed or typed letter”, and that 600 channels would suffice for normal reading speed with the aid of automatic scanning (Brindley, 1964; Brindley and Lewin, 1968b). This was supported by Sterling (1971) and later on by Cha et al. (1992a) who also looked into the factors affecting reading in phosphene-based pixelated vision. Using a phosphene simulator similar to that described in section 2.2.1, they estimated that 625 points (25 × 25 array, covering a 10° visual field) implanted within 1 cm^2 of the area representing the fovea in the visual cortex would provide 20/30 vision.

While the earlier works were aimed at estimating reading vision provided by cortical implants, researchers at Johns Hopkins University set out to investigate the potential vision of 3 different retinal prosthesis arrays, namely 4 × 4, 6 × 10, and 16 × 16, using a head-mounted prosthetic vision simulator (as described in section 2.2.1) (Hayes et al., 2003). They estimated that the potential visual acuity achievable with each of these arrays were 20/1810, 20/1330, and 20/420 respectively. Reading was achievable in all 8 participants with the 16 × 16 array and 36-point fonts, with 2 of them able to read 27-point fonts (equivalent of 20/450 reading acuity). With the 6 × 10 array, 2 participants were able to read 72-point fonts with an average reading speed of 1.02 words per minute. The reading speed could be vastly improved with good text scanning technique, achieving a reading speed of 30–60 words per minute using the 16 × 16 array (Dagnelie et al., 2006). Sommerhalder et al. (2003) also estimated that as few as 300 pixels would be adequate for close to perfect reading of 4-letter words (>90% correctly read words) when presented within the central 10° of visual field, while 600 pixels distributed over a retinal surface of 3 mm × 2 mm would be required for reading of a full-page text (Sommerhalder et al., 2004).

In summary, the above studies have shown theoretically that while more than 600 pixels would allow near normal functioning such as reading and navigation, reasonable visual function could be achieved with far fewer pixels (16 × 16 array, 4 grey levels and drop-out rate of less than 30%). The current Argus® II Retinal Prosthesis with 6 × 10 pixels would be predicted to provide reasonable navigational and some reading vision – as borne out by some patients from the Argus® II phase I/II clinical trials (Humayun et al., 2012). There is also evidence that training and practice by way of visual rehabilitation improve the performance of visual tasks (Sommerhalder et al., 2003, 2004). However, as will be discussed in section 3 later, there is still a substantial discrepancy between the predicted performance and the actual functional capability in all the Argus® II patients. This is in part due to the fact that these pixelated vision simulations were based on the assumption that each phosphene was perceived as uniform, discrete dots, which appear and disappear in accordance with the duration of electrical stimuli. In reality, although many percepts were indeed reported as white/yellow dots, the shapes, forms and persistence of many phosphenes elicited from epiretinal electrical stimulation are much more complex and vary greatly between subjects.

As previously discussed, Rizzo et al. (2003b) have observed that frequently, more than one phosphene of indiscriminate shape was described by subjects following single electrode stimulation. Furthermore, the same percept was not always described by the subject despite using identical stimulating parameters. This finding was also reported by Nanduri et al. (2008, 2011, 2012), who further demonstrated changes in phosphene shape, size and brightness with varying stimulating frequency and amplitude. Additionally, phosphene perception has been found to have poor temporal correlation with the duration of the electrical stimuli. They were frequently reported to last less than 2 s, despite persisting electrical stimulation, and there is a wide inter-subject variability (Pérez Fornos et al., 2012). Due to the number of factors involved and the variability in perception within and between subjects, the actual number of pixels required to produce useful vision has remained difficult to predict.

3. Clinical outcomes

Despite a plethora of theoretical predictions and extensive animal testing, confirmation of successful stimulation of the inner retina with matching perceptions by the patients has only become available since the commencement of long-term human implantation trials. The Argus I trial began in 2002 and the international multi-centre phase II clinical trial of the Argus® II began in 2007 (ClinicalTrials.gov Identifier: NCT00407602).

3.1. Safety profile

Given that the aim of the Argus® II programme was to develop a commercially implantable retinal prosthesis, the safety of chronic implantation was central to the early clinical studies. The interim report of a 6-month to 2.7-year follow-up of the first 30 Argus® II patients showed a good initial safety profile, with 21 patients (70%) manifesting no severe adverse events (SAEs) during this period (Humayun et al., 2012). Of the 9 patients who experienced SAEs, the commonest complication was conjunctival erosion or dehiscence (5 patients). All except one of them were satisfactorily treated with re-suturing. This patient suffered from recurrent conjunctival erosion, hypotony with 360° choroidal effusions and retinal detachment, resulting in subsequent explantation of the device. The retinal detachment was successfully treated post-explantation with silicone oil tamponade and the patient's intraocular pressure returned to normal without further sequelae. Other SAEs included: 2 cases of retinal detachment (including the above-mentioned patient), 2 cases of hypotony with choroidal effusions (including the above-mentioned patient), 3 cases of culture-negative presumed endophthalmitis and 2 cases of retinal tack dislocation requiring re-tacking. Except for the one patient who underwent eventual explantation, all of the other patients' SAEs were treated successfully either surgically or medically (e.g. intravitreal antibiotics for

endophthalmitis), and they retained good functional use of their device during the follow-up period. Most of the SAEs (82%) occurred within the first 6 months, with 70% occurring within the first 3 months. After some protocol adjustment halfway through the trial including device design improvement, surgical modifications, and the addition of a prophylactic intra-vitreal antibiotic injection at the end of surgical implantation, the rate of SAEs reduced significantly, and there were no further cases of endophthalmitis in the second half of the study (i.e. the last 15 cases) (Humayun et al., 2012).

More recently, Rizzo et al. (2014) reported the outcome of a 12-month follow-up of 6 patients who received the implant in a single centre performed by a single surgeon. There were no SAEs such as wound dehiscence, endophthalmitis or retinal detachment that required further surgery. There was one patient with post-operative elevation of intraocular pressure which was managed medically, and one patient with moderate choroidal detachment which resolved spontaneously. These outcomes are markedly better than the safety profile observed during the clinical trial phase of the Argus® II Retinal Prosthesis.

3.2. Visual function

The level and nature of vision afforded by the current generation of visual prostheses falls below the level that is normally assessed with standard visual acuity tests (e.g. logMAR/Snellen acuity, contrast sensitivity). As such, new ways of assessing visual function have been proposed and validated and these will be discussed below.

As the Argus® II Retinal Prosthesis System can be switched off, each Argus® II patient has been used as the internal control and their visual function was assessed by comparing tasks carried out with the device switched on versus off. The range of visual function facilitated by the use of the Argus® II Retinal Prosthesis can be grossly categorised into: a) form discrimination/recognition; b) target localisation; c) motion detection; and d) navigation.

3.2.1. Form discrimination/recognition

The ability to differentiate visual forms with the view to recognising objects and elements of 'real life' relies on 2 assumptions: a) stimulating electrodes are able to reproducibly elicit distinguishable, discrete phosphenes; and b) the phosphenes are represented in a retinotopic manner to convey spatial resolution. These assumptions have been tested and will be discussed under the following 3 headings:

1. Direct Electrode Stimulation Studies;
2. Two-Dimensional Screen-based Studies; and
3. Three-Dimensional Object Recognition Study.

3.2.1.1. Direct electrode stimulation studies. To test the retinotopic correlations of the electrodes in the array, Dorn et al. (2010) bypassed the use of video-camera for image capture, and directly activated the electrode array with known geometric patterns (e.g. parallel lines, "H", "L" and triangles) via VPU control. They demonstrated that in one patient, the stimulation pattern of the electrode array corresponded well with the visual percept and allowed recognition of complex geometric forms.

With direct electrode stimulation, Lauritzen et al. (2011) sought to estimate the spatial resolution of Argus® II subjects by systematically stimulating single and paired electrodes to find the minimal electrode separation that allowed perception of 2 discrete phosphenes. As expected, the probability of resolving 2 separate phosphenes increased with increasing inter-electrode separation. However other factors, such as electrode–retina distance, also affected two-point discrimination. In general, the authors found a strong correlation between a subject's ability to resolve 2 phosphenes at a given inter-electrode distance, and their visual acuity measured by identifying the orientation of gratings as described by Caspi et al. (2009) (see section 1.6). As with many other early Argus® II studies, the studies were performed on a relatively small number of patients.

3.2.1.2. Two-dimensional screen-based studies. The direct electrode stimulation studies discussed above suggested that form vision was viable and further studies moved onto assessing the use of the Argus® II Retinal Prosthesis with external camera image capture.

With the camera as the source of input and the restricted visual field (20° visual angle at best) afforded by the Argus® II Retinal Prosthesis, the patients tend to use a head scanning technique as a way of systemically surveying an area of interest, in order to identify the position and form of a shape or object in space. Due to this scanning manoeuvre, there were some doubts as to whether the Argus® II patients were in fact using the device as a light detection device, and that form vision was inferred from the proprioceptive information from head scanning rather than true perception of form from the elicited visual percepts. In order to address this query, a "signal-scrambling" mode control was introduced in later studies. "Signal-scrambling" mode (hereinafter referred to as scrambled mode) allows transmission of electrical impulses to the electrode array, but the pattern of array activation is systemically altered such that it no longer reflects spatial form, essentially turning the Argus® II into a light detection device (Caspi et al., 2009). For example, if the subject were looking at a white line on a black background in standard mode, a line of electrodes would be activated. However, in scrambled mode, the same number of electrodes would be activated in random positions across the array without any resemblance of linearity. If the subject were using the Argus® II as a light detection device and inferring form vision, then there would be no difference in outcome between standard and scrambled mode. Conversely, any difference in the performance with the device in standard mode versus scrambled mode would therefore reflect the degree of perception of spatial information originating from the device, rather than inference of form from head scanning.

3.2.1.3. Shape recognition. Arsiero et al. (2011) demonstrated in 11 Argus® II patients from Europe that they were able to recognise 8 geometrically distinct, high contrast shapes significantly better with the device switched on than switched off. The shapes were presented in white against a black background on a 15-inch flat LCD screen, 30 cm away from the seated patient (see Fig. 9). Each of the 8 shapes was presented 5 times in random order and the patient was allowed up to 1 min to give a forced-choice answer. The mean percentage of correct identification ± standard deviation (SD) with the System on was 25.0 ± 15.0%, and with the System off was 13.4 ± 4.2% ($P = 0.02$, Wilcoxon Signed Rank test), with a chance rate of 12.5% (see Fig. 10). The accuracy of the shape identification could be significantly improved ($P < 0.001$, Wilcoxon Signed Rank test) by presenting the shapes in schematic outlines rather than in

Fig. 9. Illustration of the 8 geometric solid shapes presented to the patients during the Shapes Recognition study. The shapes were presented in white against a black background on a 15-inch flat LCD screen in random order, 30 cm away from the seated patient. The patient was given up to 1 min to identify each shape. The study was performed with the Argus® II device switched on versus off.

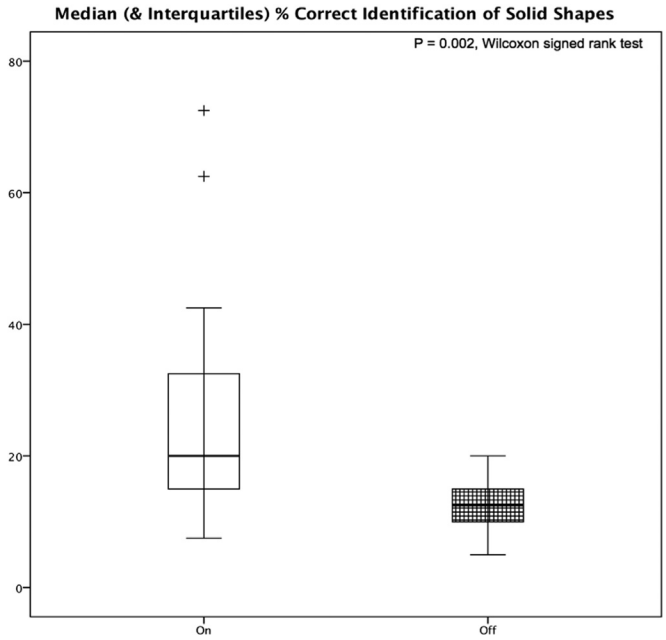

Fig. 10. Box and whisker plot showing the median (and interquartile range) percentage of correct identification of solid shapes with the device switched on versus the device switched off. The patients performed significantly better with the device on versus off (P = 0.002, Wilcoxon Signed Rank Test).

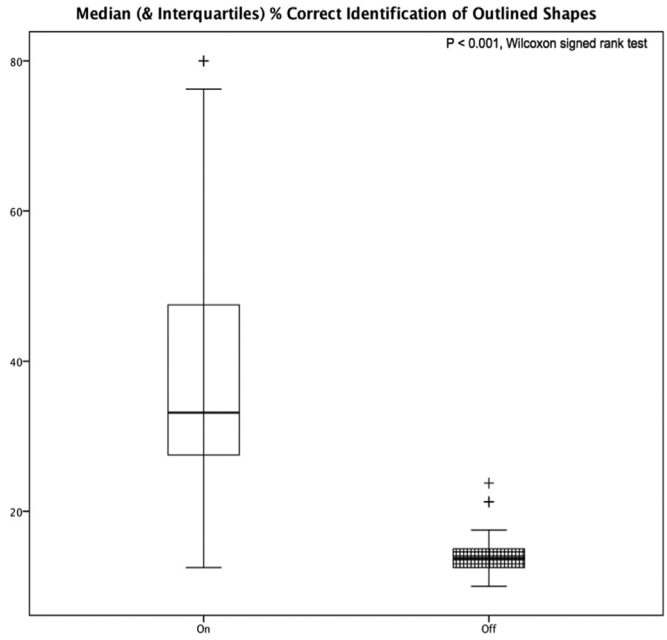

Fig. 12. Box and whisker plot showing the median (and interquartile range) percentage of correct identification of outlined shapes with the device switched on versus the device switched off. The patients performed significantly better with the device on versus off (P < 0.001, Wilcoxon Signed Rank Test).

solid forms (see Figs. 11 and 12). In these outlined forms, the mean percentage of correct identification with the System on was 41.25 ± 16.4%, and with the System off was 15.1 ± 4.4% (P < 0.001, Wilcoxon Signed Rank test).

Within this group of 11 patients, there were 2 patients who performed substantially better than the rest of the group achieving 62.5% and 30% correct identification of the filled-in shapes and 76.25% and 50% correct identification of the outlined shapes respectively.

3.2.1.4. Letter reading. Perhaps the most compelling evidence so far of form vision perception in Argus® II patients was demonstrated by daCruz et al. (2013). The authors investigated the ability of 21 eligible patients to discriminate high contrast, large letters presented on flat LCD screens with the Argus® II System, as a way of assessing spatial resolution (see Fig. 13). Three aspects of letter reading were assessed: a) the ability to resolve letters of different typographical complexity; b) the minimal letter size for letter recognition; and c) the ability to discern clusters of letters separately to enable word recognition.

In the first instance, the letters were divided into 3 groups according to their typographical complexity. All the letters were presented in the same size of 41.27° in height (26.33 cm viewed at 30 cm). Group A consisted of letters of the simplest form, involving only vertical and horizontal lines (i.e. E, F, H, I, J, L, T, U). Group B consisted of letters with oblique components involving the full height of the letter, or letters with a minor variation on the circle (i.e.

Fig. 11. Illustration of the schematic outlines of the 8 geometric shapes (i.e. outlined shapes) presented to the patients during the second part of the Shapes Recognition study. The outlined shapes were also presented in white against a black background on a 15-inch flat LCD screen in random order, 30 cm away from the seated patient. The patient was given up to 1 min to identify each shape.

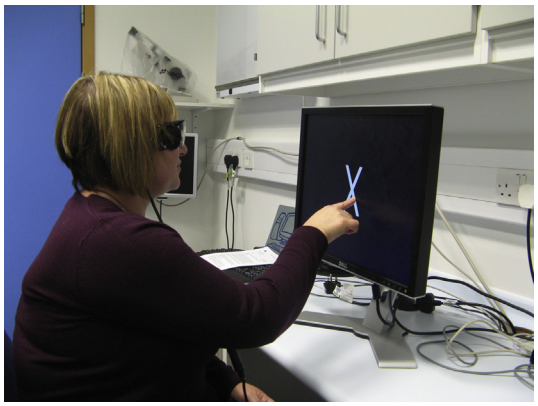

Fig. 13. Photograph showing a patient performing the letter identification task. High contrast, Century Gothic font letters were presented in white on a black LCD screen 30 cm away from the seated patient.

A, C, D, M, N, O, Q, V, W, Z). Group C consisted of letters with an oblique or curved component involving half of the height of the letter (i.e. B, G, K, P, R, S, X, Y). All the 21 patients participated in the identification of Group A letters, 19 patients participated in the identification of Group B letters and 20 patients participated in the identification of Group C letters. Collectively, the patients were able to identify the letters significantly more accurately with the device switched on for all 3 letter groups (mean percentage of correct identification ± standard deviation for Group A letters = 72.3 ± 24.6%; Group B letters = 55.0 ± 27.4%; and Group C letters = 51.7 ± 28.9%), versus the device switched off (17.7 ± 12.9%, 11.8 ± 10.7% and 15.3 ± 7.4% for Group A, B and C letters respectively; P < 0.001 for all 3 groups).

A subset of 6 patients who identified more than 50% of Group A letters correctly under 60 s (i.e. the high-performers) went on to participate in the identification of letters of decreasing sizes. Furthermore, as well as comparing the performance with the device

switched on versus off, scrambled mode control was also introduced in this study. The patients were able to correctly identify the letters significantly better with the device on (standard mode), than in scrambled mode, or with the device switched off ($P < 0.05$ for both comparisons). There did not appear to be much difference in performance with the device in scrambled mode versus the device switched off. The smallest letter identifiable was 1.7° in height (0.90 cm viewed at 30 cm), which is comparable to the theoretical resolution limit of the Argus® II device with 200 μm electrode size and inter-electrode distance (centre-to-centre) of 575 μm (Stronks and Dagnelie, 2014). The minimal letter size identified by these 6 patients, in degrees of visual angle (height in cm viewed at 30 cm) was, in increasing letter sizes: 1.7° (0.9 cm), 2.1° (1.1 cm), 3.4° (1.8 cm), 6.8° (3.6 cm), 6.8° (3.6 cm), and 32.4° (18.0 cm).

Similarly, 4 patients (from the 6 high-performers) were able to identify unrehearsed two-, three- and four-letter words substantially better with the device in standard mode (median number of words recognised = 7 out of 10 words; mean = 6.8 words), than with the device in scrambled mode (median number of words recognised = 0 out of 10 words; mean = 0.3 words), or with the device switched off (median number of words recognised = 0 out of 10 words; mean = 0.5 words). The letter sizes presented were: 33.39° (19.77 cm) for two-, 26.81° (15.16 cm) for three- and 21.33° (11.71 cm) for four-letter words.

The significantly better performance seen with the device in standard mode versus scrambled mode indicated that, at least in the 6 high-performers, letter identification was in part derived from spatial resolution contained within the visual percept, rather than inference from the proprioceptive information from head scanning. Using the aforementioned orientation of gratings method, the best grating visual acuity achieved with Argus® II Retinal Prosthesis to date is logMAR 1.8 (Snellen equivalent of 20/1262) (Humayun et al., 2012).

In comparison, patients from the alpha-IMS sub-retinal implant group were asked to read white letters of 10° (5.30 cm viewed at 30 cm) against a black background (26-alternative forced choice test). Out of a total of 29 patients, 4 patients (14%) correctly identified the letter ≥52% of the time. However, the collective performance of the subjects was not statistically significantly better with the implant switched on versus off (Stingl et al., 2015).

3.2.1.5. Three-dimensional object recognition study. Following on from the screen-based Shape Recognition Study, Luo et al. (2014a) further investigated a subset of 7 patients from the UK to look at their ability to recognise 8 common daily life objects. The 8 objects were suggested by the study patients to reflect objects that they would encounter in daily life (see Fig. 14). All of the objects were presented in high contrast settings (i.e. white/metallic objects against a black felt background) in ambient room light. Each object was presented twice in random order per trial, and the patient was allowed 30 s to give a forced-choice answer. The trials were performed with the Argus® II System under 3 settings: a) device on (standard mode), b) device in scrambled mode, and c) device off.

The results showed that the patients were able to identify the objects significantly better with the device in standard mode and in scrambled mode, than with the device off (see Fig. 15). The mean percentage of correct identification ± standard deviation was: 35.7 ± 14.6% with the device on (standard mode), 27.2 ± 12.8% with the device in scrambled mode, and 12.5 ± 7.2% with the device off, with a chance rate of 12.5% ($P = 0.016$, Friedman test). However, there was no statistical difference in the performance with the device in standard mode versus scrambled mode ($P = 0.193$, Wilcoxon Signed Rank test), indicating that the patients used other clues such as overall luminance and size to identify the objects, rather than the visual form.

Fig. 14. Photograph of the 8 real life objects chosen by the patients for the Objects Recognition study. All the objects were presented in high contrast settings (i.e. white/metallic objects against black felt background) in ambient room light. Each object was presented twice in random order per trial, and the patient was allowed 30 s to give a forced-choice answer. The trials were performed with the Argus® II system under 3 settings: a) device on (standard mode), b) device off and c) device in scrambled mode.

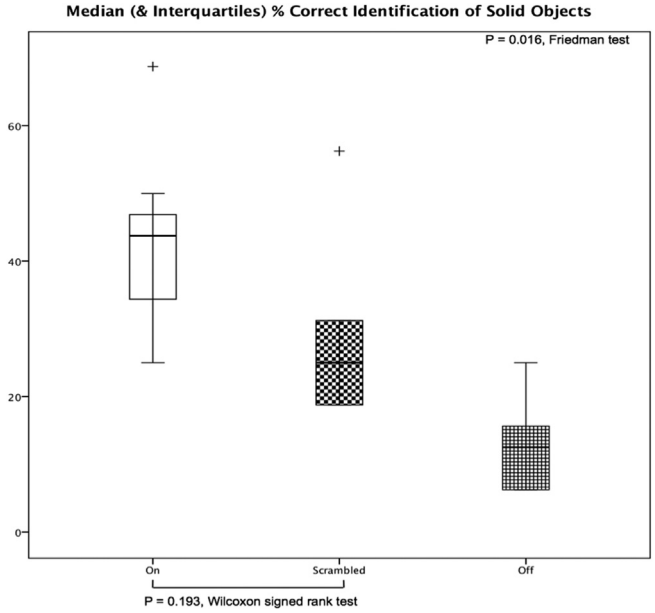

Fig. 15. Box and whisker plot showing the median (and interquartile range) percentage of correct identification of solid objects, with the device switched on (standard mode) versus "scrambled" mode, versus device switched off. The patients were able to identify the objects significantly better with the device on (standard mode) and in scrambled mode, than with the device off ($P = 0.016$, Friedman test). However, there is no statistical difference in the performance with the device in standard mode versus scrambled mode ($P = 0.193$, Wilcoxon Signed Rank test), indicating that the patients used other clues such as overall luminance and size to identify the objects, rather than the visual form.

Similar to the findings from the Shape Recognition Study, the accuracy of object identification could be significantly improved ($P = 0.015$, Wilcoxon Signed Rank test) by enhancing the borders of each object to maximise the contrast at the edges (see Fig. 16). The mean percentage of correct identification of outlined objects was: 35.7 ± 14.6% with the device in standard mode, 27.2 ± 12.9% with the device in scrambled mode, and 12.5 ± 7.2% with the device off ($P = 0.006$, Friedman test). With the outlined objects, the performance was clearly superior with the device in standard mode than in scrambled mode ($P = 0.002$, Wilcoxon Signed Rank test), indicating that the patients were able to use retinotopically represented visual form as well as other non-geometric cues to identify the objects (see Fig. 17).

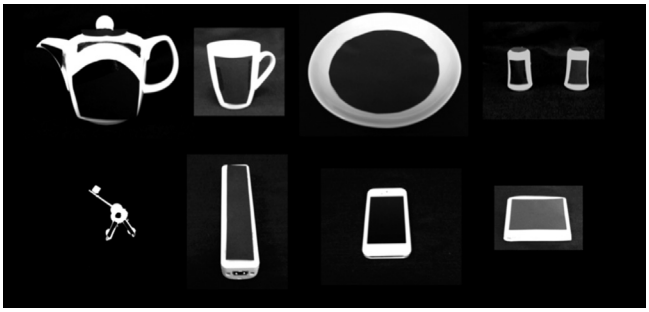

Fig. 16. Photograph of the 8 real life objects partially covered by a cut-out cardboard to enhance their borders and maximise the contrast at the edges (i.e. outlined objects). During the second part of the Object Recognition study, these outlined objects were also presented in high contrast settings (i.e. white/metallic objects against black felt background) in ambient room light. Each object was presented twice in random order per trial, and the patient was allowed 30 s to give a forced-choice answer. The trials were performed with the Argus® II system under 3 settings: a) device on (standard mode), b) device off and c) device in scrambled mode.

Unsurprisingly, the same two patients who performed well in shape recognition and letter reading tasks, also performed substantially better than the rest of the group in this object recognition task, achieving 68.8% and 37.5% correct identification of the solid objects, and 75% and 50% correct identification of the outlined objects respectively. Although the number of the patients is too small to draw any strong conclusions, the results from the above studies suggest that a subset of patients were able to utilise the prosthetic vision to differentiate visual form much more effectively than the rest. The reasons for this difference in performance ability between subjects remain unclear. However, it does appear that the ability to identify screen-based geometric shapes or recognise letters appears to correlate well with the identification of 3-dimensional real life objects.

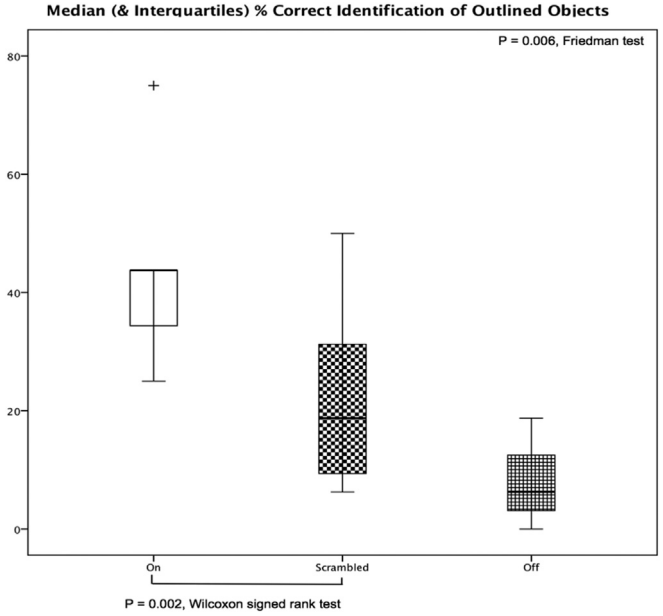

Fig. 17. Box and whisker plot showing the median (and interquartile range) percentage of correct identification of outlined objects, with the device switched on (standard mode) versus "scrambled" mode, versus device switched off. The patients were able to identify the objects significantly better with the device on (standard mode) and in scrambled mode, than with the device off ($P = 0.006$, Friedman test). Moreover, the performance was clearly superior with the device in standard mode than in scrambled mode ($P = 0.002$, Wilcoxon Signed Rank test), indicating that the patients were able to use retinotopically represented visual form as well as other non-geometric cues to identify the objects.

Interestingly, the outcomes of the 2 high-performers far exceeded the predictions from the simulated pixelated vision study (described in section 2.2.2), in which the normal sighted participants were able to describe the object, but were unable to correctly identify the object with the simulated 6×10 pixelated vision. The use of forced-choice answer design in this study may have improved the accuracy of identification, while additional training and practice in the post-operative period, as demonstrated in the simulation study, may also have improved the outcome.

Multiple regression analysis from the letter reading study suggested that younger age at the time of device implantation was a statistically significant indicator of better performance, possibly reflecting relatively healthier residual retina status in these younger patients (daCruz et al., 2013). Other factors such as a greater number of electrodes activated at the time of study, and a later age of diagnosis were also plausible indicators of a favourable outcome, but neither achieved statistical significance in the analysis.

3.2.2. Target localisation

One of the main criticisms of the use of an external camera for image capture in a retinal prosthesis system is the dissociation between the visual scene captured by the camera (which is always directed straight ahead), and that of the patient's eye position. In a normally sighted person, the sense of an object's location within one's visual field is directly correlated with the position of the image on the retina and its displacement from the fovea. As such, proprioceptive skills such as hand–eye co-ordination are often developed in relation to one's eye position. In an Argus® II patient, the image captured by the external camera is always projected onto a fixed area of the retina determined by the placement of the electrode array. Such misalignment between the camera position and the patient's eye could interfere with the patient's perception of spatial localisation, as demonstrated by Sabbah et al. (2014).

In terms of resolving the head and eye position, however, it has been shown that the Argus® II patients in the clinical trials have developed an effective compensatory mechanism, whereby they were taught to keep their gaze straight ahead at all times while using the device, and to move their head (rather than eyes) to change the direction of gaze. With this technique, 96% of the 27 Argus® II subjects were able to localise and point to bright squares on a touch screen with higher accuracy than without the device (Ahuja et al., 2011). This technique was also effective in localising objects in a 3-dimensional space and allowed for development of hand-camera co-ordination to achieve object prehension with high accuracy and efficiency (66–100% successful prehension with the system on, versus 0% with the system off) (Luo et al., 2014b).

It is interesting to note that most of the patients performed well in this task, and the two high-performers in the form discrimination/recognition tasks did not show superior performance. There was also no statistical difference in the performance of object prehension with the Argus® II system in standard mode versus scrambled mode (Kotecha et al., 2014), as would be expected from the nature of the task. This was another indication that the Argus® II patients relied on mechanisms such as head/neck proprioception, rather than the image location on the retina, to develop hand-camera co-ordination to complete target localisation tasks.

3.2.3. Motion detection

The ability to detect motion relies on the ability of the Argus® II patient to detect sequential changes in the spatial activation of the electrode array, and requires both intact, accurate retinotopy and temporal processing within the inner retina. From a group of 28

patients from the phase II clinical trial, just over half (15/28) were able to detect a high-contrast (white) bar moving across a black screen more accurately with the system on than with their native vision (system off) (Dorn et al., 2013). Of these 15 patients, 10 of them also showed significantly better performance with the system in standard mode versus in scrambled mode, showing some degree of retinotopic preservation in the retina of these patients. However, this outcome could have been confounded by multiple factors, including electric charge leakages and cross-talking between adjacent electrodes, and the synchronised activation of multiple electrodes (Horsager et al., 2010). It is therefore difficult to be certain of the mechanism by which the patients achieved this direction of motion detection, despite it being functionally present.

3.2.4. Navigation/orientation & mobility

To date, the largest report on the performance of Argus® II patients' orientation and mobility functions was by Humayun et al. (2012) in the international clinical trial interim report. The patients were asked to complete 2 tasks: to follow a 15 cm wide × 6 m long white line on a dark floor, and to locate a dark door (1 m wide × 2.1 m high) on a white wall 6 m away. Collectively, the patients performed significantly better at both tasks with the system switched on compared with switched off ($P < 0.05$) at various time points during the follow-up period.

Ultimately, due to the limited visual field and the problem with variable duration of a perceived image despite constant stimulation, the Argus® II Retinal Prosthesis is recommended by the FDA to be used in conjunction with a walking cane or a guide dog as an adjunct to navigation, rather than as an independent device for this purpose.

3.3. Magnetic resonance imaging compatibility

Magnetic resonance imaging (MRI) is a frequently used investigative tool in modern clinical medicine. Of the 30 million MRIs performed annually in the USA (OECD, 2012) 22% are brain scans. As with many chronic implantable devices, MRI compatibility of the Argus® II Retinal Prosthesis would be highly desirable.

Weiland et al. (2012) first assessed the safety of performing MRI scans in Argus® II patients based on in-vitro experimental findings with phantoms. They concluded that MRIs performed up to 3-T field strength in the absence of the external components (i.e. camera-embedded glasses and VPU) should be compatible. Luo et al. (2013) later reported two cases of Argus® II patients who underwent MRI brain scans at 1.5-T for unrelated medical conditions. There was no change in implant position (as seen in colour fundus photographs and optical coherence tomography, OCT) in either patient after the MRI, and no associated complications of implant dislocation or retinal detachment. Functionally, there was no substantial change in electrode impedance and threshold in either patient after the MRI. The patients were able to carry out visual rehabilitation tasks as before the MRI scan, and did not report any subjective change in device functionality after the scan.

Overall, MRI brain scans appear to have no detrimental effect on either the patient or the function of the implant. The Argus® II device produced an artefact of around 50 mm × 50 mm in size which prevented visualisation of orbital structures, but visualisation of surrounding tissues outside this area was unaffected (see Fig. 18).

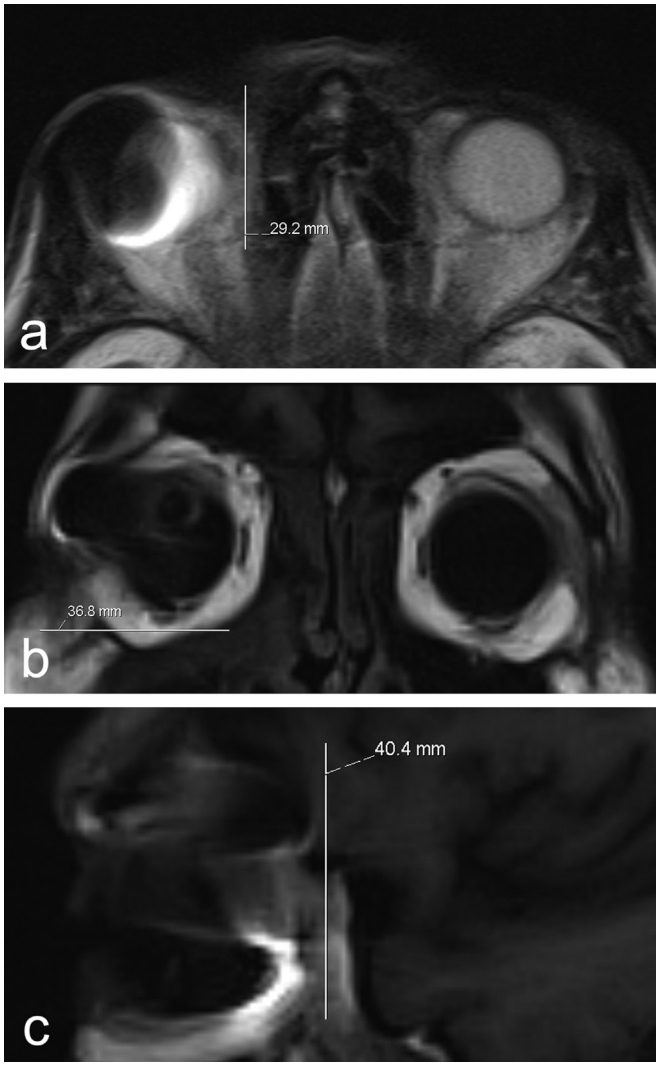

Fig. 18. Magnetic Resonance Imaging at 1.5-T with the Argus II retinal implants in the right eye of two patients, on a) axial T2-weighted, b) coronal T1-weighted and c) sagittal T1-weigthed acquisitions. The measurements are the maximal dimensions of the artifact (in millimetres) in the anterior–posterior (AP), transverse (TR) and superior–inferior (SI) planes.
(Reproduced with permission from Luo et al. (2013).)

4. Future developments

Future developments in the Argus® II Retinal Prosthesis System have been described and envisaged at both the software level and the hardware level of the device.

4.1. Software development

Without changing the current hardware configuration of the Argus® II System, adjustments to the image processing software have already been applied to improve the level of vision obtainable with the device. Early studies on shape and object recognition have shown an improvement in performance by enhancing the outlines of the targets, thereby maximising edge contrast. This finding has led to the on-going development of edge-detection and enhancement as part of image processing. Such innovation has also shown the potential for future software changes to improve patient function, while using the existing device.

Another example of software improvement was recently presented by Sahel et al. (2013), who described an image processing software known as Acuboost™. Acuboost™ utilises a combination of image magnification and minimisation (zoom), as well as some image enhancement features to achieve a visual resolution that exceeds the limit set by the number of electrodes. Using 16× magnification, it allowed one Argus® II patient to achieve an

equivalent vision of logMAR 1.0 (20/200) on gratings acuity measurement, while 4× magnification allowed the patient to read large-print (2.3 cm) letters from a notebook at 30 cm.

Other image processing features under development include signal coding for facial or obstacle recognition, whereby the camera automatically recognises a face (or obstacle), and the image is processed such that the facial image is extracted from the rest of the visual scene and presented alone to the patient in a zoomed-out view. This allows efficient identification and localisation of the face by the patient, and in real-life situations, allows the patient to look at the other person's face during conversations (Stanga et al., 2013).

More experimentally, Horsager et al. (2010, 2011) described the spatiotemporal interaction between adjacent active electrodes. Through phase difference interference of the electromagnetic waves, it may be possible to create intermediate stimulating signals, thereby effectively creating pseudo-electrodes (as observed in cochlear implants) to increase the potential resolution of the retinal implant.

4.2. Hardware development

In terms of hardware development, increasing the number of electrodes with or without reducing the size of the electrodes, and increasing the area of retina stimulated and therefore visual field are the most immediate areas of need.

The Second Sight Company has alluded to a next generation device with possibly 240 electrodes, with the possibility of adding peripheral electrodes to increase the visual field (Stronks and Dagnelie, 2014). In terms of electrode size, the ultimate aim would be to have individual electrodes comparable in size to that of RGC soma so as to allow individual RGC activation. At present this is not possible as the charge density of an electrode, being inversely proportional to the surface area of the electrode (πr^2), renders this calibre of electrode unsafe.

Ahuja et al. have demonstrated that the most critical factor affecting the electrode threshold is the electrode–retina distance (Ahuja et al., 2013; Ahuja and Behrend, 2013). To minimise this electrode–retina distance, OCT-guided custom-made electrode arrays have been proposed, which take into account the different curvatures of individual patients' eyes to maximise array apposition (Opie et al., 2014). Researchers from California Institute of Technology, CA, USA have also described an origami implant design, whereby a 3D integration technique is employed to construct a spherical, 512-channel epiretinal implant conforming to the curvature of the macula. This would allow for larger areas of retina to be stimulated, while maintaining good electrode–retina contact (Liu et al., 2013; Monge and Emami, 2014; Monge et al., 2013).

To mitigate the misalignment between the glasses-mounted external camera position and a patient's eye position (as described in section 3.2.2) so as to improve the patient's perception of spatial localisation, intraocular cameras have been proposed (Hauer and Weiland, 2011; Hauer, 2009). The intraocular camera would be placed within the capsular bag of the crystalline lens after lensectomy, and the visual information could either be transmitted wirelessly to an external VPU for processing before being transmitting back to the epiretinal microelectrode array for stimulation, or the image processing could be performed entirely intraocularly. This has the potential advantage of controlling the direction of vision with eye movements rather than head movements, thereby allowing for the development of more natural hand–eye coordination.

4.3. Deciphering the neural code

Despite the effort to increase the number of stimulating electrodes (thereby improving the potential resolution of the prosthetic vision), and the use of various image processing techniques to maximise the vision obtainable with the current Argus® II System, the functional outcomes remain wanting. The greatest obstacles to progress remain the lack of understanding of the electric field interaction between the active electrodes, the amplitude and frequency coding for signal transmission along the visual pathway to the visual cortex, and signal integration and interpretation at the cortical level. Without an understanding of the signal encoding and integration at this level, improvement in prosthetic vision synthesis would be limited irrespective of the number of electrodes available. This premise has already been demonstrated with the alpha-IMS subretinal implant which despite having 1500 channels in its stimulating array, does not have an appreciably greater acuity, only achieving a visual acuity of logMAR 1.43 (20/546) with Landolt C rings, and grating acuity of up to 3.3 cycles/degree at best (Stingl and Zrenner, 2013).

Nirenberg and Pandarinath (2012) demonstrated the importance of encoding visual information into patterns of action potentials that could potentially be understood by the visual cortex. Using data generated from stimulation of normal mice retina as a model, they developed a signal encoder consisting of a linear–nonlinear (LN) cascade – to capture stimulus/response relations for a broad range of visual stimuli; and the Poisson spike generator – to convert the visual stimuli into corresponding action potential patterns. The signal encoder therefore worked as a retinal input/output model, performing the role of information processing, as would a normal retina.

Using blind *rd* mice and the Channelrhodopsin-2 (ChR2) optogenetic retinal prosthesis model, the authors showed that when visual scenes (captured by an external camera) were presented to the *rd* mice using standard optogenetic retinal prosthesis stimulation without the signal encoder, the RGC firing patterns appeared haphazard. When the visual scenes were processed by the signal encoder first to generate the appropriate patterns for optogenetic prosthetic stimulation, the subsequent RGC firing patterns resembled that of the visual stimulation of a normal retina. Furthermore behaviourally, presentation of shifting sine wave gratings elicited optomotor eye tracking in normal mice as well as in blind *rd* mice stimulated with signal encoder-enhanced optogenetic prosthetic stimulation, but not when the standard optogenetic prosthetic stimulation (without the signal encoder) was applied.

Other groups have also described different models to mimic the intricate image processing carried out by the retina, in the hope of replicating the physiological, interpretable output sent to the visual cortex. Olmedo-Payá et al. (2013) described the *RetinaStudio* model whereby processing of the visual scenes is broken down into 3 stages. The first stage involves splitting the images into the 3 colour channels, red, green and blue (R, G and B), mimicking the outer plexiform layer. The second stage involves spatial filtering using the *Difference of Gaussian (DoG)* filters, mimicking the inner plexiform layer. The third stage mimics the ganglion cell layer, using the leaky-Integrate&Fire spiking neuron model. More importantly, they have also shown that incorporation of the effects of natural eye movements such as micro-saccades, drifts and tremors, improved the modelling of visual processing with greater sensitivity to light changes and improved edge recognition. Lorach et al. (2012) on the other hand, focused on reproducing the spatial and temporal properties of the different major types of RGCs, using an event-based, asynchronous dynamic vision sensor (DVS) to mimic the fundamentally asynchronous nature of biological vision.

Perhaps more promisingly, Jepson et al. (2014) described a method of mapping spatio-temporal patterns of retinal activity in a group of identified RGCs, using a multi-electrode recording system in isolated primate (macaque monkey) retinas. It has been shown

that ON parasol cells in particular could be electrically stimulated with high spatial and temporal precision to match the activity from visual stimuli.

Although an understanding and deciphering of the neural code may be useful, it needs to be remembered that intra-retinal remodelling and aberrant nerve regeneration in the degenerate retina may disrupt and interfere with normal spatio-temporal interaction (Marc et al., 2007, 2003). As such, it may be that the signal characteristics need to be individualised to account for the variance in disease and the state of the patient's residual retina.

5. Conclusion

The Argus® II Retinal Prosthesis System has played an important role in establishing retinal prostheses as a viable and potentially beneficial treatment option in blinding outer retinal conditions. The ability of this device to provide stable, chronic retinal stimulation in a relatively safe manner over many years has been recognised and has led to regulatory approval across many countries. However, despite the increasing volume of published outcomes from clinical trials using the Argus® II device and a cumulative experience of over two hundred patient years, it still remains difficult to predict the outcome and usefulness of the device for a given patient. The future development of this treatment option will depend not only on improvements in the device hardware and software, but also on a greater understanding of retinal and central neural pathology. Furthermore, any scientific advances will have to address the specific functional needs of the recipient patient group, before the milestone achieved by the Argus® II as a first generation retinal prosthesis consolidates into a routine treatment for blinding outer retinal diseases.

References

Abramian, M., Dokos, S., Morley, J.W., Lovell, N.H., 2010. Activation of ganglion cell axons following epiretinal electrical stimulation with hexagonal electrodes. Conf. Proc. IEEE Eng. Med. Biol. Soc. 2010, 6753–6756. http://dx.doi.org/10.1109/IEMBS.2010.5626002.

Abramian, M.M., Lovell, N.H.N., Morley, J.W.J., Suaning, G.J.G., Dokos, S.S., 2011. Activation of retinal ganglion cells following epiretinal electrical stimulation with hexagonally arranged bipolar electrodes. J. Neural Eng. 8 http://dx.doi.org/10.1088/1741-2560/8/3/035004, 035004–035004.

Addi, M.M., Dokos, S., Preston, P.J., Dommel, N., Wong, Y.T., Lovell, N.H., 2008. Charge recovery during concurrent stimulation for a vision prosthesis. Conf. Proc. IEEE Eng. Med. Biol. Soc. 2008, 1797–1800. http://dx.doi.org/10.1109/IEMBS.2008.4649527.

Ahuja, A.K., Behrend, M.R., 2013. The Argus™ II retinal prosthesis: factors affecting patient selection for implantation. Prog. Retin. Eye Res. 36, 1–23. http://dx.doi.org/10.1016/j.preteyeres.2013.01.002.

Ahuja, A.K., Dorn, J.D., Caspi, A., McMahon, M.J., Dagnelie, G.G., daCruz, L., Stanga, P., Humayun, M.S., Greenberg, R.J., Argus, I.I.S.G., 2011. Blind subjects implanted with the Argus II retinal prosthesis are able to improve performance in a spatial-motor task. Br. J. Ophthalmol. 95, 539–543. http://dx.doi.org/10.1136/bjo.2010.179622.

Ahuja, A.K., Yeoh, J., Dorn, J.D., Caspi, A., Wuyyuru, V., McMahon, M.J., Humayun, M.S., Greenberg, R.J., daCruz, L., 2013. Factors affecting perceptual threshold in Argus II retinal prosthesis subjects. Transl. Vis. Sci. Technol. 2, 1. http://dx.doi.org/10.1167/tvst.2.4.1.

Arsiero, M., daCruz, L., Merlini, F., Sahel, J.A., Stanga, P.E., Hafezi, F., Greenberg, R.J., Group, A.I.S., 2011. Subjects blinded by outer retinal dystrophies are able to recognize shapes using the Argus II Retinal Prosthesis System. In: ARVO Meeting Abstracts 2011, 4951–4951.

Beebe, X., Rose, T.L., 1988. Charge injection limits of activated iridium oxide electrodes with 0.2 ms pulses in bicarbonate buffered saline. IEEE Trans. Biomed. Eng. 35, 494–495. http://dx.doi.org/10.1109/10.2122.

Behrend, M.R., Ahuja, A.K., Humayun, M.S., Chow, R.H., Weiland, J.D., 2011. Resolution of the epiretinal prosthesis is not limited by electrode size. IEEE Trans. Neural Syst. Rehabil. Eng. 19, 436–442. http://dx.doi.org/10.1109/TNSRE.2011.2140132.

Brindley, G.S., 1964. The number of information channels needed for efficient reading. J. Physiol. 44.

Brindley, G.S., Lewin, W.S., 1968a. The visual sensations produced by electrical stimulation of the medial occipital cortex. J. Physiol. 194, 54.

Brindley, G.S., Lewin, W.S., 1968b. The sensations produced by electrical stimulation of the visual cortex. J. Physiol. 196, 479–493.

Brummer, S.B., Turner, M.J., 1977. Electrochemical considerations for safe electrical stimulation of the nervous system with platinum electrodes. IEEE Trans. Biomed. Eng. 24, 59–63. http://dx.doi.org/10.1109/TBME.1977.326218.

Brummer, S.B.S., Robblee, L.S.L., Hambrecht, F.T.F., 1983. Criteria for selecting electrodes for electrical stimulation: theoretical and practical considerations. Ann. N. Y. Acad. Sci. 405, 159–171. http://dx.doi.org/10.1111/j.1749-6632.1983.tb31628.x.

Caspi, A., Dorn, J.D., McClure, K.H., Humayun, M.S., Greenberg, R.J., McMahon, M.J., 2009. Feasibility study of a retinal prosthesis: spatial vision with a 16-electrode implant. Arch. Ophthalmol. 127, 398–401. http://dx.doi.org/10.1001/archophthalmol.2009.20.

Cha, K., Horch, K., Normann, R.A., 1992a. Simulation of a phosphene-based visual field: visual acuity in a pixelized vision system. Ann. Biomed. Eng. 20, 439–449. http://dx.doi.org/10.1007/BF02368135.

Cha, K., Horch, K.W., Normann, R.A., 1992b. Mobility performance with a pixelized vision system. Vis. Res. 32, 1367–1372.

Chen, S.-J., Mahadevappa, M., Roizenblatt, R., Weiland, J., Humayun, M., 2006. Neural responses elicited by electrical stimulation of the retina. Trans. Am. Ophthalmol. Soc. 104, 252–259.

daCruz, L., Coley, B.F., Dorn, J., Merlini, F., Filley, E., Christopher, P., Chen, F.K., Wuyyuru, V., Sahel, J., Stanga, P., Humayun, M., Greenberg, R.J., Dagnelie, G.G., Argus II Study Group, 2013. The Argus II epiretinal prosthesis system allows letter and word reading and long-term function in patients with profound vision loss. Br. J. Ophthalmol. 97, 632–636. http://dx.doi.org/10.1136/bjophthalmol-2012-301525.

Dagnelie, G.G., Barnett, D., Humayun, M.S., Thompson, R.W., 2006. Paragraph text reading using a pixelized prosthetic vision simulator: parameter dependence and task learning in free-viewing conditions. Invest. Ophthalmol. Vis. Sci. 47, 1241–1250. http://dx.doi.org/10.1167/iovs.05-0157.

Dagnelie, G.G., Keane, P., Narla, V., Yang, L., Weiland, J., Humayun, M., 2007. Real and virtual mobility performance in simulated prosthetic vision. J. Neural Eng. 4, S92–S101. http://dx.doi.org/10.1088/1741-2560/4/1/S11.

Dagnelie, G.G., Stronks, H.C., 2014. (16:30) Electrically elicited ERGs and VEPs in Argus II recipients: a window into signal processing in the degenerated RP retina. Doc. Ophthalmol. 1, 34–35.

Dobelle, W.H., 2000. Artificial vision for the blind by connecting a television camera to the visual cortex. ASAIO J. 46, 3.

Dorn, J.D., Ahuja, A.K., Arsiero, M., Caspi, A., McMahon, M.J., Nanduri, D., Greenberg, R.J., Group, A.I.S., 2010. The Argus™ II retinal prosthesis provides complex form vision for a subject blinded by retinitis pigmentosa. In: ARVO Meeting Abstracts 51, p. 3020.

Dorn, J.D., Ahuja, A.K., Caspi, A., daCruz, L., Dagnelie, G.G., Sahel, J.-A., Greenberg, R.J., McMahon, M.J., Group, F.T.A.I.S., 2013. The detection of motion by blind subjects with the epiretinal 60-electrode (Argus II) retinal prosthesis blind subjects and motion detection. JAMA Ophthalmol. 131, 183–189. http://dx.doi.org/10.1001/2013.jamaophthalmol.221.

Foerster, O., 1929. Beiträge zur Pathophysiologie der Sehbahn und der Sehsphäre. J. Psychol. Neurol. 463–485.

Friedman, M.W., 1958. The scleral buckling procedure. Trans. Pac. Coast Otoophthalmol. Soc. Annu. Meet. 39, 319–327 (discussion 327–8).

Greenberg, R.J., Velte, T.J., Humayun, M.S., Scarlatis, G.N., de Juan, E., 1999. A computational model of electrical stimulation of the retinal ganglion cell. IEEE Trans. Biomed. Eng. 46, 505–514.

Grover, S.S., Fishman, G.A.G., Anderson, R.J.R., Tozatti, M.S.M., Heckenlively, J.R.J., Weleber, R.G.R., Edwards, A.O.A., Brown, J.J., 1999. Visual acuity impairment in patients with retinitis pigmentosa at age 45 years or older. Ophthalmology 106, 1780–1783. http://dx.doi.org/10.1016/S0161-6420(99)90342-1.

Guadagni, V., Novelli, E., Piano, I., Gargini, C., Strettoi, E., 2015. Pharmacological approaches to retinitis pigmentosa: a laboratory perspective. Prog. Retin. Eye Res. http://dx.doi.org/10.1016/j.preteyeres.2015.06.005.

Guo, T., Lovell, N.H., Tsai, D., Twyford, P., Fried, S., Morley, J.W., Suaning, G.J., Dokos, S., 2014. Selective activation of ON and OFF retinal ganglion cells to high-frequency electrical stimulation: a computational modeling study. In: Presented at the Engineering in Medicine and Biology Society (EMBC), 2014 36th Annual International Conference of the IEEE IS. IEEE, pp. 6108–6111. http://dx.doi.org/10.1109/EMBC.2014.6945023.

Güven, D., Weiland, J.D., Fujii, G., Mech, B.V., Mahadevappa, M., Greenberg, R., Roizenblatt, R., Qiu, G., Labree, L., Wang, X., Hinton, D., Humayun, M.S., 2005. Long-term stimulation by active epiretinal implants in normal and RCD1 dogs. J. Neural Eng. 2, S65–S73. http://dx.doi.org/10.1088/1741-2560/2/1/009.

Hartong, D.T., Berson, E.L., Dryja, T.P., 2006. Retinitis pigmentosa. Lancet 368, 1795–1809. http://dx.doi.org/10.1016/S0140-6736(06)69740-7.

Hauer, M., Weiland, J.D., 2011. An intraocular camera for retinal prostheses: restoring sight to the blind. In: Advanced Series in Applied Physics. Optical Processes in Microparticles and Nanostructures, pp. 385–429.

Hauer, M.C., 2009. Intraocular camera for retinal prostheses: refractive and diffractive lens systems.

Hayes, J.S., Yin, V.T., Piyathaisere, D., Weiland, J.D., Humayun, M.S., Dagnelie, G.G., 2003. Visually guided performance of simple tasks using simulated prosthetic vision. Artif. Organs 27, 1016–1028. http://dx.doi.org/10.1046/j.1525-1594.2003.07309.x.

Hodgkin, A.L., Huxley, A.F., 1952. A quantitative description of membrane current and its application to conduction and excitation in nerve. J. Physiol. 117, 500–544. http://dx.doi.org/10.1113/jphysiol.1952.sp004764.

Holmes, G., 1945. Ferrier lecture: the organization of the visual cortex in man on JSTOR. In: Presented at the Proceedings of the Royal Society of London Series B.
Horsager, A., Boynton, G.M., Greenberg, R.J., Fine, I., 2011. Temporal interactions during paired-electrode stimulation in two retinal prosthesis subjects. Invest. Ophthalmol. Vis. Sci. 52, 549–557. http://dx.doi.org/10.1167/iovs.10-5282.
Horsager, A., Greenberg, R.J., Fine, I., 2010. Spatiotemporal interactions in retinal prosthesis subjects. Invest. Ophthalmol. Vis. Sci. 51, 1223–1233. http://dx.doi.org/10.1167/iovs.09-3746.
Horsager, A., Greenwald, S.H., Weiland, J.D., Humayun, M.S., Greenberg, R.J., McMahon, M.J., Boynton, G.M., Fine, I., 2009. Predicting visual sensitivity in retinal prosthesis patients. Invest. Ophthalmol. Vis. Sci. 50, 1483–1491. http://dx.doi.org/10.1167/iovs.08-2595.
Humayun, M., Propst, R., de Juan, E., McCormick, K., Hickingbotham, D., 1994. Bipolar surface electrical stimulation of the vertebrate retina. Arch. Ophthalmol. 112, 110–116. http://dx.doi.org/10.1001/archopht.1994.01090130120028.
Humayun, M.S., 2001. Intraocular retinal prosthesis. Trans. Am. Ophthalmol. Soc. 99, 271.
Humayun, M.S., de Juan, E., Dagnelie, G.G., Greenberg, R.J., Propst, R.H., Phillips, D.H., 1996. Visual perception elicited by electrical stimulation of retina in blind humans. Arch. Ophthalmol. 114, 40–46. http://dx.doi.org/10.1001/archopht.1996.01100130038006.
Humayun, M.S., de Juan, E., Weiland, J.D., Dagnelie, G.G., Katona, S., Greenberg, R., Suzuki, S., 1999. Pattern electrical stimulation of the human retina. Vis. Res. 39, 2569–2576.
Humayun, M.S., Dorn, J.D., daCruz, L., Dagnelie, G.G., Sahel, J.-A., Stanga, P.E., Cideciyan, A.V., Duncan, J.L., Eliott, D., Filley, E., Ho, A.C., Santos, A.A., Safran, A.B., Arditi, A., Del Priore, L.V., Greenberg, R.J., Argus II Study Group, 2012. Interim results from the international trial of second sight's visual prosthesis. Ophthalmology 119, 779–788. http://dx.doi.org/10.1016/j.ophtha.2011.09.028.
Humayun, M.S., Freda, R., Fine, I., Roy, A., Fujii, G., Greenberg, R.J., Little, J., Mech, B., Weiland, J.D., de Juan, E.J., 2005. Implanted intraocular retinal prosthesis in six blind subjects. In: ARVO Meeting Abstracts 46, p. 1144.
Humayun, M.S., Weiland, J.D.J., Fujii, G.Y.G., Greenberg, R.R., Williamson, R.R., Little, J.J., Mech, B.B., Cimmarusti, V.V., Van Boemel, G.G., Dagnelie, G.G., de Juan, E.E., 2003. Visual perception in a blind subject with a chronic microelectronic retinal prosthesis. Vis. Res. 43, 2573–2581. http://dx.doi.org/10.1016/S0042-6989(03)00457-7.
Jensen, R.J., Rizzo, J.F., Ziv, O.R., Grumet, A., Wyatt, J., 2003a. Thresholds for activation of rabbit retinal ganglion cells with an ultrafine, extracellular microelectrode. Invest. Ophthalmol. Vis. Sci. 44, 3533–3543.
Jensen, R.J., Ziv, O.R., Rizzo, J.F., 2003b. Thresholds for direct and indirect activation of ganglion cells with an epiretinal electrode: effect of stimulus duration and electrode size. In: ARVO Meeting Abstracts 44, p. 5048.
Jepson, L.H., Hottowy, P., Mathieson, K., Gunning, D.E., Dabrowski, W., Litke, A.M., Chichilnisky, E.J., 2013. Focal electrical stimulation of major ganglion cell types in the primate retina for the design of visual prostheses. J. Neurosci. 33, 7194–7205. http://dx.doi.org/10.1523/JNEUROSCI.4967-12.2013.
Jepson, L.H., Hottowy, P., Weiner, G.A., Dąbrowski, W., Litke, A.M., Chichilnisky, E.J., 2014. High-fidelity reproduction of spatiotemporal visual signals for retinal prosthesis. Neuron 83, 87–92. http://dx.doi.org/10.1016/j.neuron.2014.04.044.
Kolb, H., 2003. How the retina works. Am. Sci. 91, 28–35. http://dx.doi.org/10.4249/Scholarpedia.
Kotecha, A., Zhong, J., Stewart, D., daCruz, L., 2014. The Argus II prosthesis facilitates reaching and grasping tasks: a case series. BMC Ophthalmol. 14, 71. http://dx.doi.org/10.1186/1471-2415-14-71.
Lauritzen, T.Z., Nanduri, D., Weiland, J., Dorn, J.D., McClure, K., Greenberg, R., Group, A.I.S., 2011. Inter-electrode discriminability correlates with spatial visual performance in Argus™ II subjects. In: ARVO Meeting Abstracts 52, p. 4927.
Lilly, J.C., Hughes, J.R., Alvord, E.C., Galkin, T.W., 1955. Brief, noninjurious electric waveform for stimulation of the brain. Science 121, 468–469. http://dx.doi.org/10.1126/science.121.3144.468.
Liu, Y., Park, J., Lang, R.J., Emami-Neyestanak, A., Pellegrino, S., Humayun, M.S., Tai, Y.-C., 2013. Parylene origami structure for intraocular implantation. In: Presented at the Solid-State Sensors, Actuators and Microsystems (TRANSDUCERS & EUROSENSORS XXVII), 2013 Transducers & Eurosensors XXVII: the 17th International Conference on IS – SN – VO. IEEE, pp. 1549–1552. http://dx.doi.org/10.1109/Transducers.2013.6627077.
Lorach, H., Benosman, R., Marre, O., Ieng, S.-H., Sahel, J.A., Picaud, S., 2012. Artificial retina: the multichannel processing of the mammalian retina achieved with a neuromorphic asynchronous light acquisition device. J. Neural Eng. 9 http://dx.doi.org/10.1088/1741-2560/9/6/066004, 066004–066004.
Lovell, N.H., Dokos, S., Preston, P., Lehmann, T., Dommel, N., Lin, A., Wong, Y.T., Opie, N., Hallum, L.E., Chen, S., Suaning, G.J., 2005. A retinal neuroprosthesis design based on simultaneous current injection. In: Presented at the 2005 3rd IEEE/EMBS Special Topic Conference on Microtechnology in Medicine and Biology. IEEE, pp. 98–101. http://dx.doi.org/10.1109/MMB.2005.1548394.
Luo, Y.H.-L., Zhong, J.J., Merlini, F., Anaflous, F., Arsiero, M., Stanga, P.E., daCruz, L., 2014a. The use of Argus® II retinal prosthesis to identify common objects in blind subjects with outer retinal dystrophies. In: Presented at the ARVO Meeting Abstracts, p. 1834.
Luo, Y.-L., Zhong, J., daCruz, L., 2014b. The use of Argus® II retinal prosthesis by blind subjects to achieve localisation and prehension of objects in 3-dimensional space. Graefe's Arch. Clin. Exp. Ophthalmol. = Albrecht von Graefes Archiv fur klinische und experimentelle Ophthalmologie 1–8. http://dx.doi.org/10.1007/s00417-014-2912-z.
Luo, Y.H.-L., Davagnanam, I., daCruz, L., 2013. MRI brain scans in two patients with the Argus II retinal prosthesis. Ophthalmology 120. http://dx.doi.org/10.1016/j.ophtha.2013.04.021, 1711–1711.e8.
Machemer, R., Buettner, H., Norton, E.W., Parel, J.M., 1971. Vitrectomy: a pars plana approach. Trans. – Am. Acad. Ophthalmol. Otolaryngol. 75, 813–820. http://dx.doi.org/10.1016/S0002-7154(71)30199-1.
Machemer, R., Parel, J.M., Norton, E.W., 1972. Vitrectomy: a pars plana approach. Technical improvements and further results. Trans. – Am. Acad. Ophthalmol. Otolaryngol. 76, 462–466. http://dx.doi.org/10.1016/S0002-7154(72)30104-3.
Marc, R.E., Jones, B.W., Anderson, J.R., Kinard, K., Marshak, D.W., Wilson, J.H., Wensel, T., Lucas, R.J., 2007. Neural reprogramming in retinal degeneration. Invest. Ophthalmol. Vis. Sci. 48, 3364–3371. http://dx.doi.org/10.1167/iovs.07-0032.
Marc, R.E., Jones, B.W., Watt, C.B., Strettoi, E., 2003. Neural remodeling in retinal degeneration. Prog. Retin. Eye Res. 22, 607–655.
Margalit, E., Maia, M., Weiland, J.D., Greenberg, R.J., Fujii, G.Y., Torres, G., Piyathaisere, D.V., O'Hearn, T.M., Liu, W., Lazzi, G., Dagnelie, G.G., Scribner, D.A., de Juan Jr., E., Humayun, M.S., 2002. Retinal prosthesis for the blind. Surv. Ophthalmol. 47, 335–356. http://dx.doi.org/10.1016/S0039-6257(02)00311-9.
Mathieson, K., Loudin, J., Goetz, G., Huie, P., Wang, L., Kamins, T.I., Galambos, L., Smith, R., Harris, J.S., Sher, A., Palanker, D., 2012. Photovoltaic retinal prosthesis with high pixel density. Nat. Phot. 6, 391–397. http://dx.doi.org/10.1038/nphoton.2012.104.
Menzel-Severing, J.J., Laube, T.T., Brockmann, C.C., Bornfeld, N.N., Mokwa, W.W., Mazinani, B.B., Walter, P.P., Roessler, G.G., 2012. Implantation and explantation of an active epiretinal visual prosthesis: 2-year follow-up data from the EPIRET3 prospective clinical trial. Eye (Lond.) 26, 501–509. http://dx.doi.org/10.1038/eye.2012.35.
Milam, A.H., Li, Z.Y., Fariss, R.N., 1998. Histopathology of the human retina in retinitis pigmentosa. Prog. Retin. Eye Res. 17, 175–205.
Monge, M., Emami, A., 2014. Design considerations for high-density fully intraocular epiretinal prostheses. In: Presented at the Biomedical Circuits and Systems Conference (BioCAS), 2014 IEEE IS – SN – VO. IEEE, pp. 224–227. http://dx.doi.org/10.1109/BioCAS.2014.6981703.
Monge, M., Raj, M., Honarvar-Nazari, M., Chang, H.-C., Zhao, Y., Weiland, J., Humayun, M., Tai, Y.-C., Emami-Neyestanak, A., 2013. A fully intraocular 0.0169 mm^2/pixel 512-channel self-calibrating epiretinal prosthesis in 65 nm CMOS. In: Presented at the Solid-State Circuits Conference Digest of Technical Papers (ISSCC), 2013 IEEE International IS. IEEE, pp. 296–297. http://dx.doi.org/10.1109/ISSCC.2013.6487742.
Nadig, M.N., 1999. Development of a silicon retinal implant: cortical evoked potentials following focal stimulation of the rabbit retina with light and electricity. Clin. Neurophysiol. 110, 1545–1553.
Nanduri, D., 2011. Prosthetic Vision in Blind Human Patients: Predicting the Percepts of Epiretinal Stimulation. University of Southern California Dissertations and Theses. University of Southern California.
Nanduri, D., Dorn, J.D., Humayun, M.S., Greenberg, R.J., Weiland, J.D., 2011. Percept properties of single electrode stimulation in retinal prosthesis subjects. In: ARVO Annual Meeting Abstract Search and Program Planner 2011, 442–442.
Nanduri, D., Fine, I., Horsager, A., Boynton, G.M., Humayun, M.S., Greenberg, R.J., Weiland, J.D., 2012. Frequency and amplitude modulation have different effects on the percepts elicited by retinal stimulation. Invest. Ophthalmol. Vis. Sci. 53, 205–214. http://dx.doi.org/10.1167/iovs.11-8401.
Nanduri, D., Humayun, M.S., Greenberg, R.J., McMahon, M.J., Weiland, J.D., 2008. Retinal prosthesis phosphene shape analysis. Conf. Proc. IEEE Eng. Med. Biol. Soc. 2008, 1785–1788. http://dx.doi.org/10.1109/IEMBS.2008.4649524.
Nirenberg, S., Pandarinath, C., 2012. Retinal prosthetic strategy with the capacity to restore normal vision. Proc. Natl. Acad. Sci. U. S. A. 109, 15012–15017. http://dx.doi.org/10.1073/pnas.1207035109.
Normann, R.A., Greger, B., House, P., Romero, S.F., Pelayo, F., Fernandez, E., 2009. Toward the development of a cortically based visual neuroprosthesis. J. Neural Eng. 6, 035001. http://dx.doi.org/10.1088/1741-2560/6/3/035001.
OECD, 2012. Magnetic resonance imaging (MRI) exams, total 2012/2. oecd-ilibrary.org. http://dx.doi.org/10.1787/mri-exam-total-table-2012-2-en.
Olmedo-Payá, A., Martínez-Álvarez, A., Cuenca-Asensi, S., Ferrández-Vicente, J., Fernandez, E., 2013. Modeling the effect of fixational eye movements in natural scenes. In: Ferrández Vicente, J., Álvarez Sánchez, J., la Paz López, de F., Toledo Moreo, F.J. (Eds.), Lecture Notes in Computer Science, Lecture Notes in Computer Science. Springer, Berlin, Heidelberg, pp. 332–341. http://dx.doi.org/10.1007/978-3-642-38637-4_34.
Opie, N.L., Ayton, L.N., Apollo, N.V., Ganesan, K., Guymer, R.H., Luu, C.D., 2014. Optical coherence tomography-guided retinal prosthesis design: model of degenerated retinal curvature and thickness for patient-specific devices. Artif. Organs 38, E82–E94. http://dx.doi.org/10.1111/aor.12287.
Palanker, D., Huie, P., Vankov, A., Aramant, R., Seiler, M., Fishman, H., Marmor, M., Blumenkranz, M., 2004. Migration of retinal cells through a perforated membrane: implications for a high-resolution prosthesis. Invest. Ophthalmol. Vis. Sci. 45, 3266. http://dx.doi.org/10.1167/iovs.03-1327.
Panetsos, F., Diaz-De Cerio, E., Sanchez-Jimenez, A., Herrera-Rincon, C., 2009. Thalamic visual neuroprostheses: comparison of visual percepts generated by natural stimulation of the eye and electrical stimulation of the thalamus. In: Presented at the Neural Engineering, 2009. NER '09. 4th International IEEE/EMBS Conference on, pp. 56–59. http://dx.doi.org/10.1109/NER.2009.5109233.
Panetsos, F., Sanchez-Jimenez, A., Cerio, E.D.-D., Diaz-Guemes, I., Sanchez, F.M.,

2011. Consistent phosphenes generated by electrical microstimulation of the visual thalamus. An experimental approach for thalamic visual neuroprostheses. Front. Neurosci. 5, 84. http://dx.doi.org/10.3389/fnins.2011.00084.
Pérez Fornos, A., Sommerhalder, J., daCruz, L., Sahel, J.-A., Mohand-Said, S., Hafezi, F., Pelizzone, M., 2012. Temporal properties of visual perception on electrical stimulation of the retina. Invest. Ophthalmol. Vis. Sci. 53, 2720–2731. http://dx.doi.org/10.1167/iovs.11-9344.
Potts, A.M., Inoue, J., 1970. The electrically evoked response of the visual system (EER) III. Further contribution to the origin of the EER. Invest. Ophthalmol. Vis. Sci. 9, 814–819.
Potts, A.M., Inoue, J., 1969. The electrically evoked response (EER) of the visual system. II. Effect of adaptation and retinitis pigmentosa. Invest. Ophthalmol. 8, 605–612.
Potts, A.M., Inoue, J., Buffum, D., 1968. The electrically evoked response of the visual system (EER). Invest. Ophthalmol. Vis. Sci. 7, 269–278.
Rizzo, J.F., Wyatt, J., Loewenstein, J., Kelly, S., Shire, D., 2003a. Methods and perceptual thresholds for short-term electrical stimulation of human retina with microelectrode arrays. Invest. Ophthalmol. Vis. Sci. 44, 5355–5361.
Rizzo, J.F., Wyatt, J., Loewenstein, J., Kelly, S., Shire, D., 2003b. Perceptual efficacy of electrical stimulation of human retina with a microelectrode array during short-term surgical trials. Invest. Ophthalmol. Vis. Sci. 44, 5362–5369.
Rizzo, S., Belting, C., Cinelli, L., Allegrini, L., Genovesi-Ebert, F., Barca, F., Di Bartolo, E., 2014. The Argus II retinal prosthesis: 12-month outcomes from a single-study center. Am. J. Ophthalmol. 157, 1282–1290.
Rose, T.L., Robblee, L.S., 1990. Electrical stimulation with Pt electrodes. VIII. Electrochemically safe charge injection limits with 0.2 ms pulses (neuronal application). IEEE Trans. Biomed. Eng. 37, 1118–1120. http://dx.doi.org/10.1109/10.61038.
Sabbah, N., Authie, C.N., Sanda, N., Mohand-Said, S., Sahel, J.-A., Safran, A.B., 2014. Importance of eye position on spatial localization in blind subjects wearing an Argus II retinal prosthesis. Invest. Ophthalmol. Vis. Sci. 55, 8259–8266. http://dx.doi.org/10.1167/iovs.14-15392.
Sahel, J., Mohand-Said, S., Stanga, P., Caspi, A., Greenberg, R., Argus II Study Group, 2013. Acuboost™: enhancing the maximum acuity of the Argus II Retinal Prosthesis System. In: ARVO Meeting Abstracts 54, p. 1389.
Sakaguchi, H., Kamei, M., Fujikado, T., Yonezawa, E., Ozawa, M., Cecilia-Gonzalez, C., Ustariz-Gonzalez, O., Quiroz-Mercado, H., Tano, Y., 2009. Artificial vision by direct optic nerve electrode (AV-DONE) implantation in a blind patient with retinitis pigmentosa. J. Artif. Organs 12, 206–209. http://dx.doi.org/10.1007/s10047-009-0467-2.
Sakaguchi, H., Kamei, M., Nishida, K., Terasawa, Y., Fujikado, T., Ozawa, M., 2012. Implantation of a newly developed direct optic nerve electrode device for artificial vision in rabbits. J. Artif. Organs 15, 295–300. http://dx.doi.org/10.1007/s10047-012-0642-8.
Santos, A.A., 1997. Preservation of the inner retina in retinitis pigmentosa. Arch. Ophthalmol. 115, 511. http://dx.doi.org/10.1001/archopht.1997.01100150513011.
Schepens, C.L., 1957. The scleral buckling procedures. AMA Arch. Ophthalmol. 58, 797–811. http://dx.doi.org/10.1001/archopht.1957.00940010819003.
Sekirnjak, C., 2006. Electrical stimulation of mammalian retinal ganglion cells with multielectrode arrays. J. Neurophysiol. 95, 3311–3327. http://dx.doi.org/10.1152/jn.01168.2005.
Sekirnjak, C., Hottowy, P., Sher, A., Dabrowski, W., Litke, A.M., Chichilnisky, E.J., 2008. High-resolution electrical stimulation of primate retina for epiretinal implant design. J. Neurosci. 28, 4446–4456. http://dx.doi.org/10.1523/JNEUROSCI.5138-07.2008.
Sekirnjak, C., Hulse, C., Jepson, L.H., Hottowy, P., Sher, A., Dabrowski, W., Litke, A.M., Chichilnisky, E.J., 2009. Loss of responses to visual but not electrical stimulation in ganglion cells of rats with severe photoreceptor degeneration. J. Neurophysiol. 102, 3260–3269. http://dx.doi.org/10.1152/jn.00663.2009.
Sommerhalder, J., Oueghlani, E., Bagnoud, M., Leonards, U., Safran, A.B., Pelizzone, M., 2003. Simulation of artificial vision: I. Eccentric reading of isolated words, and perceptual learning. Vis. Res. 43, 269–283. http://dx.doi.org/10.1016/S0042-6989(02)00481-9.
Sommerhalder, J., Rappaz, B., de Haller, R., Fornos, A.P., 2004. Simulation of artificial vision: II. Eccentric reading of full-page text and the learning of this task. Vis. Res.
Sommerhalder, J.R., Perez Fornos, A., Chanderli, K., Colin, L., Schaer, X., Mauler, F., Safran, A.B., Pelizzone, M., 2006. Minimum requirements for mobility in unpredictable environments. In: ARVO Meeting Abstracts 47, p. 3204.
Stanga, P., Sahel, J., Mohand-Said, S., daCruz, L., Caspi, A., Merlini, F., Greenberg, R., Argus II Study Group, 2013. Face detection using the Argus(R) II retinal prosthesis system. In: ARVO Meeting Abstracts 54, p. 1766.
Sterling, T.D., 1971. Visual Prosthesis, the Interdisciplinary Dialogue.
Stingl, K., Bartz-Schmidt, K.U., Besch, D., Braun, A., Bruckmann, A., Gekeler, F., Greppmaier, U., Hipp, S., Hörtdörfer, G., Kernstock, C., Koitschev, A., Kusnyerik, A., Sachs, H., Schatz, A., Stingl, K.T., Peters, T., Wilhelm, B., Zrenner, E., 2013. Artificial vision with wirelessly powered subretinal electronic implant alpha-IMS. Proc. Biol. Sci. R. Soc. 280, 20130077. http://dx.doi.org/10.1098/rspb.2013.0077.
Stingl, K., Bartz-Schmidt, K.U., Besch, D., Chee, C.K., Cottriall, C.L., Gekeler, F., Groppe, M., Jackson, T.L., MacLaren, R.E., Koitschev, A., Kusnyerik, A., Neffendorf, J., Nemeth, J., Naeem, M.A.N., Peters, T., Ramsden, J.D., Sachs, H., Simpson, A., Singh, M.S., Wilhelm, B., Wong, D., Zrenner, E., 2015. Subretinal visual implant alpha IMS – clinical trial interim report. Vis. Res. 111, 149–160. http://dx.doi.org/10.1016/j.visres.2015.03.001.
Stingl, K., Zrenner, E., 2013. Electronic approaches to restitute vision in patients with neurodegenerative diseases of the retina. Ophthalmic Res. 50, 215–220. http://dx.doi.org/10.1159/000354424.
Stone, J.L., 1992. Morphometric analysis of macular photoreceptors and ganglion cells in retinas with retinitis pigmentosa. Arch. Ophthalmol. 110, 1634. http://dx.doi.org/10.1001/archopht.1992.01080230134038.
Stronks, H.C., Barry, M.P., Dagnelie, G.G., 2013. Electrically elicited visual evoked potentials in Argus II retinal implant wearers. Invest. Ophthalmol. Vis. Sci. 54, 3891–3901. http://dx.doi.org/10.1167/iovs.13-11594.
Stronks, H.C., Dagnelie, G.G., 2014. The functional performance of the Argus II retinal prosthesis. Expert Rev. Med. Dev. 11, 23–30. http://dx.doi.org/10.1586/17434440.2014.862494.
Terasawa, Y., Fujikado, T., Yagi, T., 2002. Simulation of visual prosthesis in virtual space. Int. J. Appl.
Thompson, R.W., 2003. Facial recognition using simulated prosthetic pixelized vision. Invest. Ophthalmol. Vis. Sci. 44, 5035–5042. http://dx.doi.org/10.1167/iovs.03-0341.
Twyford, P., Cai, C., Fried, S., 2014. Differential responses to high-frequency electrical stimulation in ON and OFF retinal ganglion cells. J. Neural Eng. 11, 025001. http://dx.doi.org/10.1088/1741-2560/11/2/025001.
Velikay-Parel, M., Ivastinovic, D., Georgi, T., Richard, G., Hornig, R., 2013. A test method for quantification of stimulus-induced depression effects on perceptual threshold in epiretinal prosthesis. Acta Ophthalmol. 91, e595–602. http://dx.doi.org/10.1111/aos.12179.
Velikay-Parel, M., Ivastinovic, D., Langmann, G., Hornig, R., Georgi, T., Wedrich, A., 2009. First experience with the IRIS retinal implant system. Acta Ophthalmol. 87 http://dx.doi.org/10.1111/j.1755-3768.2009.3115.x.
Walter, P., Heimann, K., 2000. Evoked cortical potentials after electrical stimulation of the inner retina in rabbits. Graefe's Arch. Clin. Exp. Ophthalmol. = Albrecht von Graefes Archiv fur klinische und experimentelle Ophthalmologie 238, 315–318.
Walter, P., Kisvárday, Z.F., Görtz, M., Alteheld, N., Rössler, G., Stieglitz, T., Eysel, U.T., 2005. Cortical activation via an implanted wireless retinal prosthesis. Invest. Ophthalmol. Vis. Sci. 46, 1780–1785. http://dx.doi.org/10.1167/iovs.04-0924.
Wang, K., Li, X.-Q., Li, X.-X., Pei, W.-H., Chen, H.-D., Dong, J.-Q., 2011. Efficacy and reliability of long-term implantation of multi-channel microelectrode arrays in the optical nerve sheath of rabbit eyes. Vis. Res. 51, 1897–1906. http://dx.doi.org/10.1016/j.visres.2011.06.019.
Wang, L., Yang, L., Dagnelie, G.G., 2008. Virtual wayfinding using simulated prosthetic vision in gaze-locked viewing. Optom. Vis. Sci. 85, E1057–E1063. http://dx.doi.org/10.1097/OPX.0b013e31818b9f36.
Weiland, J.D., Anderson, D.J., Humayun, M.S., 2002. In vitro electrical properties for iridium oxide versus titanium nitride stimulating electrodes. IEEE Trans. Biomed. Eng. 49, 1574–1579. http://dx.doi.org/10.1109/TBME.2002.805487.
Weiland, J.D., Faraji, B., Greenberg, R.J., Humayun, M.S., Shellock, F.G., 2012. Assessment of MRI issues for the Argus II retinal prosthesis. Magn. Reson. Imaging 30, 382–389. http://dx.doi.org/10.1016/j.mri.2011.12.005.
Weiland, J.D., Humayun, M.S., Dagnelie, G.G., de Juan, E., Greenberg, R.J., Iliff, N.T., 1999. Understanding the origin of visual percepts elicited by electrical stimulation of the human retina. Graefe's Arch. Clin. Exp. Ophthalmol. = Albrecht von Graefes Archiv fur klinische und experimentelle Ophthalmologie 237, 1007–1013.
Yanai, D., Weiland, J.D., Mahadevappa, M., Fujii, G.Y., de Juan, E.J., Greenberg, R.J., Williamson, R., Cimmarusti, V., Humayun, M.S., 2003. Visual perception in blind subjects with microelectronic retinal prosthesis. In: ARVO Meeting Abstracts 44, p. 5056.
Zrenner, E., Bartz-Schmidt, K.U., Benav, H., Besch, D., Bruckmann, A., Gabel, V.-P., Gekeler, F., Greppmaier, U., Harscher, A., Kibbel, S., Koch, J., Kusnyerik, A., Peters, T., Stingl, K., Sachs, H., Stett, A., Szurman, P., Wilhelm, B., Wilke, R., 2011. Subretinal electronic chips allow blind patients to read letters and combine them to words. Proc. Biol. Sci. R. Soc. 278, 1489–1497. http://dx.doi.org/10.1098/rspb.2010.1747.

Vision Research 111 (2015) 149–160

Contents lists available at ScienceDirect

Vision Research

journal homepage: www.elsevier.com/locate/visres

Subretinal Visual Implant Alpha IMS – Clinical trial interim report

Katarina Stingl [a], Karl Ulrich Bartz-Schmidt [a], Dorothea Besch [a], Caroline K. Chee [b], Charles L. Cottriall [c], Florian Gekeler [a,d], Markus Groppe [c], Timothy L. Jackson [e], Robert E. MacLaren [c], Assen Koitschev [f], Akos Kusnyerik [g], James Neffendorf [e], Janos Nemeth [g], Mohamed Adheem Naser Naeem [b], Tobias Peters [h], James D. Ramsden [l], Helmut Sachs [i], Andrew Simpson [e], Mandeep S. Singh [b], Barbara Wilhelm [h], David Wong [j], Eberhart Zrenner [k,a,*]

[a] Centre for Ophthalmology, University of Tübingen, Schleichstr. 12-16, 72076 Tübingen, Germany
[b] Department of Ophthalmology, National University Health System, 1E Kent Ridge Road, Singapore 119228, Singapore
[c] Oxford Eye Hospital and Nuffield Laboratory of Ophthalmology, University of Oxford, Oxford OX3 9DU, United Kingdom
[d] Klinikum Stuttgart – Katharinenhospital, Eye Clinic, Kriegsbergstraße 60, 70174 Stuttgart, Germany[1]
[e] King's College Hospital and King's College London, Denmark Hill, London SE5 9RS, United Kingdom
[f] Klinikum Stuttgart – Olgahospital, ORL-Department, Pediatric Otorhinolaryngology and Otology, Kriegsbergstr. 62, 70176 Stuttgart, Germany
[g] Department of Ophthalmology, Semmelweis University, Maria utca 39, H-1085 Budapest, Hungary
[h] STZ Eyetrial, Center for Ophthalmology, University of Tübingen, Schleichstr. 12-16, 72076 Tübingen, Germany
[i] Klinikum Dresden Friedrichstadt, Univ. Teaching Hospital, Eye Clinic, Friedrichstr. 41, 01067 Dresden, Germany
[j] Li Ka Shing Faculty of Medicine, University of Hong Kong, 301 Block B, Cyberport 4, Hong Kong
[k] Werner Reichardt Centre for Integrative Neuroscience (CIN), University of Tübingen, Schleichstr. 12-16, 72076 Tübingen, Germany
[l] Department of Otolaryngology, Oxford University Hospitals NHS Trust, Oxford OX3 9DU, United Kingdom

ARTICLE INFO

Article history:
Received 6 May 2014
Received in revised form 18 February 2015
Available online 23 March 2015

Keywords:
Subretinal Implant Alpha IMS
Neuroprosthetics
Retinitis pigmentosa
Artificial vision
Hereditary retinal diseases
Photoreceptor degeneration

ABSTRACT

A subretinal visual implant (Alpha IMS, Retina Implant AG, Reutlingen, Germany) was implanted in 29 blind participants with outer retinal degeneration in an international multicenter clinical trial. Primary efficacy endpoints of the study protocol were a significant improvement of activities of daily living and mobility to be assessed by activities of daily living tasks, recognition tasks, mobility, or a combination thereof. Secondary efficacy endpoints were a significant improvement of visual acuity/light perception and/or object recognition (clinicaltrials.gov, NCT01024803).

During up to 12 months observation time twenty-one participants (72%) reached the primary endpoints, of which thirteen participants (45%) reported restoration of visual function which they use in daily life. Additionally, detection, localization, and identification of objects were significantly better with the implant power switched on in the first 3 months.

Twenty-five participants (86%) reached the secondary endpoints. Measurable grating acuity was up to 3.3 cycles per degree, visual acuities using standardized Landolt C-rings were 20/2000, 20/2000, 20/606 and 20/546. Maximal correct motion perception ranged from 3 to 35 degrees per second. These results show that subretinal implants can restore very-low-vision or low vision in blind (light perception or less) patients with end-stage hereditary retinal degenerations.

1. Introduction

Hereditary retinal degenerations (e.g. retinitis pigmentosa, RP) are characterised by progressive loss of rod and/or cone function over years or decades, frequently leading to blindness in middle age. Several therapeutic approaches are under development for hereditary degeneration of the outer retina, including gene-therapy (Bainbridge et al., 2008; Busskamp et al., 2012; Maguire et al., 2009), electrostimulation (Schatz et al., 2011) and microelectronic visual implants (Humayun et al., 2012; Stingl et al., 2013b; Stingl & Zrenner, 2013b; Zrenner et al., 2011).

Many of the attempts are in preclinical stage; some are in clinical trials. Their applicability depends on various factors: early stages of photoreceptor degenerations may benefit from gene therapy or neuroprotection. Gene replacement therapy has been successfully applied in several gene mutations causing hereditary

* Corresponding author at: Werner Reichardt Centre for Integrative Neuroscience (CIN), Centre for Ophthalmology, University of Tübingen, Schleichstr. 12-16, 72076 Tübingen, Germany. Fax: +49 7071 295038.
E-mail address: ezrenner@uni-tuebingen.de (E. Zrenner).
[1] Present address.

http://dx.doi.org/10.1016/j.visres.2015.03.001
0042-6989/

photoreceptor degenerations (Bainbridge et al., 2008; Maguire et al., 2009), where not only rescue of the remaining vision, but also an improvement in several patients in a 3-years follow-up has been reported (Testa et al., 2013). Neuroprotective effects via release of endogenous growth factors have been demonstrated by transcorneal electrostimulation (Schatz et al., 2011) or intraocularly applied growth factors (Sieving et al., 2006), however their degree of efficacy has not yet been finally evaluated. In late stages of hereditary retinal degenerations rods and cones are almost completely lost. Treatment options considered in such cases are "optogenetics" where inner retina cells are made light sensitive by means of channel rhodopsins, or stem cells, all applied so far not yet in clinical studies. At present only electronic implants are available for patients blind from hereditary retinal degenerations.

Several types of electronic retinal implants have either been approved as commercial products such as Argus II, (Second Sight, Sylmar, CA, see Humayun et al., 2012) and Alpha IMS (Retina Implant AG, Reutlingen, Germany, see Stingl et al., 2013b) or are under development (Ayton et al., 2014; Guenther, Lovell, & Suaning, 2012; Luo & da Cruz, 2014; Menzel-Severing et al., 2012; Stingl & Zrenner, 2013; Zrenner, 2013) for the treatment of hereditary retinal degenerations. Their aim is to restore some vision in end-stage disease for patients who are completely blind or who have light perception without light localization. All of these implants consist of a light-capturing unit (an external camera or an intraocular photodiode array) and an electrode array for stimulation of retinal neurons, mostly those in the inner retina. By electrically stimulating the remaining neurons, the implants initiate a visual percept, replacing to some extent the lost photoreceptor function with artificial vision.

The two types of implants available commercially, the subretinal implant Alpha IMS (Retina Implant AG; Reutlingen, Germany) and the epiretinal implant Argus II (Second Sight, Sylmar, CA) differ in their function in two major aspects: the epiretinal implant has an external head mounted camera and stimulates the ganglion cells of the retina, the third visual pathway neuron whose axons build the optic nerve. The number of stimulation electrodes reaches currently up to 60 and the signal is processed in an external computer and decoded via an epibulbar device that drives the 60 electrodes via transocular wires for an optimal stimulation of the ganglion cells at the retinal output. In contrast, the subretinal implant has a light sensitive 1500 photodiode-array positioned in the layer of the degenerated photoreceptors (subretinally) and stimulates the bipolar cells layer at the retinal input (the second visual pathway neuron, which is connected to the photoreceptors in a healthy eye) and thereby uses the processing power of the neuronal network of the inner retina. The photodiodes are coupled via 1500 amplifiers directly to the stimulation electrodes in an array of independent 1500 "pixels".

A consortium led by the University of Tübingen has been developing various types of active subretinal visual implants since the 1990s (Zrenner, 2002; Zrenner et al., 1999). After preclinical biocompatibility, safety, and biostability tests (Gekeler et al., 2007; Guenther et al., 1999; Kohler et al., 2001; Schwahn et al., 2001), a first wire-bound version of the subretinal implant with 1500 pixels was tested in a pilot study in 11 blind volunteers, where a retroauricular transdermal cable connected the visual implant with an external battery supply. Surprising functional outcomes in three of the subjects, allowing for recognition of unknown objects and even reading large letters, including the detection of spelling errors, were published (Stingl et al., 2013c; Zrenner et al., 2011). Subsequently, a version with wireless transmission of power and signals (transdermally via coils in the retroauricular region, see Figs. 1 and 2), the subretinal implant Alpha IMS of Retina Implant AG, Reutlingen, Germany was implanted in further 29 eyes of 29 blind participants with degeneration of the outer retina in an ongoing clinical trial that consists of module 1 (a single centre study in Tübingen) and module 2 (a multicentre trial at authors' sites). Primary efficacy endpoints were a significant improvement of activities of daily living and mobility shown via activities of daily living tasks, recognition tasks, mobility, or a combination thereof. Secondary efficacy endpoints were a significant improvement of visual acuity/light perception and/or object recognition (clinicaltrials.gov, NCT01024803). Results from the nine participants in module 1 have been published (Stingl et al., 2012, 2013b,c). This manuscript describes the results obtained in the multicentre trial, with a combined analysis of the original nine module-1-participants and the additional 20 participants recruited in module 2.

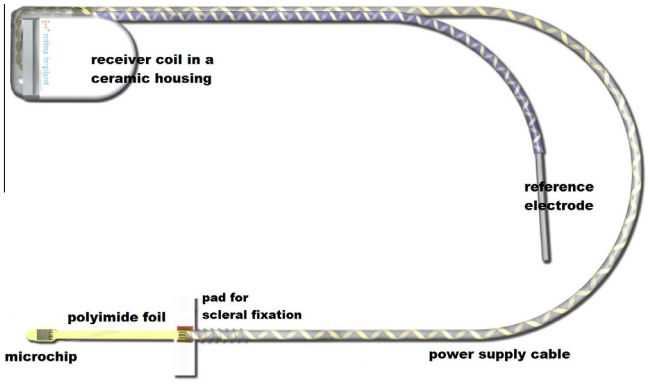

Fig. 1. Retina Implant Alpha IMS: detail on the device. The Retina Implant Alpha IMS consists of the vision chip (multiphotodiodes array) on a polyimide foil (both placed subretinally), a power supply cable connecting the microchip with the receiver coil in a ceramic housing and the reference electrode placed subdermally at the temple and retroauricular region.

2. Material and methods

2.1. Participants

Twenty-nine participants (13 females, 16 males) with a mean age (±standard deviation) of 53.8 ± 8.2 years (range 35–71 years) were enrolled in the clinical trial (www.clinicaltrials.gov, NCT01024803) and received the implant in one eye. Visual function prior to implantation was light perception without projection (20 participants) or no light perception (9 participants) as tested by the ophthalmologist using the standard flashlight test manually by direct illumination of the eye from 5 directions. The loss of vision was caused by hereditary degenerations of the photoreceptors (25 participants had retinitis pigmentosa, 4 had cone-rod dystrophy). None of the participants had other eye diseases that might have affected the visual pathway. Written informed consent was obtained from all participants and the trial was conducted in accordance with the declaration of Helsinki. Research ethics committee approval was obtained for all 7 sites.

2.2. Subretinal Implant Alpha IMS

The Retina Implant Alpha IMS (Fig. 1) consists of a subretinal microphotodiode-array (MPDA, the "microchip") on a polyimide foil and a cable for power supply and signal control, ending in a receiver coil, housed together with electronic circuits in a small subdermal box behind the ear, similar to technology used in cochlear implants (Fig. 2). A separate short cable connects the return electrode to the subdermal box. The MPDA consists of 1500 independent photodiode-amplifier-electrode units, each of which transforms the local luminance information into an electrical current that is amplified for the stimulation of the adjacent

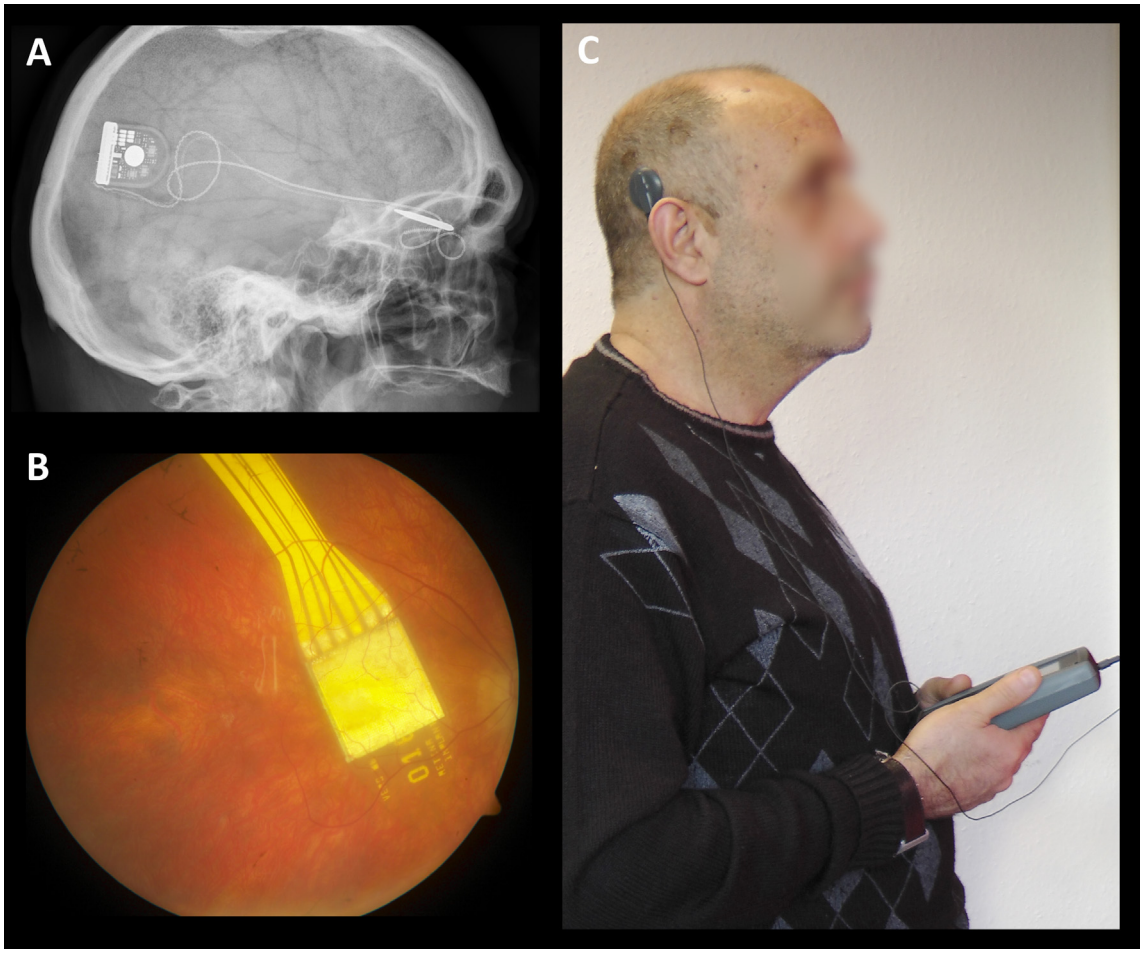

Fig. 2. Retina Implant Alpha IMS: clinical setting. (A) Illustration of the placement of the receiver coil and the power supply cable in an X-ray image. (B) Image of the Retina Implant Alpha IMS on the eye fundus. (C) Handling of the hand held unit: for activation of the visual chip the transmitter coil has to be put on top of the receiver coil and is kept in place magnetically behind the ear. The coils provide a wireless inductive transfer of energy and control signals. The participant can switch on or off the device on the hand held unit, as well as adjust contrast sensitivity and brightness manually via two knobs (adapted from Stingl et al., 2013b).

bipolar cells (Eickenscheidt et al., 2012; Stett et al., 2000) via a 50×50 μm titanium nitride electrode. Thus, a point-by-point electrical image of the luminance information is forwarded to bipolar cells and processed in the inner retina and the afferent visual pathway. Each electrode of the chip typically releases 1 ms pulses in a defined frequency, usually 5 Hz, creating a slightly flickering perception consisting of up to 9 grey levels (Zrenner et al., 2011). As each photodiode-electrode unit theoretically works independently from the neighbouring ones (although in vitro experiments point out that there might be interferences of the electric fields of each electrode), the image reported by the patients reminds of a blurred screen of a black-and white television set allowing for shape perception up to a theoretical two-point resolution of 0.25° of visual angle.

An external battery-driven power supply equipped with a transmitter coil permits an inductive transfer of energy and control signals (Fig. 2). A special feature of the subretinal implant is that the light-to-voltage conversion of the luminance information falling onto the retina, used for electric stimulation of the retinal bipolar cells (Eickenscheidt et al., 2012; Stett et al., 2000), maintains retinotopy in the moving eye. On the external device Retina Implant Alpha IMS has manual adjustment of contrast and brightness for defining the transfer characteristic output curve allowing optimal contrast vision in different luminance conditions. Further technical details have been published earlier (Stingl et al., 2013b; Zrenner et al., 2011, including electronic data supplements).

2.3. Surgical implantation

The subretinal implant was surgically implanted into one eye, under general anesthesia. As depicted in Fig. 2, the polyimide foil that carries the microchip leads subretinally toward the retinal periphery, where it exits the intraocular space through the choroid and sclera. By means of a sealed ceramic connector piece, sutured onto the sclera, the gold wires printed on the foil connect to the round cable that makes a loop within the orbital space (to allow for free eye movement) before it leads to the retroauricular electronic box. Further details on surgical technique have been published (Besch et al., 2008; Sachs et al., 2010).

2.4. Study procedures

Primary efficacy endpoints of the study protocol were a significant improvement of activities of daily living and mobility to be assessed by activities of daily living tasks, recognition tasks, mobility, or a combination thereof. Secondary efficacy endpoints were a significant improvement of visual acuity/light perception and/or object recognition (clinicaltrials.gov, NCT01024803).

Protocol-mandated follow-up extended to 1 year, and included serial retinal imaging with multiple tests of visual function, and adverse event reporting (Stingl et al., 2013a). It was not possible to simulate sham surgery, hence participants served as their own internal controls, comparing the visual function with the implant

power switched on or off. The status of the chip power ON or OFF was not indicated to the patient. Additionally, in most of the patients, tests were performed using light levels that were not visible via the remaining photoreceptors in the eye, if those photoreceptors had retained light perception. The following tests (Stingl et al., 2013a; Zrenner et al., 2011) were repeated in up to 7 follow-up visits during the year of observation.

2.4.1. Basic visual functions ("screen tasks")

Light threshold perception, light source localization, and motion detection of dot patterns were tested on a 60 cm distant screen as 2- or 4-alternatives forced-choice (AFC) tests (Basic Light and Motion – BaLM test) in 8 or 12 trials each. The methodology of the BaLM test that is now mentioned by the FDA as one of the possible tests for electronic implants has been described in detail (Bach et al., 2010, Food and Drug Administration. Investigational Device Exemption Guidance for Retinal Prostheses, 2013) and was used here to measure the secondary endpoints of the study.

The participant was asked whether he/she has seen a flash of light (2AFC, light threshold perception), to localize the illuminated part of the screen (4AFC, light source localization) and to determine the movement direction of a dot pattern (4AFC, motion detection). The first speed tested was 3.3 degrees per second (dps) as the default value set in BaLM. If the participant passed the motion detection, the speed was increased to 5 dps, 7 dps or higher values according to the examiners' consideration. The participant responded via a keyboard or verbally. Due to simplicity of the screen tasks there were no training procedures.

At least 75% (in 2-AFC) or 62.5% (in 4-AFC) correct responses were required to pass the test (defined by the inflection point of the sigmoid psychometric curve). Feedback was given after completion of each test.

2.4.2. Spatial resolution

Grating acuity and visual acuity (VA) with standardized Landolt C-rings in contrast reversal (white ring on black background), the secondary endpoints of the study, were tested on a 60 cm distant screen as 2- or 4-alternatives forced-choice tests in 8 or 12 trials per resolution level. The participant was asked to tell the orientation of the grating and the direction of the C-ring gap respectively. The participants responded via a keyboard or verbally without time limitations. In most of the patients a short training was performed prior to the very first test by showing and explaining the vertical grating pattern and/or the C-Ring in the middle of the screen. At least 75% (in 2-AFC) or 62.5% (in 4-AFC) correct responses were required to pass the test. Feedback was given after completion of each test.

2.4.3. Activities of daily living and recognition tasks

Recognition tasks and activities of daily living (ADL) tasks, the primary endpoints of the study, were performed on a black table using white objects. A short training procedure preceded the tests, except "grey scales", to make the volunteer acquainted with the objects visually and by touch. After completion of each test trial, feedback about correctness of the responses was given. The luminance of the white objects on the table was usually around 200–600 cd/m^2, that of the black table cloth usually below 30 cd/m^2.

2.4.3.1. Geometric shapes. Four objects of about 5° visual angle each were placed in front of the participant, who was not informed about the number of the objects. The participant had to report how many objects were present, point to their position, and describe what they were (shape description and localization) with a timeout of 4 min. Correct responses were documented as scores (from 0 to 4 for each of the three questions; for example, if the patient reported 'I can see three shapes: a circle (points toward the crescent), a triangle (points toward the triangle) and a square (points toward the square)', the documented scores are identification 3, recognition 2 and localization 3).

2.4.3.2. Table setup. Four dining objects (such as cups and cutlery) were placed around a white large plate in front of the participant, who was not informed about the number of the objects. The participant had to report how many objects were present around the plate, localize them, and identify them (shape description) with a timeout of 4 min. Correct responses were documented as scores (from 0 to 4 for each of the three questions).

2.4.3.3. Clock task. White clock hands were placed at angles of 0°, 90° or 180° to each other indicating a clock time. This therefore presented a 16-alternative forced choice test; a response rate above 53% was taken as a pass. The participant was asked to "tell the time" with a timeout of 2 min. During each test (one per study visit) the participant had to read a randomly set clock, 12 times.

2.4.3.4. Letters. Participants were asked to read white letters on a black background (26-alternative forced choice test; a response rate above 52% was taken as a pass). The letter size subtended a visual angle of up to 10°. Timeout of each letter reading was 2 min.

2.4.3.5. Grey levels. The aim of this test was to define the number of grey levels which can be distinguished within the luminance transfer function. An intermediate grey color was presented on one half of a screen with one of six different levels of grey on the other half of the screen: three brighter levels (Michelson contrast in comparison to the intermediate grey 0.29, 0.52 and 0.63) and three darker levels (Michelson contrast in comparison to the intermediate grey 0.96, 0.56 and 0.33). Each of the six combinations was presented three times in random order. Participants were asked which side of the monitor was brighter. Combinations of different grey levels which were distinguished correctly at least twice were documented as recognized. Number of recognized grey scales was the endpoint result of the test. A full screen at the intermediate grey level served as control. There was no timeout for the responses.

The light levels for the screen tests were usually adapted individually to interfere as little as possible with eventually present remaining light perception and light sensitivity of the MPDA was set such that the dark areas of the screen evoked minimum currents and the light areas evoked maximum currents; the bright light level of the screen tasks was usually between 100 and 2500 cd/m^2 and of the black areas approx. 0.1–50 cd/m^2, respectively.

2.4.3.6. Patients' reports. Additionally, patients used the implant at their homes and in daily living and reported subjectively their visual experiences. These reports were documented to analyze improvements in orientation and mobility in daily lives of the participants (one of the primary endpoints of the study).

3. Results

Twenty-one participants (72%) reached the primary efficacy endpoints as set in the study protocol ("significant improvement of activities of daily living and mobility shown via activities of daily living tasks, recognition tasks, mobility, or a combination thereof"). Twenty-five participants (86%) reached the secondary endpoints ("significant improvement of visual acuity/light perception and/or object recognition"). The following paragraphs give details on the performance for the particular tests. For summary of results with the implant switched on for each patient see Table 1.

Table 1
Table shows the best achieved results for each participant in the function tests with the implant power on. In AFC tests (Light perception, Light source localization, clock task, reading letters) " + " indicates the participant passed the test, "–" indicates he/she failed. Motion perception results show the highest speed where the participant was able to distinguish the motion direction correctly ("dps" means degrees per second). Grating acuity results is documented in cycles per degree ("cpd"), the visual acuity as tested by Landolt C-rings in the Snellen fraction. For grey levels the number of correctly distinguished shades of grey is shown. For the categorization of daily life experiences please see the text.

	Light	Location	Motion [dps]	Grating acuity [cpd]	Landolt C VA	Grey levels	Clock	Letters	Daily life experiences
TU-01	–	na	na	na	na	na	–	na	None
TU-02	+	+	–	–	–	na	+	+	Useful
TU-05	+	+	3	0,33	–	na	–	–	Useful
TU-06	+	–	–	–	na	na	–	na	Little
TU-07	+	+	na	0,3	20/2000	na	–	–	Useful
TU-08	+	+	7	0,3	–	3	na	+	Useful
TU-09	+	+	35	3,3	20/546	na	+	+	Useful
TU-10	+	+	5	0,5	–	4	na	–	Little
TU-12	+	+	5	1	–	3	+	+	Little
TU-14	+	+	na	–	na	5	na	na	None
TU-15	+	+	–	1	na	1	–	na	Little
BU-01	–	–	–	–	–	–	–	–	None
BU-02	+	–	–	–	na	4	–	–	Useful
DD-01	+	+	–	–	na	na	na	na	Useful
DD-03	+	–	na	na	na	–	–	–	None
LO-01	+	–	3,3	0,33	na	2	–	na	Useful
LO-07	+	+	–	0,1	na	na	–	+	Useful
LO-08	+	+	–	–	na	na	na	na	None
LO-16	+	+	–	–	na	2	na	na	Little
OX-01	+	–	–	–	–	3	–	–	Little
OX-02	+	+	–	0,33	na	5	–	–	Useful
OX-03	+	–	–	0,33	na	4	–	–	Useful
OX-04	+	+	–	1	–	4	–	–	Useful
OX-05	+	+	–	0,33	–	4	+	–	Little
OX-06	+	+	–	1	20/2000	6	+	–	Useful
SI-01	–	–	–	na	na	na	na	na	None
SI-02	+	–	–	–	–	–	–	–	Little
HK-01	+	–	–	na	20/606	6	–	–	None
HK-02	–	–	–	–	–	–	–	na	None
% passed	86%	59%	21%	48%	14%	52%	17%	14%	45%

"na" means not assessable; the visual function of the patient did not allow to perform the test.

3.1. Primary endpoints

3.1.1. Activities of daily living and recognition tasks

3.1.1.1. ADL: geometric shapes. Scores with implants on and off were compared pair-wise with a non-parametric (Wilcoxon) test. Detection, localization, and recognition of geometric shapes in a good contrast was significantly better with the implant power on compared to off during the first three months (Fig. 3). From the month 6 visits and beyond, the statistical significance decreased ($p > 0.05$) for most of the on–off comparisons, (Fig. 3). This might be due to fewer data, as well as to a slight increase in the performance with the implant power off, as discussed below.

3.1.1.2. ADL: table setup. Scores with the implant on and off were compared pair-wise using all available data and the Wilcoxon test. Detection, localization, and recognition of table objects in a good contrast was significantly better with the implant on compared to off during the first three months (Fig. 3). From the month 6 visits and beyond, the statistical significance decreased ($p > 0.05$) for most of the on–off comparisons (Fig. 3). This might also be due to fewer data and a slight increase in the performance with the implant power off.

3.1.1.3. Clock task. Using the non-parametric (Wilcoxon) test the performance over all subjects was not statistically significantly better with implant on vs. off for the clock task (Fig. 4A). Five participants passed the test at least once during the trial visits and could read the clock hands and tell the time (Table 1). One participant passed the clock task once with the implant turned off.

3.1.1.4. Letters. Using the non-parametric (Wilcoxon) test the performance over all subjects was not statistically significantly better with implant on vs. off for the clock task (Fig. 4B). Four participants passed the test at least once during the trial visits and could read letters (Table 1). Additionally, one participant (TU-12) passed the test with the implant turned on as well as off at the end of the study (month 9), probably using a peripheral residual field with widened pupils, whereas the patient could not read letters at the time of screening; this positive development may be due to beneficial effects described for electrical stimulation treatment (see Section 4).

3.1.1.5. Grey levels. Using the non-parametric (Wilcoxon) test the performance over all subjects was significantly better ($p < 0.05$) with implant on vs. off for grey levels recognition in months 1, 2 and 12 (Fig. 4C).

Fifteen participants (52%) were able to recognize at least one grey level, ranging up to six (only six levels were tested in the present study), compared to an intermediate grey level. The number of grey levels correctly distinguished is illustrated in Table 1. Eight participants (28%) recognized up to three grey levels with the implant off.

3.1.2. Daily life experiences

Participants used the visual implant during their daily life, at home, outdoors, or at work, usually up to 2–3 h daily. The type of vision experienced was described as a blurred image, consisting of shapes of different grey levels, slightly flickering (due to the working frequency of the implant, typically 5 Hz), in a square-shaped visual field of up to 15° diagonally (Stingl et al., 2012, 2013b). Several participants spontaneously reported a slight improvement of the remaining light perception with the implant off during the course of the study; however, none of them could see objects without the implant power being switched on.

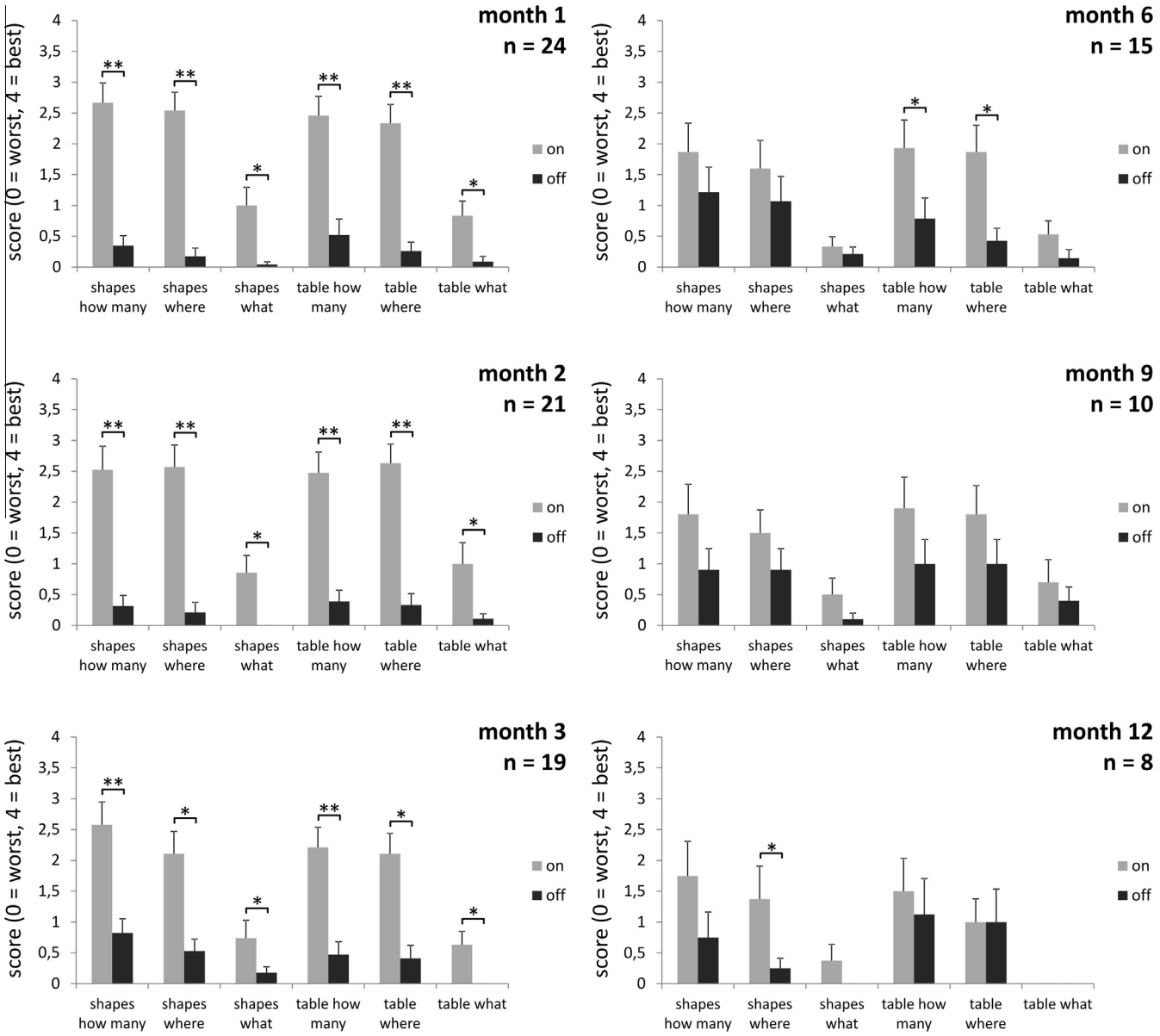

Fig. 3. ADL tasks. ADL tasks for shapes and table setups (see Section 2.4.3). Nonparametric testing showed significant differences between the scores achieved with the implant power switched on vs. off for all test questions in the first three months (see Sections 3.1.1.1 and 3.1.1.2). "*n*" indicates number of participants with available data for the particular visit; * and ** indicate statistic significances of $p < 0.05$ and $p < 0.001$ resp. The value for "table what" score at month 12 is zero.

Eight participants (28%, including the four who did not have any light perception via the implant) did not benefit in daily life. A further eight participants (28%) could localize objects with a good contrast in their daily life, but could not recognize shapes or details (Fig. 5). Thirteen participants (45%) reported useful new daily life experiences with the implant, being able to see shapes and/or details of objects in grey scales (Table 1, Fig. 5). Some of their visual experiences match the criteria of improving independence and social connectedness as proposed recently for the endpoints of visual prostheses (see The Lasker/IRRF Initiative for Innovation in Vision Science, 2014a, chap. 3). The following visual experiences were described with the implant power on (examples).

3.1.2.1. Facial and other personal features. Participants reported seeing the shape of another person's head, mouth, glasses, a baby in a white dress, scarf around the neck, and other features.

3.1.2.2. Buildings. For example, house outlines, windows, town-hall silhouette, and curtain stripes.

3.1.2.3. Outdoors. Street lamps at night showing the direction of the street, pavement lines, arches of a viaduct, landmarks, and others.

3.1.2.4. Vehicles. Car lights moving at night, car reflexions, recognizing different types of buses.

3.1.2.5. Nature. Sunflower stalk, river on the horizon, dog-tail wagging, garden table, moon, and others.

3.1.2.6. Own body. Hand, head silhouette in the mirror, striped jacket in the mirror.

3.1.2.7. Indoors. Such as picture frame on the wall, fluorescent tubes, kitchen objects, plates in a good contrast, bottles, cup handle, washbasin, and bottles on shelves.

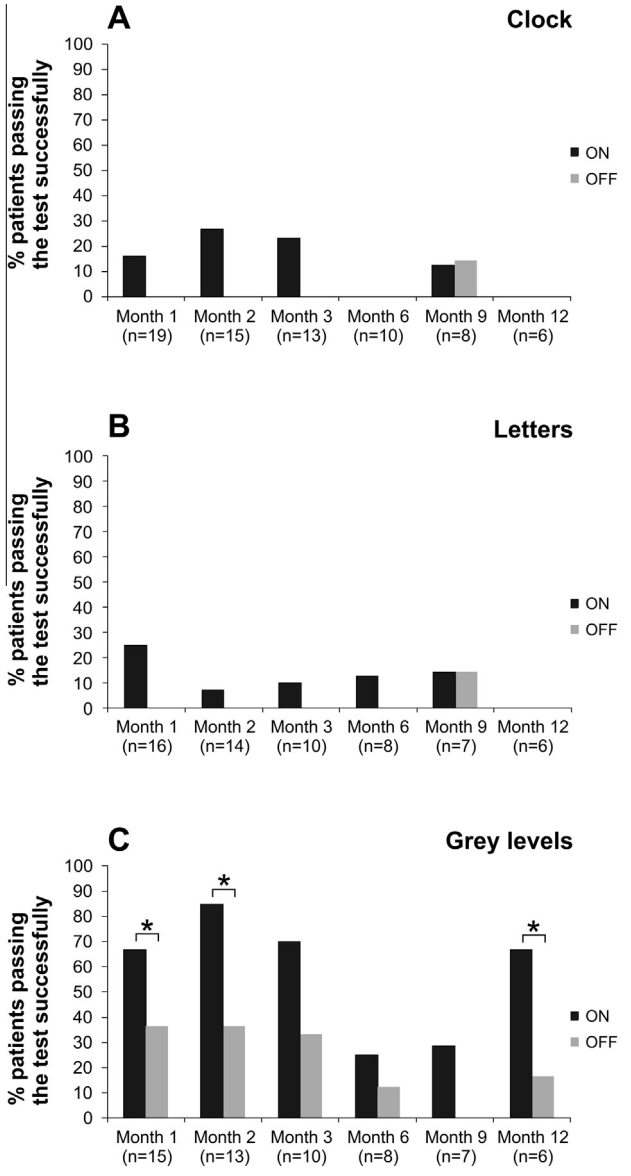

Fig. 4. Recognition tasks. Recognition tasks: (A) clock task, (B) reading letters, (C) recognition of grey levels (for setup see Sections 2.4.3.3–2.4.3.5). The bars depict percentages of patients who passed successfully the particular AFC tasks with the implant power switched on (black bars) and off (grey bars) in all study visits (for details see Sections 3.1.1.3–3.1.1.5). *Above the bars indicate statistical significance ($p < 0.05$) if compared on vs. off in a non-parametric (Wilcoxon) test. "*n*" describes the number of subjects who performed the particular test in the visits.

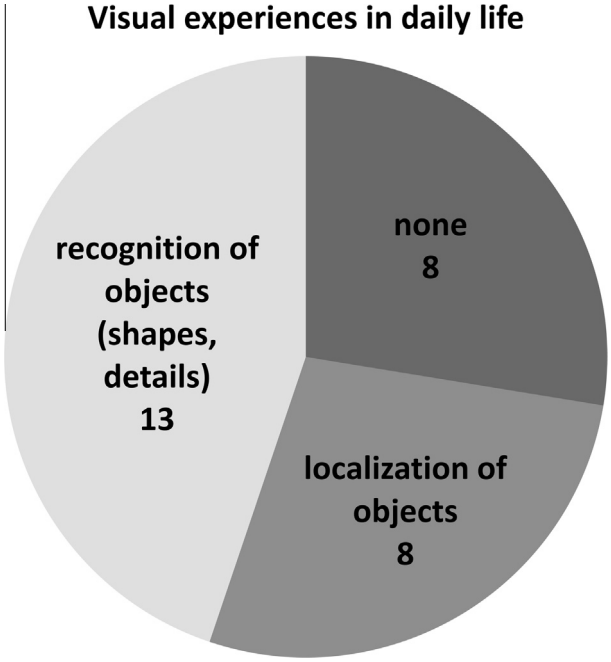

Fig. 5. Daily life experiences. Numbers of participants grouped according to their reports of visual experiences in daily life. Eight participants did not benefit from the visual implant in daily life. Further eight participants could only localize objects. 13 participants reported regained visual experiences with descriptions of shapes or details in scales of grey. For details of the descriptions see Section 3.1.2.

3.2. Secondary endpoints

3.2.1. Basic visual functions

Of 29 participants, four could not perceive any light using the subretinal implant. The most probable reasons in these cases were: (1) intraoperative touch of the optic nerve during device insertion, with subsequent optic disc swelling interrupting MPDA signal propagation by the ganglion cells; (2) retinal edema after implant repositioning; (3) suspected retinal perfusion problems overlying the MPDA; and (4) technical failure of the implant. The remaining 25 participants (86%) were able to perceive light via the subretinal implant tested in a 2 alternative forced choice mode.

Using the non-parametric (Wilcoxon) test the performance over all subjects was significantly better ($p < 0.05$) with implant on vs. off for light perception in all visits and for light localization in months 1, 2, 3 and 6 (Fig. 6A–C).

The highest speed for which the direction was correctly recognized with the implant switched on ranged from 3 to 35 degrees per second (Table 1). With the implant power off, one patient passed the motion task (3.3 degrees per second) in a 4-AFC task once by reaching 62.5% correct responses (Fig. 6C), but volunteered that this was by guessing.

3.2.2. Spatial resolution

Using the non-parametric (Wilcoxon) test the performance over all subjects was significantly better ($p < 0.05$) with implant on vs. off for the grating acuity in months 1, 2 and 3 (Fig. 7).

The grating acuity resolutions with implant power on ranged from 0.1 to 3.3 cycles per degree (Table 1). Five participants passed a 2 alternative forced choice grating acuity task once by reaching 75% correct responses despite chip power being switched off; four of them indicated that it was done by guessing (Fig. 7A), whereas in all five patients the grating acuity with implant power switched off was lower than with the implant power on. Four participants successfully completed standardized visual acuity (VA) testing using contrast reversal Landolt C-rings, with VAs of 20/2000, 20/2000, 20/606 and 20/546 (Table 1).

3.3. Safety

Two serious adverse events (SAEs) were reported during the trial: an increase of intraocular pressure up to 46 mmHg that was successfully treated and resolved without sequelae; and retinal detachment immediately after explantation of the device, treated surgically with laser coagulation and silicone oil, which resolved but with local retinal fibrotic changes.

Safety analyzes of the first, monocentric part of the trial (module 1, see Section 1) have been published recently (Kitiratschky et al., 2014). A detailed description of the whole cohort of the clinical trial safety data, including the non-serious adverse events (AEs) will be presented in another publication. The adverse events

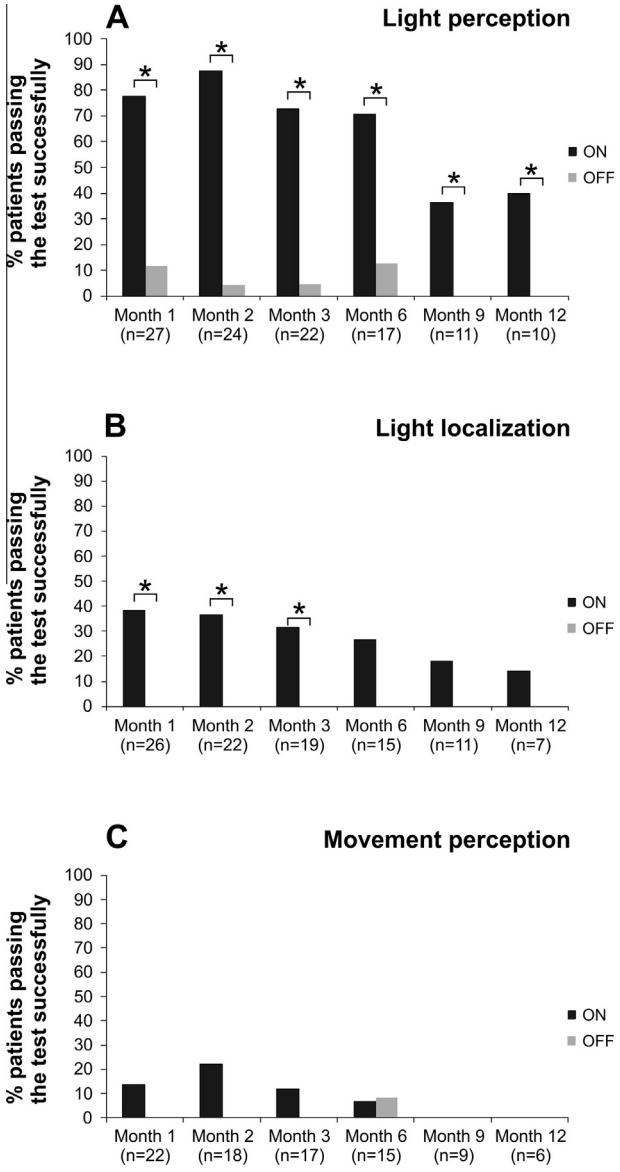

Fig. 6. Basic visual functions ("screen tasks"). Basic visual functions as assessed by the BaLM test: (A) light perception, (B) light localization, (C) movement detections (for setup see Section 2.4.1). The bars depict percentages of patients who passed successfully the particular AFC tasks with the implant power switched on (black bars) and off (grey bars) in all study visits (for details see Section 3.2.1). *Above the bars indicate statistical significance ($p < 0.05$) if compared on vs. off in a non-parametric (Wilcoxon) test. "*n*" describes the number of subjects who performed the particular test in the visits.

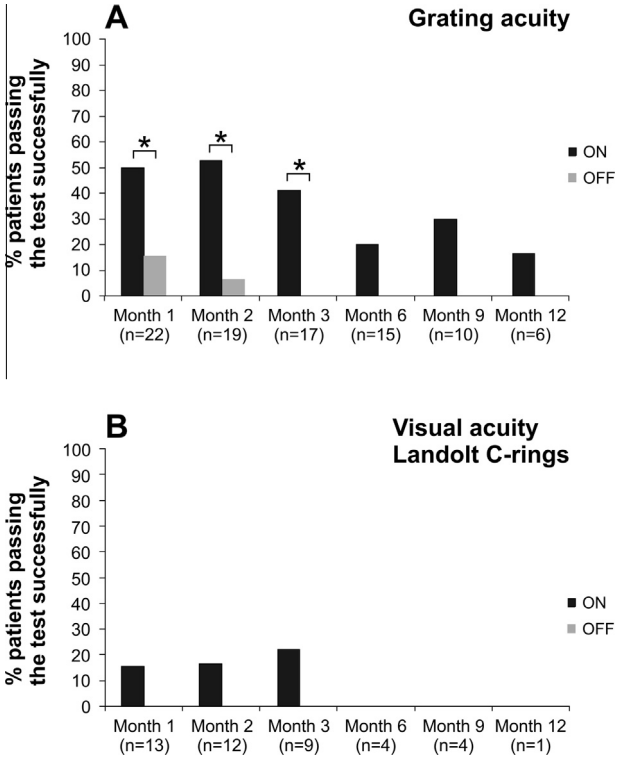

Fig. 7. Spatial resolution. Measures of spatial resolution: (A) grating acuity, (B) visual acuity measured with Landoldt C-rings (for setup see Section 2.4.2). The bars depict percentages of patients who passed successfully the particular AFC tasks with the implant power switched on (black bars) and off (grey bars) in all study visits (for details see Section 3.2.2). *Above the bars indicate statistical significance ($p < 0.05$) if compared on vs. off in a non-parametric (Wilcoxon) test. "*n*" describes the number of subjects who performed the particular test in the visits.

were almost all transient, were treated where possible and did not cause persistent or significant health impairments. Two serious adverse events occuring during module 1 phase could be treated (Kitiratschky et al., 2014).

4. Discussion

These results provide proof of principle that a subretinal implant can restore reliably measurable visual function and potentially useful vision in low-vision or very low-vision range in selected patients with end-stage degenerations of the outer retina such as RP.

Vision with a subretinal implant differs from natural vision in a healthy eye in several ways. Firstly, there is limited spatial resolution. The distance between the light-sensitive photodiodes is 70 μm in a square-shaped-array, allowing for a theoretical maximum VA of approximately 20/250. Preclinical work (Stett et al., 2000) indicates that a distance of less than 50 μm between the single planar electrodes does not improve spatial resolution without additional measures, due to the dissipation of electrical currents within the retinal tissue. Grating acuity and VA results from some of our participants show that the measured VA comes close to this theoretical limit; one participant achieved a grating acuity of 3.3 cycles per degree, corresponding to 20/200. Optotype and grating acuity, however, should not be directly compared (Katz & Sireteanu, 1989), because grating acuity relies on cues derived from angles of lines across a large visual field (even when lines are interrupted), whereas optotype VA depends on the recognition of single optotype features in a very small visual field. The best Landolt C-rings acuity of the same participant was 20/546.

Secondly, electronic implants with planar electrodes do not replicate normal color perception. The images perceived with the subretinal implant are composed of grey levels, as the photodiodes transform the luminance information into an electrical current that, for each electrode, stimulates all color coding bipolar cell types beneath the electrode. Most of the patients are able to distinguish several levels of grey. With a subretinal implant stimulating an end-stage degenerated retina, the 70 μm × 70 μm pixels cover approximately 16 bipolar cells (Stingl et al., 2013c), a number that also depends on the degree of retinal degeneration, with approximately 80% of bipolar cells still present after many years of blindness (Santos et al., 1997). To date, it is not possible to stimulate the cellular connections established earlier in life for green, red and blue selectively and thereby restore natural color vision.

Thirdly, the visual field is limited to the area of the photodiode array. The square of the submacular implant measures

3 mm × 3 mm, which results in a square-shaped visual field of up to 15° of visual angle diagonally. This is sufficient for orientation, given that RP patients can quite well navigate with fields of this size, but it still far more constricted than a normal visual field.

Fourthly, contrast perception and brightness must be adjusted manually in response to ambient illumination and patient preference. On the hand-held battery unit, there are two knobs for manual adjustment of both parameters. With visual training, patients learn to adjust the transmission characteristics of the implant during the first days or weeks after implantation. The procedure is reminiscent of optimizing the image in older black-and-white television sets with two separate knobs for brightness and contrast. The working range of the implant is relatively broad, with luminance from 1 to 100,000 cd/m^2.

Lastly, the perceived image has a blinking character based on the working frequency of the implant. Typically, this is set to 5 Hz, leading to a relatively constant image, but several participants preferred a lower frequency in order to prevent image fading, other reached 20 Hz repetition rate. The origin of these differences in temporal resolution without fading is not clear; there are indications that the ability to use the involuntary microsaccades that allow refreshing the images may play a role and that utilization of such microsaccades may improve over time or that an intrinsic characteristic of the degenerated retina leads to different temporal resolution capability.

Interestingly, the time necessary for re-learning vision is relatively short. Localization of dots and direction of lines was possible usually from the first days, improving within days to weeks to the best possible vision of the particular individual. An evidence for this authors' observation can be taken from the figures Figs. 3, 4, 6 and 7, showing that the results from the "month 1" visit are comparable to visit "month 2", followed by a slight decrease of the functional results from the third month on (caused by technical difficulties as described below).

Activities of daily living as well as real-life visual experiences show that this type of subretinal multi-photodiode array can stimulate the inner retina to obtain a useful perception. The increase in visual function from blindness to a low-vision or very-low vision range can provide significant help for participants who became blind from a chronically progressive degeneration of the retina. The majority of the participants could at least localize objects with a good contrast within their own environments. Almost half of the participants gained useful visual experiences by being able to recognize the details of objects or shapes in real life. The ADL laboratory tests were performed with high contrast (white objects on a black table) and showed a significant improvement of the detection, localization, and identification of objects in the near-vision range, compared to the results with the implant off during the first three months.

The improved vision seen in some participants after several months with the implant power being switched off might possibly be explained by the well-known release of growth factors that occurs after electrical stimulation. Both pre-clinical (Morimoto et al., 2012; Schmid et al., 2009) and clinical studies (Schatz et al., 2011) suggest that this can in turn improve visual function. Indeed, a few participants spontaneously reported an improved light perception with the implant off, especially at the end of the study. Such observations of improvement of remaining vision have been made also in previous attempts to restore vision by subretinal implants in RP patients (Chow et al., 2004). Although those implants – due to very peripheral position and lack of electronic amplification – did not provide vision restoration, central vision in such patients improved considerably, probably due to effects of growth factors (Pardue et al., 2005). We assume that the functional improvements seen in our patients during the course of the study also with non-activated implants may be due to such well established treatment effects after continued electrical stimulation in patients that had still light perception preoperatively.

Additionally, in almost all tests a decrease of function over time with the implant power switched on was observed in a number of participants (Figs. 3, 4, 6 and 7). There are no indications that this phenomenon is caused by biological reasons such as retinal structure changes or local adverse events. Rather, the decrease of the functional performance after implantation was caused by technical failures of the implants occurring in some cases already after 3–12 months after implantation, which is also one of the reasons why the number of participants performing the tests in the later visits decreases. In some patients breaks in the intraorbital cable part caused by the mechanical stress from eye movements occurred (Kernstock et al., 2011). This problem has meanwhile been successfully solved by a surgical technique leading the intraorbital part of the cable in a parabulbar loop minimizing the mechanical stress onto the cable during eye movements, so that this problem did not occur beyond the seventh participant of the trial. Other modes of technical failures have been solved by improving encapsulation of the electronic chip which in laboratory tests showed a considerably prolonged lifetime, currently assessed also in the ongoing clinical trial.

The reaction time was limited to 4 min in the ADL tasks and to 2 min in the recognition tasks. In the screen tasks there were mostly no timeout as usually the responses took several seconds only; however, some participants wanted the pattern presented up to several minutes. The authors learned that this measure is more an expression of the patient's personality than a functionality parameter; some patients report their first impression immediately, whereas many patients try check more times or have difficulties to make a decision in an AFC test, prolonging thus the reaction time although they commented afterwards that their first impression did not change much.

As we published previously, the best visual function is obtained if the chip is located in a subfoveal position (Stingl et al., 2013c; Zrenner et al., 2011). Before surgery, the desired subfoveal position is determined (Kusnyerik et al., 2012). However, due to adhesions, foveal thinning, the curvature of the eye, and the length and flexibility of the polyimide foil, it is not always possible to precisely position the chip. Among the 29 participants, the foveola was on the MPDA in 11 cases, on the chip but close to the MPDA border in 12 cases, and not on the MPDA in 6 cases (usually with a parafoveal position, but up to 3.8 mm away from the nearest chip border). An evaluation of best achieved functional measures for each individual shows also in this cohort, that a parafoveal position most likely limits the best possible spatial resolution (Fig. 6); grating acuity and visual acuity with Landolt C-rings are achievable in more participants and of higher value if the fovea is on the microchip surface (Fig. 8A and B). However, the fovea placement in relation to the microchip does not seem to play a big role for most daily life experiences or the number of distinguishable grey scales (Fig. 8C and D). This might be explained by the low level of vision (low-vision or very-low-vision) that the implant can restore, which is biologically achievable in the whole macular region. Also the amount of distinguishable grey levels is not a direct capability of the fovea alone.

We do not see any direct effect of age or disease duration on the functional outcome. However, the authors have an impression that a kind of ability and motivation to learn a "new perception" and understand the principal function and technical possibilities of the implant might be advantageous, but this is not a measure which could be objectively documented.

Worldwide, currently subretinal, epiretinal, suprachoroidal, cortical and optic nerve implant are under development (Brelén et al., 2010; Humayun et al., 2012; Schmidt et al., 1996; Weiland, Cho, & Humayun, 2011; Zrenner, 2002, 2012, 2013). At present,

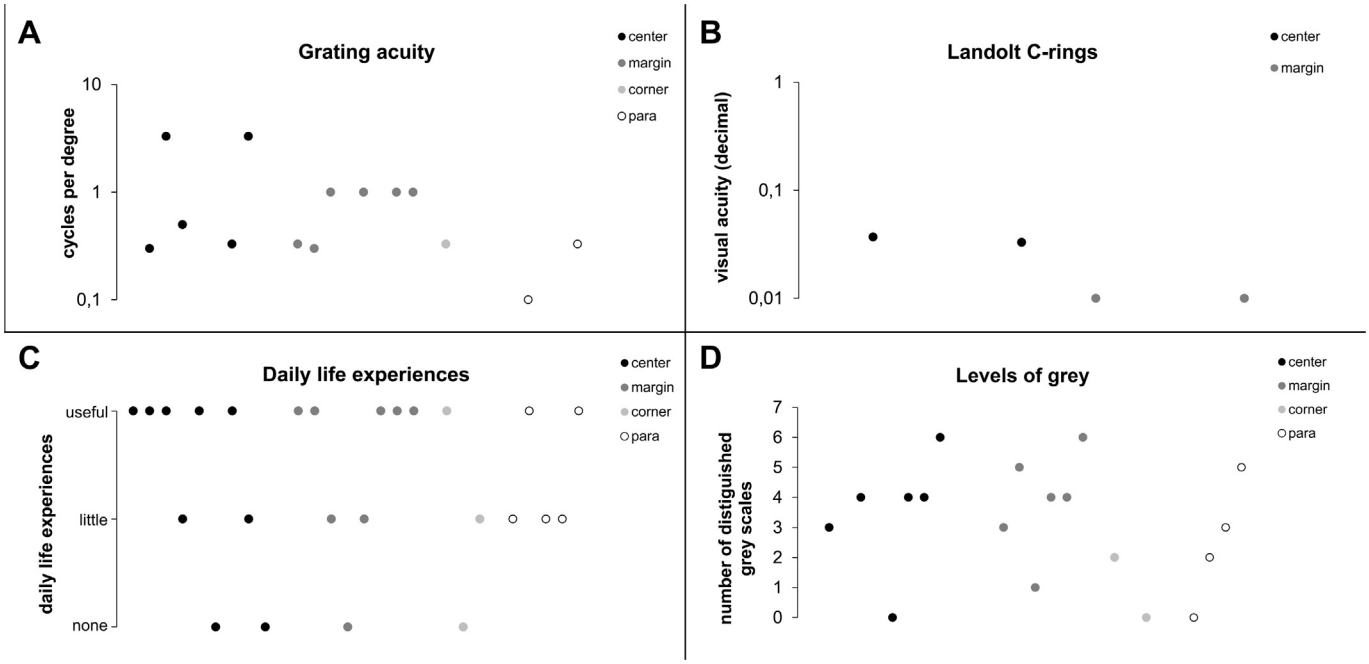

Fig. 8. Effect of the position of the fovea to the subretinal microchip. The color-coded dots represent participants, for whom the results of grating acuity (A), visual acuity (B), daily life reports (C) and number of correctly documented grey scales (D) were available. The colors of the dots represent where the fovea was placed in relation on to the microchip in the particular participant: para (chip was parafoveally, thus the fovea was not on the chip surface), corner (fovea was in the region of the chip corner), margin (fovea was close to the chip border) and centre (fovea was on the microchip surface, not in the proximity of the border). (A) Grating acuity and (B) visual acuity with Landolt C-rings were better and more often measureable if the fovea was stimulated by the chip (chip not parafoveally). (C) Daily life experiences and (D) number of distinguishable grey levels do not show such a tendency.

only the epiretinal Argus II (Second Sight Medical Products Inc. Sylmar USA) prosthesis with the FDA approval and the subretinal Alpha IMS (Retina Implant AG, Reutlingen Germany) implant, both having received the CE mark for use in Europe, have been the subjects of long-term clinical studies in blind patients with hereditary retinal degenerations. Recently also a small number of patients with a suprachoroidal implant have been reported (Ayton et al., 2014). Moreover, there are earlier reports on human patients with a passive subretinal implant (Chow et al., 2010) and EPIRET3, another epiretinal prosthesis (Menzel-Severing et al., 2012) who did not report on daily life experiences, mediated regularly by electronic implant devices.

Both subretinal implant Alpha IMS and the epiretinal implant Argus II could show improvement of the vision in end-stage retinitis pigmentosa patients. However, there are several differences in both systems. The epiretinal prosthesis uses an external camera affixed to spectacles and stimulates directly the ganglion cells with a transformed signal via 60 electrodes, and thus does not primarily involve the bipolar and amacrine cells. This might be an advantage in cases where the bipolar cells layer has degenerated profoundly and ganglion cell system being intact which is rarely the case; to our opinion, including the bipolar cell and amacrine cell circuitry in the visual processing is an enormous advantage for a more natural perception and fast restoration. Inner retina circuitry carries out a number of important processes such as contrast enhancement or movement perception and enable – in contrary to the long ganglion cells axons – a good retinotopy of the image. Moreover, histological work show that the bipolar cell layer usually – despite some reorganization – is present in most patients after years of blindness (Santos et al., 1997) and does not degenerate profoundly even in end-stage disease. Further, the use of an external camera eliminates the chance of utilizing natural eye movements which are important not only for visual search but also serve to prevent image fading on the retina by small involuntary eye movements that refresh images during visual perception and maintain image position stability by the efference copy transmission to the brain, for which the utilization of the extraocular muscle system is instrumental.

Indeed, patients with Subretinal Implant Alpha IMS move their eyes in order to find and localize the objects. In the screen tasks, once they have found the object on the area of the microchip, most patients can see the spatial characteristics and shape without using gaze or head movements. For outdoor use or during scanning larger areas such as table, head movements are necessary, too. Patients wearing a subretinal implant also perform microsaccades with their eyes, refreshing thus the image on the retina (Hafed et al., publication in progress).

Nevertheless an external camera and image pre-processing as necessary for the epiretinal approach brings additional advantages. Accommodation and magnification by zooming in the camera system can improve perception of details (Humayun et al., 2012) and preprocessing of images might enable some additional encoding of information, although such technical measures cannot improve visual acuity, as assessed in proper ophthalmological terms. Moreover, optical magnifying devices for low vision such as lenses can be applied with subretinal implants as well.

Another advantage of the epiretinal approach is an easier surgical insertion – the median implant surgery time is 4 h (Humayun et al., 2012) compared to six to eight hours in the case of the subretinal implantation. The epiretinal system has also shown longer observation times the follow-up of patients wearing the epiretinal prosthesis reaches up to 2.7 years (Humayun et al., 2012) and meanwhile longer (>5 years).

On the other hand, the Alpha IMS with 1500 electrodes has shown better visual results so far, compared to the Argus II with 60 electrodes. The best result of grating visual acuity mediated by Argus II to date is 20/1262 (Humayun et al., 2012) (decimal 0.016), visual acuity measured by standardized Landolt C-ring tests with an epiretinal prosthesis was not reported so far. Also the range of daily life reports of patients wearing Alpha IMS is broader

and its technical stability, shown in laboratory tests, has improved several fold, presently assessed in clinical trials.

Microelectronic visual implants are designed for completely blind persons with retinal degenerations. However, especially for low vision and very low vision patients a number of non-invasive visual rehabilitation tools have been developed to allow for an improved functional performance and visual rehabilitation. Optical and electronic magnifying devices are available on the market for many years, enabling a regular or contrast-reversal magnification of up to 70-times. Mobile digital devices based on video goggles can zoom, autofocus, and adapt to ambient luminance in an enlarged visual field, but most of the devices have a bulky appearance which is socially not easily acceptable. An alternative approach is the tongue stimulator, a non-invasive device which transfers the visual image into a vibrating pattern on the tongue. With the tongue stimulator "Brainport" blind individuals can pass the light perception, time resolution and grating acuity task in a screen module similar to the setup described in the present manuscript (Nau, Bach, & Fisher, 2013). Also conversion of the image into acoustical signals is used for orientation and mobility, letter recognition and other visual tasks, as was published for congenitally blind individuals (Striem-Amit et al., 2012). For recent advances see also The Lasker/IRRF Initiative for Innovation in Vision Science, (2014b, chap. 9).

5. Conclusions

The results of our study show that a subretinal implant is able to restore rudimentary but potentially useful vision in patients blind from hereditary degenerations of the photoreceptors. Almost half of the participants could recognize object shapes and detail in daily life and almost three-quarters could localize high-contrast objects. The implant received a CE mark granting marketing authorization within the European Community in July 2013 and for some centers in Germany public health insurance negotiations for reimbursement have been positive. Nevertheless it is of utmost importance that interested patients are properly informed about the present limitations of electronic implants and that the maximum achievable visual restoration is corresponding only to very low vision of a kind that patients may have experienced just before becoming blind. Moreover, despite well maintained retinal layering, assessed by OCT, it cannot be predicted at present, which patients after implantation may have very useful object perception in daily life and which patients may have only improved light perception and how long the restoration of very-low-vision abilities will be maintained.

Conflicts of interest

Katarina Stingl: Employed by University of Tübingen by means provided by Retina Implant AG, Reutlingen for the clinical trial, travel support. Eberhart Zrenner, Florian Gekeler: Stock ownership in Retina Implant AG, Reutlingen, paid consultant, holder of patents as inventor/developer, travel support from Retina Implant AG, Reutlingen. Helmut Sachs: Stock ownership in Retina Implant AG, Reutlingen, paid consultants.

Karl Ulrich Bartz-Schmidt, Dorothea Besch, Assen Koitschev, Akos Kusnyerik, Janos Nemeth, Robert E MacLaren, Caroline Chee, Mohamed Adheem Naser Naeem, Mandeep S. Singh, Markus Groppe, Timothy L. Jackson, Charles L. Cottriall, James Neffendorf, James D. Ramsden, Andrew Simpson, David Wong: No financial conflicts of interest.

Tobias Peters, Barbara Wilhelm: CRO of the trial on behalf of Retina Implant AG, Reutlingen.

Acknowledgments

This work was supported by Retina Implant AG, Reutlingen, Germany. This study is also part of the research programme of the Bernstein Center for Computational Neuroscience, Tübingen, Germany and was funded by the German Federal Ministry of Education and Research (BMBF; FKZ: 01GQ1002), by the NIHR Oxford Biomedical Research Centre, United Kingdom and the Tistou and Charlotte Kerstan Foundation, Germany. This project was also supported by joint grant of the National University of Singapore and Baden-Wuerttemberg, Germany (BW A/C – 191-000-016-646) and the Werner Reichardt Centre for Integrative Neuroscience (CIN) at the Eberhard Karls University of Tübingen, Germany. The CIN is an Excellence Cluster funded by the Deutsche Forschungsgemeinschaft (DFG) within the framework of the Excellence Initiative (EXC 307).

The authors thank Krunoslav Stingl (Tübingen) for the statistical analysis of the data, Regina Ebenhoch (Tübingen) for the graphical design of the images and Margaret Clouse (Tübingen) for English proof reading. Special thanks are due to the many coworkers who were involved in caring for the patients and did so in a most dedicated way: Andreas Schatz, Anna Bruckmann, Christoph Kernstock and Stephanie Hipp (Tübingen), Gopal Lingam, Amutha Veluchamy Barathi, Erlangga Ariadarma Mangunkusumo, Woei-Shyang Loh, Gangadhara Sundar, Carlo Nasol, Eng Soon Go and Thet Naing (Singapore).

References

Ayton, L. N. et al. (2014). First-in-human trial of a novel suprachoroidal retinal prosthesis. *PLoS One, 9*(12), e115239. http://dx.doi.org/10.1371/journal.pone.0115239.

Bach, M. et al. (2010). Basic quantitative assessment of visual performance in patients with very low vision. *Investigative Ophthalmology & Visual Science, 51*(2), 1255–1260. http://dx.doi.org/10.1167/iovs.09-3512.

Bainbridge, J. W. B. et al. (2008). Effect of gene therapy on visual function in Leber's congenital amaurosis. *The New England Journal of Medicine, 358*(21), 2231–2239. http://dx.doi.org/10.1056/NEJMoa0802268.

Besch, D. et al. (2008). Extraocular surgery for implantation of an active subretinal visual prosthesis with external connections: Feasibility and outcome in seven patients. *British Journal of Ophthalmology, 92*(10), 1361–1368. http://dx.doi.org/10.1136/bjo.2007.131961.

Brelén, M. E. et al. (2010). Measurement of evoked potentials after electrical stimulation of the human optic nerve. *Investigative Ophthalmology & Visual Science, 51*(10), 5351–5355. http://dx.doi.org/10.1167/iovs.09-4346.

Busskamp, V. et al. (2012). Optogenetic therapy for retinitis pigmentosa. *Gene Therapy, 19*(2), 169–175. http://dx.doi.org/10.1038/gt.2011.155.

Chow, A. Y. et al. (2004). The artificial silicon retina microchip for the treatment of vision loss from retinitis pigmentosa. *Archives of Ophthalmology, 122*(4), 460–469. http://dx.doi.org/10.1001/archopht.122.4.460.

Chow, A. Y. et al. (2010). The artificial silicon retina in retinitis pigmentosa patients (an American Ophthalmological Association thesis). *Transactions of the American Ophthalmological Society, 108*, 120–154.

Eickenscheidt, M. et al. (2012). Electrical stimulation of retinal neurons in epiretinal and subretinal configuration using a multicapacitor array. *Journal of Neurophysiology, 107*(10), 2742–2755. http://dx.doi.org/10.1152/jn.00909.2011.

Food and Drug Administration. Investigational Device Exemption Guidance for Retinal Prostheses (2013). http://www.fda.gov/MedicalDevices/DeviceRegulationandGuidance/GuidanceDocuments/ucm341954.htm.

Gekeler, F. et al. (2007). Compound subretinal prostheses with extra-ocular parts designed for human trials: Successful long-term implantation in pigs. *Graefe's Archive for Clinical and Experimental Ophthalmology, 245*(2), 230–241. http://dx.doi.org/10.1007/s00417-006-0339-x.

Guenther, E. et al. (1999). Long-term survival of retinal cell cultures on retinal implant materials. *Vision Research, 39*(24), 3988–3994.

Guenther, T., Lovell, N. H., & Suaning, G. J. (2012). Bionic vision: System architectures: A review. *Expert Review of Medical Devices, 9*(1), 33–48. http://dx.doi.org/10.1586/erd.11.58.

Humayun, M. S. et al. (2012). Interim results from the international trial of Second Sight's visual prosthesis. *Ophthalmology, 119*(4), 779–788. http://dx.doi.org/10.1016/j.ophtha.2011.09.028.

Katz, B., & Sireteanu, R. (1989). The Teller Acuity Card Test: Possibilities and limits of clinical use. *Klinische Monatsblätter für Augenheilkunde, 195*(1), 17–22. http://dx.doi.org/10.1055/s-2008-1046406.

Kernstock, C. J. et al. (2011). 3D-visualisation of power supply cable of subretinal electronic implants during eye movement. *ARVO Meeting Abstracts, 52*(6), 1341.

Kitiratschky, V. B. D. et al. (2014). Safety evaluation of 'retina implant alpha IMS' – A prospective clinical trial. *Graefe's Archive for Clinical and Experimental Ophthalmology*. http://dx.doi.org/10.1007/s00417-014-2797-x.

Kohler, K. et al. (2001). Histological studies of retinal degeneration and biocompatibility of subretinal implants. *Der Ophthalmologe, 98*(4), 364–368. http://dx.doi.org/10.1007/s003470170142.

Kusnyerik, A. et al. (2012). Positioning of electronic subretinal implants in blind retinitis pigmentosa patients through multimodal assessment of retinal structures. *Investigative Ophthalmology & Visual Science, 53*(7), 3748–3755. http://dx.doi.org/10.1167/iovs.11-9409.

Luo, Y. H.-L., & da Cruz, L. (2014). A review and update on the current status of retinal prostheses (bionic eye). *British Medical Bulletin, 109*, 31–44. http://dx.doi.org/10.1093/bmb/ldu002.

Maguire, A. M. et al. (2009). Age-dependent effects of RPE65 gene therapy for Leber's congenital amaurosis: A phase 1 dose-escalation trial. *Lancet, 374*(9701), 1597–1605. http://dx.doi.org/10.1016/S0140-6736(09)61836-5.

Menzel-Severing, J. et al. (2012). Implantation and explantation of an active epiretinal visual prosthesis: 2-year follow-up data from the EPIRET3 prospective clinical trial. *Eye (London, England), 26*(4), 501–509. http://dx.doi.org/10.1038/eye.2012.35.

Morimoto, T. et al. (2012). Transcorneal electrical stimulation promotes survival of photoreceptors and improves retinal function in rhodopsin P347L transgenic rabbits. *Investigative Ophthalmology & Visual Science, 53*(7), 4254–4261. http://dx.doi.org/10.1167/iovs.11-9067.

Nau, A., Bach, M., & Fisher, C. (2013). Clinical tests of ultra-low vision used to evaluate rudimentary visual perceptions enabled by the brainport vision device. *Translational Vision Science & Technology, 2*(3), 1.

Pardue, M. T. et al. (2005). Neuroprotective effect of subretinal implants in the RCS rat. *Investigative Ophthalmology & Visual Science, 46*(2), 674–682. http://dx.doi.org/10.1167/iovs.04-0515.

Sachs, H. et al. (2010). Subretinal implant: The intraocular implantation technique. *Nova Acta Leopoldina NF III, 379*, 217–223.

Santos, A. et al. (1997). Preservation of the inner retina in retinitis pigmentosa. A morphometric analysis. *Archives of Ophthalmology, 115*(4), 511–515.

Schatz, A. et al. (2011). Transcorneal electrical stimulation for patients with retinitis pigmentosa: A prospective, randomized, sham-controlled exploratory study. *Investigative Ophthalmology & Visual Science, 52*(7), 4485–4496. http://dx.doi.org/10.1167/iovs.10-6932.

Schmid, H. et al. (2009). Neuroprotective effect of transretinal electrical stimulation on neurons in the inner nuclear layer of the degenerated retina. *Brain Research Bulletin, 79*(1), 15–25. http://dx.doi.org/10.1016/j.brainresbull.2008.12.013.

Schmidt, E. M. et al. (1996). Feasibility of a visual prosthesis for the blind based on intracortical microstimulation of the visual cortex. *Brain: A Journal of Neurology, 119*(Pt. 2), 507–522.

Schwahn, H. et al. (2001). Studies on the feasibility of a subretinal visual prosthesis: Data from Yucatan micropig and rabbit. *Graefe's Archive for Clinical and Experimental Ophthalmology, 239*(12), 961–967. http://dx.doi.org/10.1007/s004170100368.

Sieving, P. A. et al. (2006). Ciliary neurotrophic factor (CNTF) for human retinal degeneration: Phase I trial of CNTF delivered by encapsulated cell intraocular implants. *Proceedings of the National Academy of Sciences of the United States of America, 103*(10), 3896–3901. http://dx.doi.org/10.1073/pnas.0600236103.

Stett, A. et al. (2000). Electrical multisite stimulation of the isolated chicken retina. *Vision Research, 40*(13), 1785–1795. http://dx.doi.org/10.1016/S0042-6989(00)00005-5.

Stingl, K. et al. (2012). What can blind patients see in daily life with the subretinal Alpha IMS implant? Current overview from the clinical trial in Tübingen. *Der Ophthalmologe, 109*(2), 136–141. http://dx.doi.org/10.1007/s00347-011-2479-6.

Stingl, K. et al. (2013a). Safety and efficacy of subretinal visual implants in humans: Methodological aspects. *Clinical & Experimental Optometry, 96*(1), 4–13. http://dx.doi.org/10.1111/j.1444-0938.2012.00816.x.

Stingl, K. et al. (2013b). Artificial vision with wirelessly powered subretinal electronic implant alpha-IMS. *Proceedings of the Royal Society B: Biological Sciences, 280*(1757). http://dx.doi.org/10.1098/rspb.2013.0077.

Stingl, K. et al. (2013c). Functional outcome in subretinal electronic implants depends on foveal eccentricity. *Investigative Ophthalmology & Visual Science, 54*(12), 7658–7665. http://dx.doi.org/10.1167/iovs.13-12835.

Stingl, K., & Zrenner, E. (2013). Electronic approaches to restitute vision in patients with neurodegenerative diseases of the retina. *Ophthalmic Research, 50*(4), 215–220. http://dx.doi.org/10.1159/000354424.

Striem-Amit, E. et al. (2012). Visual' acuity of the congenitally blind using visual-to-auditory sensory substitution. *PLoS ONE, 7*(3), e33136. http://dx.doi.org/10.1371/journal.pone.0033136 '.

Testa, F. et al. (2013). Three-year follow-up after unilateral subretinal delivery of adeno-associated virus in patients with Leber congenital Amaurosis type 2. *Ophthalmology, 120*(6), 1283–1291. http://dx.doi.org/10.1016/j.ophtha.2012.11.048.

The Lasker/IRRF Initiative for Innovation in Vision Science (2014a). Restoring vision to the blind: The new age of implanted visual prostheses. *Translational Vision Science & Technology, 3*(7). http://dx.doi.org/10.1167/tvst.3.7.3.

The Lasker/IRRF Initiative for Innovation in Vision Science (2014b). Restoring vision to the blind: Advancements in vision aids for the visually impaired. *Translational Vision Science & Technology, 3*(7). http://dx.doi.org/10.1167/tvst.3.7.9.

Weiland, J. D., Cho, A. K., & Humayun, M. S. (2011). Retinal prostheses: Current clinical results and future needs. *Ophthalmology, 118*(11), 2227–2237. http://dx.doi.org/10.1016/j.ophtha.2011.08.042.

Zrenner, E. et al. (1999). Can subretinal microphotodiodes successfully replace degenerated photoreceptors? *Vision Research, 39*(15), 2555–2567. http://dx.doi.org/10.1016/s0042-6989(98)00312-5.

Zrenner, E. (2002). Will retinal implants restore vision? *Science (New York, N.Y.), 295*(5557), 1022–1025. http://dx.doi.org/10.1126/science.1067996.

Zrenner, E. et al. (2011). Subretinal electronic chips allow blind patients to read letters and combine them to words. *Proceedings of the Royal Society B: Biological Sciences, 278*(1711), 1489–1497. http://dx.doi.org/10.1098/rspb.2010.1747.

Zrenner, E. (2012). Artificial vision: Solar cells for the blind. *Nature Photonics, 6*(6), 344–345. http://dx.doi.org/10.1038/nphoton.2012.114.

Zrenner, E. (2013). Fighting blindness with microelectronics. *Science Translational Medicine, 5*(210), 210ps16. http://dx.doi.org/10.1126/scitranslmed.3007399.

State of the Art

Artificial Vision for the Blind by Connecting a Television Camera to the Visual Cortex

WM. H. DOBELLE

Blindness is more feared by the public than any ailment with the exception of cancer and AIDS. We report the development of the first visual prosthesis providing useful "artificial vision" to a blind volunteer by connecting a digital video camera, computer, and associated electronics to the visual cortex of his brain. This device has been the objective of a development effort begun by our group in 1968 and represents realization of the prediction of an artificial vision system made by Benjamin Franklin in his report on the "kite and key" experiment, with which he discovered electricity in 1751.* *ASAIO Journal* 2000; 46:3-9.

This new visual prosthesis produces black and white display of visual cortex "phosphenes" analogous to the images projected on the light bulb arrays of some sports stadium scoreboards. The system was primarily designed to promote independent mobility, not reading. We have also provided a battery powered, electronic interface that is RF isolated from line currents for safety. This interface can replace the camera, permitting the volunteer to directly watch television and use a computer, including access to the Internet. Because of their potential importance for education, and to help integrate blind people into the workforce, such television, computer, and Internet capabilities may prove even more valuable in the future than independent mobility. In addition, the image from the camera or interface and an overlaid simulated real-time display of the phosphene image seen by the volunteer, can be re-broadcast from the system over an RF link to a remote videotape recorder and viewing screen. This allows real-time monitoring, as well as post-trial analysis, by the experimental team.

The television camera, which is built into a pair of sunglasses, is shown in **Figure 1**; the prosthesis, as worn by the blind volunteer, is pictured in **Figure 2**, and the complete system is described schematically in **Figure 3**, including both the television/computer/Internet interface and the remote Video Screen/VCR monitor, neither of which are shown in **Figure 2**.

These efforts were inspired by a seminal paper published by Giles Brindley's group in 1968[1] Our first human experiments in 1970-1972[2] involved cortical stimulation of 37 sighted volunteers who were undergoing surgery on their occipital lobe under local anesthesia to remove tumors and other lesions. In 1972-1973 we then stimulated the visual cortex of three blind volunteers who were temporarily implanted for a few days with electrode arrays passed through a Penrose drain.[3] Our subsequent experiments have involved four blind volunteers implanted with permanent electrode arrays using percutaneous connecting pedestals. Two volunteers were implanted in 1974.[4] One array was removed 3 months after surgery and the second after 14 years.† The first five volunteers were operated on at the University of Western Ontario in London Canada. Two additional blind volunteers, including the subject of this article, were implanted in 1978 at the Columbia-Presbyterian Medical Center in New York City.[6] They have both retained their implants for more than 20 years without infection or other problems.

Figure 1. Blind volunteer with sub-miniature TV camera mounted on the right lens of his sunglasses, and the laser-pointer (position monitor) on the left temple piece.

From the Institut Dobelle AG, Zurich, Switzerland and the Dobelle Institute, Inc. at the Columbia-Presbyterian Medical Center, New York, NY.

Submitted for consideration September 1999; accepted for publication in revised form November 1999.

Reprint requests: Dr. William H. Dobelle, 3960 Broadway, New York, NY 10032

* From Watson W: An account of Mr. Benjamin Franklin's treatise, lately published, entitled Experiments and Observations on Electricity, made at Philadelphia in America. *Philos Trans R Soc London* 47: 202-211.

† The first implant was removed, as planned, after 3 months. The second volunteer agreed to continue participation but his implant was removed due to a blood borne infection that did not originate with the implant.

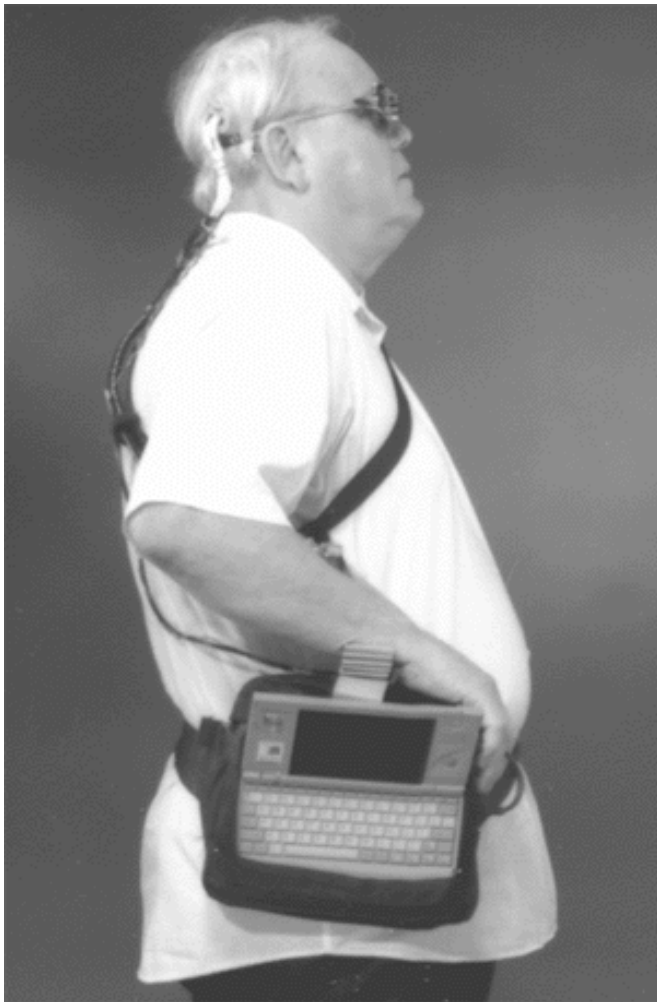

Figure 2. The complete artificial vision system showing the computer and electronics package on the belt with output cable to the electrodes on the brain.

The Volunteer and Implant

The 62 year old subject of this article traumatically lost vision in one eye at age 22, and was totally blinded at age 36 by a second trauma. He was continually employed, before and after losing his sight, as an administrator by the State of New York. He retired in 1997 after 32 years of service. The electrode was implanted in 1978 when he was 41years old. Because of discomfort during surgery caused by mechanical impingement of the teflon electrode matrix on the volunteer's falx and tentorium, his electrode array is posterior to the

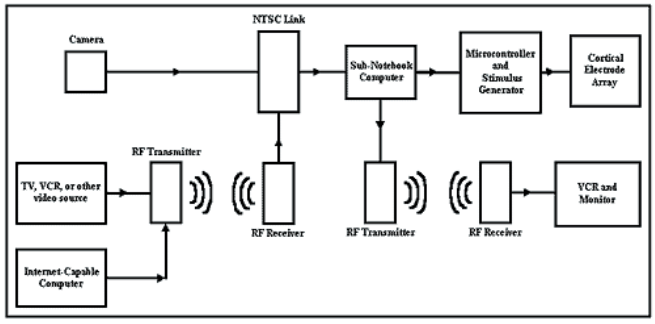

Figure 3. Schematic of artificial vision system including TV/computer/ Internet interface and VCR monitor.

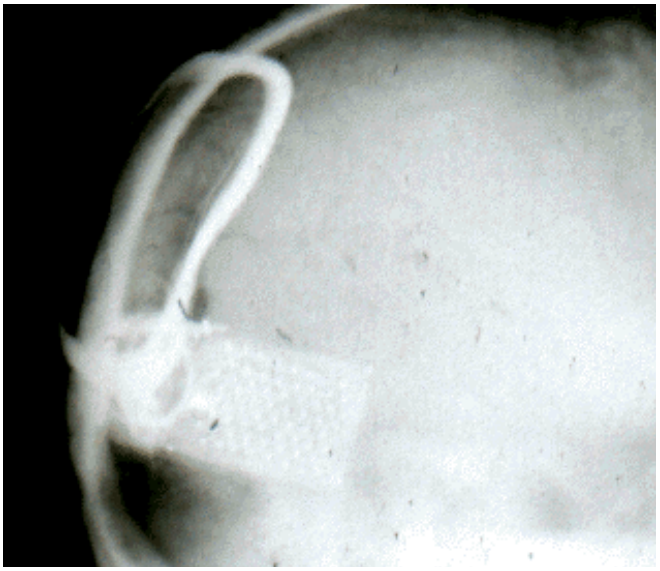

Figure 4. X-ray of electrode array on the mesial surface of the right occipital lobe.

position of the arrays implanted in our six other blind volunteers. We have been using this implanted pedestal and intracranial electrode array to experimentally stimulate the visual cortex, on the mesial surface of the right occipital lobe, for more than 20 years. However, the fifth generation externalelectronics package and software are entirely new, taking advantage of cutting edge technology that has only recently become available. An X-ray of the implanted visual cortex electrode array is shown in **Figure 4**, and the numbered electrode layout is detailed in **Figure 5**.

A platinum foil ground plant is perforated with a hexagonal array of 5 mm diameter holes on 3 mm centers, and the flat platinum electrodes centered in each hole are 1 mm in diameter. This ground plane keeps all current beneath the dura. This eliminates discomfort due to dural excitation when stimulating some single electrodes (such as number 19) and when other arrays of electrodes are stimulated simultaneously. The ground plane also eliminates most phosphene interactions[3] when multiple electrodes are stimulated simultaneously, and provides an

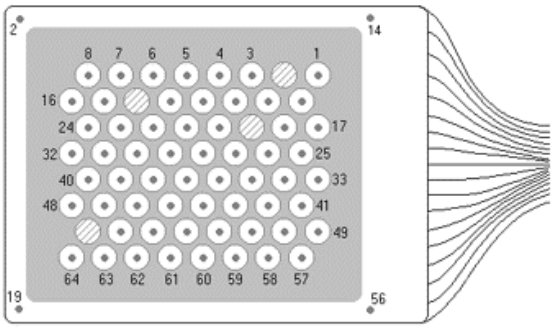

Figure 5. Electrode layout, as seen on the mesial surface of the right occipital lobe (looking through the electrode). Electrode #19 in the lower left hand corner of the array corresponds to the electrode in the lower right hand corner of the X-ray shown in Figure 4.

additional measure of electrical safety that is not possible when stimulating between cortical electrodes and a ground plane outside the skull. Each electrode is connected by a separate teflon insulated wire to a connector contained in a carbon percutaneous pedestal. Fabrication techniques for these electrodes[6] and pedestals[7] have been previously described. The original surgery in 1978 was performed under local anesthesia, and implants in future patients can probably be performed on an outpatient basis by most neurosurgeons.

Phosphenes and Their Map in The Visual Field

When stimulated, each electrode produces 1-4 closely spaced phosphenes. Each phosphene in a cluster ranges up to the diameter of a pencil at arms length. Neighboring phosphenes in each cluster are generally too close to the adjacent phosphenes for another phosphene to be located between them. These "multiples" are unlike the phosphenes described by our other blind volunteers, or those reported by Brindley's volunteers.[1] They may be due to the use of a ground plane array, although we have used a similar ground plane array in one temporarily implanted blind volunteer without producing multiple phosphenes. Other possible causes for these multiples include the fact that the volunteer lost vision in his two eyes at different times or that we may be stimulating visual association cortex (areas 18 and 19) rather than primary visual cortex (area 17).

All phosphenes flicker at a rate that seems unrelated to the pulse, repetition frequency, or any other parameter of stimulation, or to cardiac pulse, breathing rate, or other physiologic function. Using a variety of computer and manual mapping techniques, we determined that the phosphene map occupies an area roughly 8 inches in height and 3 inches wide, at arms length. The map and the parameters for stimulation both appear to be stable over the last two decades. The map of some of the phosphenes in this volunteer's visual space is shown in **Figure 6**, and is more nearly a vertical line than the larger, more two-dimensional maps reported by our earlier volunteers, or by the volunteers of Brindley.[1] We suspect, but cannot prove, that this unusual map, like the clusters of multiple phosphenes, is due to placement of the electrodes on visual association cortex (areas 18 and 19) rather than primary visual cortex (area 17). In the future we may implant up to 256 additional surface electrodes, particularly on the left occipital lobe of this volunteer, to increase the resolution of this system. However, trying to place additional electrodes within sulci is impractical, at least al this time. Our anatomic studies in cadavers (**9**) indicate the primary visual cortex (area 17) would permit placement of 256 surface electrodes on 3 mm centers on each lobe in most humans (512 electrodes total). However, stimulating adjacent visual association cortex — as we believe we are doing in this volunteer — would substantially expand the number of possible electrodes in the matrix. The organization of the stimulator is modular, and the system described here is being expanded to allow us to stimulate 256 electrodes on each hemisphere.

The Electronics Package

The 292 X 512 pixel charge coupled devices (CCD) black and white television camera is powered by a 9 V battery, and

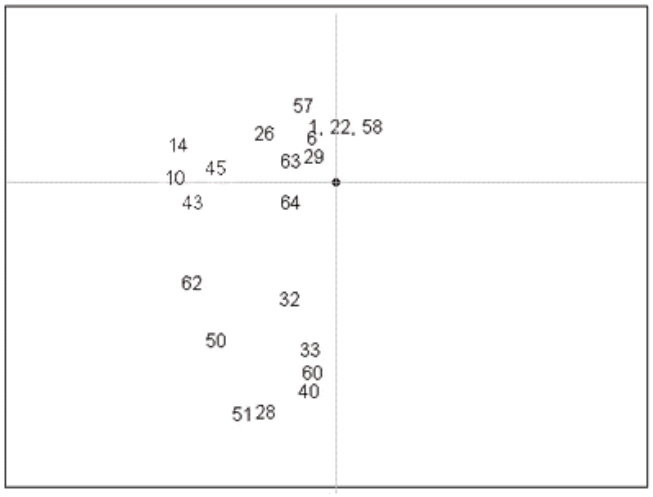

Figure 6. Phosphene map in visual space. The electrode array, on the right occipital lobe, produces an 8 inch by 3 inch array of phosphenes (at arm's length) in the left visual field. Phosphenes produced by electrodes No. 22 and No. 58 actually appear to the left of the vertical meridian, atop the phosphenes produced by electrode No. 1

connects via a battery-powered National Television Standards Committee (NTSC) link to a sub-notebook computer in a belt pack. This f 14.5 camera, with a 69° field of view, uses a pinhole aperture, instead of a lens, to minimize size and weight. It also incorporates an electronic "iris" for automatic exposure control.

The sub-notebook computer incorporates a 120 MHz microprocessor with 32 MB of RAM and a 1.5 GB hard drive. It also has an LCD screen and keyboard. It was selected because of its very small size and light weight. The belt pack also contains a second microcontroller, and associated electronics to stimulate the brain. This stimulus generator is connected through a percutaneous pedestal to the electrodes implanted on the visual cortex. The computer and electronics package together are about the size of a dictionary and weigh approximately 10 pounds, including camera, cables, and rechargeable batteries. The battery pack for the computer will operate for approximately 3 hours and the battery pack for the other electronics will operate for approximately 6 hours.

This general architecture, in which one computer interfaces with the camera and a second computer controls the stimulating electronics, has been used by us in this, and four other substantially equivalent systems, since 1969.[9] The software involves approximately 25,000 lines of code in addition to the sub-notebooks' operating system. Most of the code is written in **C++**, while some is written in **C**. The second microcontroller is programmed in assembly language.

Stimulation Parameters

Stimulation delivered to each electrode typically consists of a train of six pulses delivered at 30 Hz to produce each frame of the image. Frames have been produced with 1-50 pulses, and frame rates have been varied from 1 to 20 frames per second. As expected,[4] frame rates of 4 per second currently seem best, even with trains containing only a single pulse.

Each pulse is symmetric, biphasic (-/+) with a pulse width of 500 μsec per phase (1,000 μsec total). Threshold amplitudes of 10-20 volts (zero-peak) may vary + /-20% from day to day; they are higher than the thresholds of similar electrodes without the ground plane, presumably because current shunts across the surface of the pia-arachnoid and encapsulating membrane. The system is calibrated each morning by recomputing the thresholds for each electrode, a simple procedure that takes the volunteer approximately 15 minutes with a numeric keypad.

Performance of the System

We know of no objective method for comparing our "artificial vision" system with a cane, guide dog, or other aid for the blind. For example, there is no standard obstacle course on which such devices, or the performance of volunteers using them, can be rated. Indeed, even the vision test for drivers' licenses in most jurisdictions employs only static Snellen tests.

Furthermore, there are really no analogous low vision patients with parafoveal tunnel vision, plus scattered field defects (due to gaps between phosphenes), no color vision, and no depth perception to provide models for testing.

Initially, the volunteer was unable to recognize letters or numbers. Based on extensive personal experience in the 1960s with corneal transplant patients whose vision had been restored after many years of blindness, I expected that it might take the volunteer more than a year to learn how to use our new artificial vision system. This expectation was reinforced by the work of Valvo[10] and others. However, within 1 one-day sessions the patient learned to use the system, and he has continued to practice 3-4 hours per day 2 or 3 days per week.

With scanning he can now routinely recognize a 6 inch square "tumbling E" at five feet, as well as Snellen letters, HOTV test, Landolt rings, and Lea figures of similar size. These psychophysical tests are summarized in **Figure 7**. He can also count fingers. With the exception of finger counting, these acuity tests have been conducted using pure black characters on a pure white background at an illumination greater than 1,000 lux. Six inch characters at 5 feet corresponds to a visual acuity of approximately 20/120. A frequency-of-seeing curve for the "tumbling E" and for Landolt's ring is shown in **Figure 8**.

Paradoxically, larger characters are slightly more difficult for this volunteer because they extend well beyond the limits of his visual "tunnel." The rapid fall-off with characters smaller than 20/1200 is also quite reproducible, but the explanation is uncertain. In the future, more sophisticated psychophysical experiments may compare this volunteer with normal patients, separating effect due to processing at the retina and lateral geniculate from those occurring at cortical levels or beyond.

Similar acuity results have been achieved with the television/computer/Internet interface replacing the camera, although scanning is slower because a keypad is currently used for control, rather than neck movements. The volunteer believes that his performance will continue to improve with additional experience, particularly practice in scanning. The resolution of the system itself is ultimately limited by the analog-to-digital conversion in the NTSC link between the camera or other source and the computer, and thus can be improved by a better link, a different camera, or both.

Of course, visual acuity is normally measured with optimal

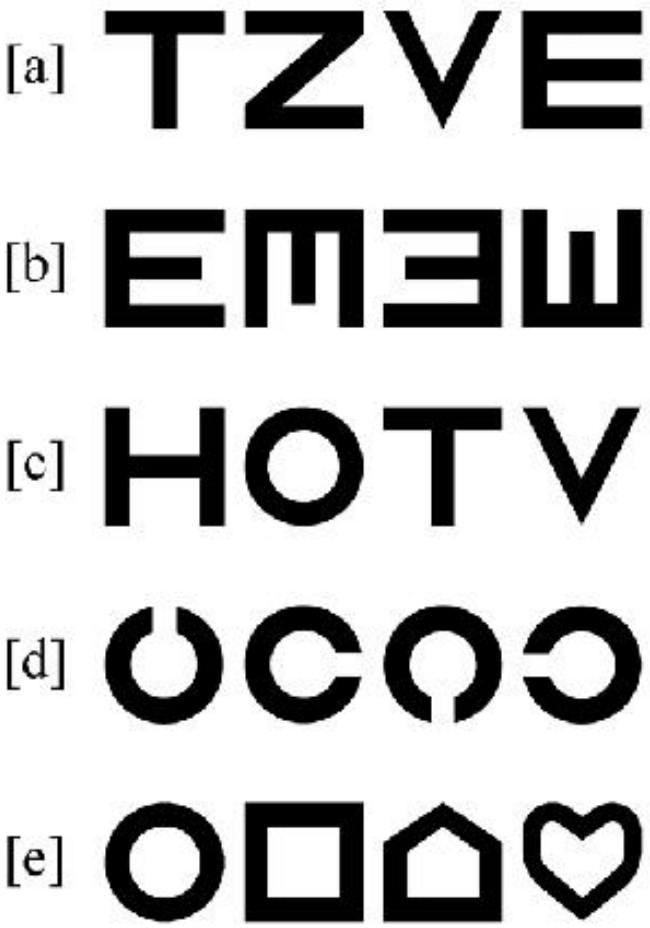

Figure 7. Character sets used in acuity tests: a, Snellen letters; b, "Tumbling E"; c, HOTV; d, Landolt rings; and e, Lea figures.

correction. Adding a lens to the existing camera is one possibility but — because of size, weight, and cosmetic considerations — we have chosen to accomplish magnification "correction" in software, which proved very difficult to write and is still being debugged. In addition, we are exploring use of image processing techniques, including edge detection. This additional computer processing required for edge detection slows the frame rate to

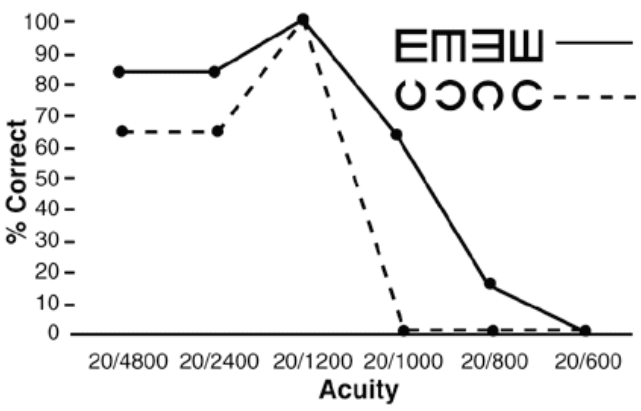

Figure 8. Frequency-of-seeing curves, which are optimal at 20/1200.

approximately 1 per second, but the volunteer is practicing use of such displays for mobility. In a larger (benchtop) development system, with a different camera, no NTSC link, and a 300 MHz processor of slightly different design, frame rates can be increased up to 7 per second.

We had expected that the patient might have trouble with apparent changes in size or shape of the phosphene image, particularly because the electrodes seem to be on visual association cortex. However, at this point there are no signs of either metamorphopsia or dysmetropsia, and corrective image processing has not been necessary.

As we have reported with earlier volunteers,[2] brightness can easily be modulated by changes in pulse amplitude.[11] However, provision of "gray scale" has not proven very valuable so far, probably because of the combination of tunnel vision and limited resolution. The phosphene display is planar, but is of uncertain distance, like the stars in the sky. We, therefore, plan to add an ultrasonic or infra-red "rangefinder"[12] in which the brightness of an easily identifiable phosphene, probably the one produced by electrode # 14 in this volunteer, is a function of distance. This is analogous to the "heads up" displays used by military pilots.

Although stimulation of visual cortex in sighted patients[2] frequently produces colored phosphenes, the phosphenes reported by this volunteer (and all previous blind volunteers to the best of our knowledge) are colorless. We speculate that this is the result of post-deprivation deterioration of the cells and/or senaphtic connections required for color vision. Consequently, color vision may never be possible in this volunteer or in future patients. However, optical filters could help differentiate colors, and it is also conceivable that chromatic sensations could be produced if future patients are implanted shortly after being blinded, before atrophy of the neural network responsible for color vision.

Contrast is entirely a function of the software, with adjustment by the experimental team depending on the experimental situation. The system also allows "reversal" in which the world looks much like a black and white photographic negative. Reversal is particularly useful when presenting black characters on a white background. These characters are then reversed by the computer so they appear as a matrix of white phosphenes on the patient's (otherwise dark) visual field.

The phosphene map is not congruent with the center of the volunteer's visual field. Phosphenes also move with eye movement. However, the volunteer's ability to fixate with this artificial vision system is a function of aiming the camera using neck muscles, rather than eye muscles. It helps that the camera image is displayed on the remote video screen for monitoring by the experimental team. In addition, we use a laser point in the temple-piece of the volunteer's glasses so the experimental team can tell at any moment where the camera is aimed by looking for the red dot.

Low vision patients often follow lines, including the junction between the wall and the floor, and/or lines of lights on the ceiling, and this volunteer has been practicing this approach. People with very limited vision can also achieve excellent mobility by following people. The volunteer has been practicing use of the system for this purpose as well, and can easily follow an 8 year old child.

The volunteer frequently travels alone in the New York metropolitan area, and to other cities, using public transport. He believes that one of the most dangerous errors in mobility is to mistake the space between subway cars for an open car door. He has been using the artificial vision system to practice this differentiation, while we monitor his performance with the remote VCR and viewing screen.

Discussion

In the United States, there are more than 1.1 million legally blind people, including 220,00 with light perception or less. [13] Similar statistics are thought to prevail in other economically developed countries. Unlike some other artificial vision proposals, such as retinal stimulators, cortical stimulators are applicable to virtually all causes of blindness. Our device may also help some legally blind low vision patients because the cortex of sighted people responds to stimulation similarly to the cortex of blind people. We believe that some blind children will be particularly good candidates for this new artificial vision system, because of their ability to quickly learn to use the system. In addition, without visual input, the visual cortex of blind children may not develop and this would prevent their use of artificial vision in the future. For example, the second patient implanted on the same day in 1978 as the volunteer reported here, was blinded in an accident at age 5 and implanted at age 62. Although he has retained his implant for more than 20 years, he has never seen phosphenes. However, our device is contraindicated in the very small number of blind people with severe chronic infections and the even smaller number blinded by stroke or cortical trauma.

None of the seven blind volunteers in our series have ever exhibited epileptic symptoms or other systemic problems related to the implant. Based on our clinical experience during the last 30 years, implanting thousands of patients in more than 40 countries with other types of neurostimulators (to control breathing, pain, and the urogenital system),[14] we believe the principal risk of our artificial vision device is infection, which might require removal of the implant in addition to antibiotic therapy.

To control costs and ensure easy maintenance, our design uses commercial off-the-shelf (COTS) components. The computer, stimulating electronics, and software are all external, facilitating upgrades and repairs. However, despite ongoing software improvements and use of larger numbers of electrodes in the future, it is unlikely that patients will be able to drive an automobile in the foreseeable future, much less get legal approval to do so.

Development of implanted medical devices such as this artificial vision system progresses in three stages. First there is speculation,[15] then there is hope,[1] and finally there is promise.

Given our considerable experience with neurostimulator implantation, we believe that we can promise a 512 electrode system that will be cost-competitive with a guide dog. More important, that cost can be expected to drop dramatically in the future, while performance should continue to improve.

Acknowledgements

I thank W.J. Kolff, the mentor and friend who enabled me to begin this project from 1968 to 1976. I also thank this blind volunteer and his family, as well as the more than 50 other sighted, blind, and deaf volunteers who have been involved as surgical subjects in our sensory prostheses research, as well as the thousands of patients in over 40 countries who have been implanted with our clinical neurological

† Deceased.

stimulators since 1969. I also thank (alphabetically) R. Avery, G. Brindley, M. Dobelle †, M.D. Dobelle, C. Eyzaguirre, D. Evans †, H.K. Hartline †, B. Lisan, E.F. McNichol, Jr., W. Partridge, W. Penfield †, K.Reemtsma, D. Rushton and T. Stockham, for reasons best known to each of them. J. Girvin has been our principle neurosurgical collaborator since 1970. He implanted all seven of our blind patients assisted by J. Antunes, D. Fink, M. McDonald, D. Quest, T. Roberts and T. Stanley among others. D. Dohn, C. Drake†, P. Gildenberg, M.G. Yasergil and many others have also provided neurosurgical advice and assistance. M. Mladejovsky and more recently P. Ning have guided our computer engineering efforts over the past 30 years with programming assistance from a group including D. Eddington, J. Evans, A. Halpert, M. O'Keefe, and J. Ochs. More than 300 other scientists, physicians, engineers and surgeons have been involved in our experiments since 1968, including K. Aron, B. Besser, M. D'Angelo, G. Dulmage, S. Fidone, B. Goetz, R. Goldbaum, J. Hanson, D. Hill, R. Huber, D. Kiefer, G. Klomp, T. Lallier, L. Pape, B. Seelig, K. Smith, L. Stensaas, S. Stensaas and M. Womack III †. J. Andrus and L. Homrighausen (Surdna Foundation, New York, NY), Max Fleischman Foundation (Reno, Nevada), H. Geneen † (IT&T Corp., New York, NY), E. Grass (Gross Instruments, Boston, Mass.), Wm. Randolph Heart Foundation (San Francisco, CA), E. Land † (Polaroid Corp., Cambridge, Mass.), S. Olsen (Digital Equipment Corp., Maynard Mass.), D. Rose † (New York, NY), M. Shapiro † (General Instrument Co., New York, NY), Wm. Volker Fund (Monterey, CA) and over 100 other individuals, and foundations provided financial support prior to 1981, without which this program would have been impossible. During that period we also received equipment donations from dozens of corporations, including Phillips Electronics, Fairchild Inc., Siguestis Inc., Soldran Inc., Bell Telephone Laboratories Inc., Hughes Aircraft Corp., Sanyo Corp., General Atomic Corp., Thermionics Inc., and TRW Inc.. Since 1981, all financial support has been provided by the Dobelle Institute, Inc. and its United States and Swiss affiliates. Financing our R&D on artificial vision entirely by sale of related neurological stimulators was conciously modeled on the Wright Brothers, who developed the airplane with proceeds from their bicycle factory. Like the airplane, the artificial vision project has entailed a high risk of failure, and a long development time, which are incompatible with conventional venture capital horizons. Advice and assistance in this respect has been provided by P. Baldi, P. Conley †, R. Downey, D. Ellis III, C. Giffuni, A. Gutman, E. Heil, I. Lustgarten †, J. McGarrahan, P.G. Pedersen, S. Sawyier, L. Towler, T. Young, and L. Weltman among others.

References

1. Brindley GS, Lewin WS: The sensations produced by electrical stimulation of the visual cortex. *J Physiol (Lond)* 196: 479-493, 1968.
2. Dobelle WH, Mladejovsky MG: Phosphenes produced by electrical stimulation of human occipital cortex, and their application to the development of a prosthesis for the blind. *J Physiol (Lond)* 243: 553-576, 1974.
3. Dobelle WH, Mladejovsky MG, Girvin JP: Artificial vision for the blind: Electrical stimulation of visual cortex offers hope for a functional prosthesis. *Science* 183: 440-444, 1974.
4. Dobelle WH, Mladejovsky MG, Evans JR, Roberts TS, Girvin JP: "Braille" reading by a blind volunteer by visual cortex stimulation. *Nature* 259: 111-112, 1976.
5. Dobelle WH, Quest D, Antunes J, Roberts T, Girvin JP: Artificial vision for the blind by electrical stimulation of the visual cortex. *Neurosurgery* 5: 521-527, 1979.
6. Klomp GF, Womack MVB, Dobelle WH: Fabrication of large arrays of cortical electrodes for use in man. *J Biomed Mater Res* 11: 347-364, 1977.
7. Klomp GF, Womack MVB, Dobelle WH: Percutaneous transmission of electrical energy in humans. *Trans ASAIO* 25: 1-7, 1979.
8. Stenaas SS, Eddington DK, Dobelle WH: The topography and variability of the primary visual cortex in man. *J Neurosurg* 40: 747-754, 1974.
9. Mladejovsky MG, Eddington DK, Evans JR, Dobelle WH: A computer-based brain stimulation system to investigate sensory prostheses for the blind and deaf. *IEEE Trans Biomed Eng* 23: 286-296, 1976.
10. Valvo A: Sight restoration after long-term blindness: The problems and behavior patterns of visual rehabilitation. New York: *American Foundation for the Blind*, 1971.
11. Henderson DC, Evans JR, Dobelle WH: The relationship between stimulus parameters and phosphene threshold/brightness, during stimulation of human visual cortex. *Trans ASAIO* 25: 367-370, 1979.
12. Dobelle WH: Artificial vision for the blind: The summit may be closer than you think. *ASAIO J* 40: 919-921, 1994.
13. Leonard R: Statistics on vision impairment: A resource manual. *Lighthouse International*, February 1999.
14. The Dobelle Group. Available at http://www.dobelle.com
15. Watson W: An account of Mr. Benjamin Franklin's treatise, lately published, entitled Experiments and Observations on Electricity, made at Philadelphia in America. *Philos Trans R Soc London* 47: 202-211, 1751-52.
16. Sobel I: Camera models and machine perception. AIM-21. Stanford Artificial Intelligence Laboratory, Palo Alto, California, 1970.

Afterword

Our team has continued to develop the hardware and software of this artificial vision system. Five key developments have occurred in the two months since submission of this paper for publication in September, 1999.

Development of a New Technique for Phosphene Mapping

Phosphene mapping is complicated by the fact that all phosphenes are produced in a relatively small area, which makes pointing difficult. This is compounded by the fact that phosphenes move with eye movements. In the refined technique, two phosphenes are selected to provide a vertical scale. The volunteer is then asked to estimate the vertical distance between each phosphene and these two references, as well as the distance to the left or right of an imaginary line connecting the reference phosphenes. This approach resulted in some small changes in the map described in (**Figure 6**), but the principal result was to "compress" the map horizontally from 3 inches across to about 2 inches across.

Use of a More Powerful Computer

Over the last two decades many improvements in our hardware and software have developed because of rapid technological advancements in computer technology ("Moore's Law"). Shortly after submission of this paper, we were able to obtain a new computer in an almost identical small package. This more powerful system employs a 233 MHz processor, 32 MB of RAM and a 4 GB hard disk. After debugging the software, the extra computing power proved important in two areas, (1) magnification in software and (2) image pre-processing, particularly edge detection.

Electronic Magnification

The pin hole camera we have been using is small, light and inconspicuous. However, it has a 69° field of view. Conventional optics would be heavy and conspicuous. Moreover, it is difficult to conceive a "zoom" version without employing a motor drive. Using the more powerful computer we were able to implement software magnification algorithms that were not possible with the initial portable system discussed above. The gray value for all pixels (120 x 160) were recorded and then 2, 4, 8, or 16 pixels were combined to create a single pixel for transmission to the patient. Using magnifications of 4 (and sometimes 8) times the patient's resolution improved to the point where he can now recognize a 2-inch high letter at 5 feet, as opposed to a 6-inch high letter at the same distance. This represents an acuity improvement from roughly 20/1200 to **20/400**. Less magnification (eg: 2x) was insufficient. Due to the patient's tunnel vision, at 16x the image far overlapped the tunnel with effects similar to the acuity degradation described for letters larger than 6 inches at 5 feet in **Figure 8** above.

Edge Detection

In 1969-1970, our team (M. Mladejovsky and W. Dobelle, unpublished data), at the University of Utah began exploring computer simulations of artificial vision displays using a head mounted display (originally designed by Ivan Sutherland) attached to a "single user" PDP-1 computer. This research was part of a much larger (unclassified) program on computerized image processing sponsored by the Advanced Research Projects Agency of the Department of Defense. Edge detection clearly extracted important information and removed "noise." However, this computer, (which occupied about 8,000 sq. feet) required hours to process a single frame. The 120 MHz system described above was able to process approximately one frame per second which is too slow for mobility. The new 233 MHz system using Sobel filters[16] for edge detection, can process and transmit images to the volunteer at speeds up to eight frames/second. A mannequin as pictured by the television camera (**Figure 1**, above) is shown in **Figure 9A**. The same scene is also shown after edge-detection processing in **Figure 9B**. We believe that such processing will be an integral part of all clinical visual prostheses.

Ultrasonic Rangefinder

Using edge detection, it is particularly helpful for the blind patient to know how far the wall is located behind the mannequin (**Figures 9A and 9B**). Ultrasonic rangefinders for the blind have been known for many years, but they have typically translated distance into audio signals which interfere with the ability of blind patients to use their hearing. (Indeed, this writer almost fell down a stairway at the University of Utah while blindfolded and trying to use an ultrasonic-to-audio conversion device. I did not hear the warning of a companion). However, by placing an electrostatic transducer on the left lens of the patient's eyeglasses (lateral to the camera and below the laser pointer) we have begun exploring the supplementary information that can be provided by modulating brightness, blink rate and identity of selected phosphenes.

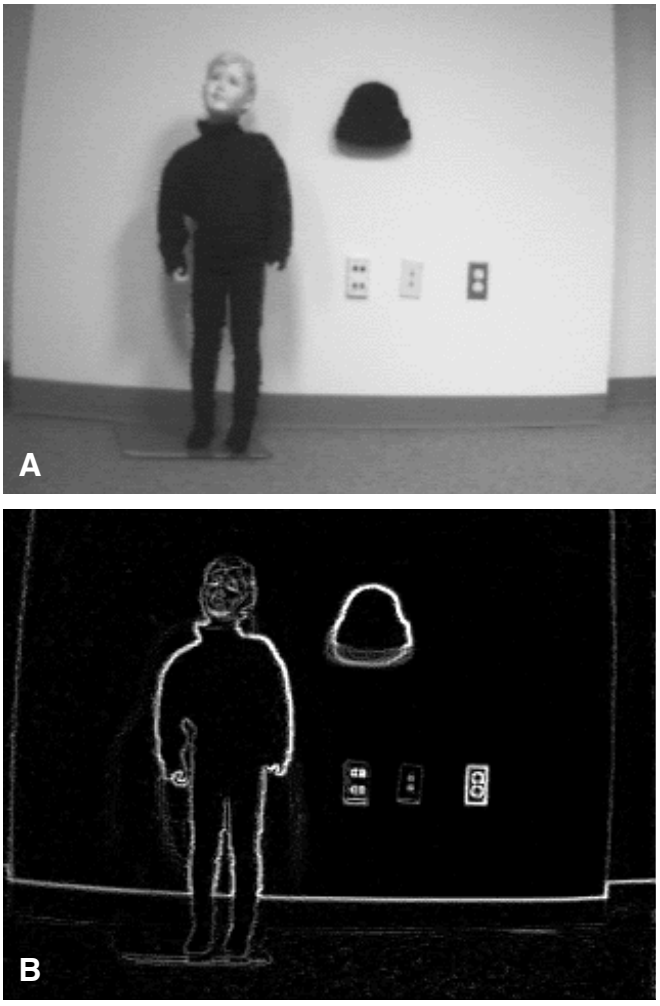

Figure 9. A, Picture of the 38 inch high child mannequin, with a second ski cap placed at a random location on the wall. B, Same scene as above, after edge-detection using Sobel filters and black/white reversal. The blind volunteer is able to easily find the cap and detect the wall outlets. Similarly, doorways appear as an outline of white phosphenes on a black background. All processing can be performed and transmitted to the patient at 8 frames/second.

Discussion

The blind volunteer is now able to navigate among a "family" of three mannequins —standing adult male, seated adult female and standing 3 year old child— randomly placed in a large room, without bumping into any of them. He can then go to the wall and retrieve a cap which has been placed on the wall at a random location. Navigating back in the direction from which he came, he can find any of the three mannequins and place the cap on the head of whichever one we request. As the volunteer gains more experience, and we make further refinements in the system, rapid progress can be expected. Even more rapid advances can be anticipated with larger electrode arrays, more powerful computers, and more sophisticated image pre-processing algorithms.

Wm. H. Dobelle, PhD
December 1, 1999
New York, NY